

MAGNETIC RESONANCE IMAGING, IN SITU HYBRIDIZATION, AND
IMMUNOHISTOCHEMISTRY-BASED ANALYSES OF EARLY
PRENATAL ETHANOL EXPOSURE-INDUCED CENTRAL NERVOUS
SYSTEM ABNORMALITIES

Elizabeth Anne Godin

A dissertation submitted to the faculty of the University of North Carolina at Chapel Hill in partial fulfillment of the requirements for the degree of Doctor of Philosophy in the Curriculum in Toxicology.

Chapel Hill

2010

Approved by:

Kathleen K. Sulik, Ph.D.
Thomas W. Bouldin, M.D.
Franck Polleux, Ph.D.
John M. Rogers, Ph.D.
Martin Styner, Ph.D.

ABSTRACT

ELIZABETH ANNE GODIN

Magnetic Resonance Imaging, In Situ Hybridization, and Immunohistochemistry-based Analyses of Early Prenatal Ethanol Exposure-Induced Central Nervous System Abnormalities

(Under the direction of Kathleen K. Sulik, Ph.D.)

Fetal alcohol spectrum disorders (FASD), the collection of defects resulting from prenatal alcohol (ethanol) exposure, has been the subject of basic and clinical investigation for four decades, but remains a major public health problem. At the severe end of the spectrum is fetal alcohol syndrome (FAS), which is characterized by the presence of growth retardation, craniofacial anomalies, and brain deficits. The research described herein was designed to advance our knowledge regarding ethanol's insult to the developing brain, with much of it directed toward testing the hypothesis that the application of magnetic resonance-based imaging to the examination of brain morphology, regional volumes and fiber tracts in ethanol-exposed fetal mice would facilitate new discoveries. As with other teratogens, it is well known that the type and severity of abnormality induced by ethanol is dependent upon the dose, timing, and pattern of maternal exposure. For this study, the CNS dysmorphology resulting from acute gestational day (GD) 7 maternal ethanol administration was examined in fetal mice utilizing state of the art imaging

techniques. This time in mouse development is consistent with that in the third week of human gestation. Magnetic resonance microscopy (MRM) allowed for linear, volumetric and 3-dimensional morphologic analyses of ethanol-induced alterations in the fetal CNS and diffusion tensor imaging (DTI) provided for assessment of fiber tract abnormalities. In addition, routine histological techniques were utilized for detailed examination of the ventromedian forebrain in ethanol-exposed embryos and fetuses.

Major new findings from these studies include the following regarding the consequences of acute GD7 ethanol exposure in mice 1) cerebral cortical heterotopias are induced; a discovery that was facilitated by MRM-based analyses, 2) fiber tract abnormalities involving the corpus callosum, anterior commissure, and fornix/fimbria occur, as evidenced by DTI, 3) fiber tract abnormalities, as identified in fetal mice, persist into periadolescent stages, 4) ventral forebrain insult preferentially involving the preoptic area and medial ganglionic eminences reduces Olig2 and GABA expression and alters the morphology of somatostatin-expressing cells. Overall, the results of this work promise to aid in clinical recognition, diagnosis, and prevention of FASD.

ACKNOWLEDGEMENTS

This dissertation would not have been possible without the help of so many people in so many ways... First and foremost, I would like to extend my sincerest gratitude to my mentor, Dr. Kathleen Sulik, for her commitment to training me as a scientist, in thinking, in speaking, and in writing. I will forever be grateful for her patience and guidance throughout my graduate career. To my dissertation committee, Drs. Tom Bouldin, Franck Polleux, John Rogers, and Martin Styner, I would like to thank each of you for your time and effort in making this dissertation possible. Your constructive criticisms, scientific questions, and helpful research suggestions helped to strengthen this dissertation.

I would like to recognize the members of the Sulik lab, who have been continuously supportive, both personally and professionally. Deborah Dehart, Drs. Shonagh O’Leary-Moore, Scott Parnell, Rob Lipinski, Shao-Yu Chen, Jiang Dong, and Yan Dong, it has been a pleasure to work alongside such bright scientists. I would like to specifically acknowledge Dr. Shonagh O’Leary-Moore for her time and dedication with the DTI project. To our “students”, Amber Kahn, Jake Ament, and Steve Pecevich, thanks for all your help with the tedious work of segmenting the many brains within this study!

While the next 100 some odd pages reflect my time spent in the laboratory over the past 6 years, the times in between were critical for encouraging the science.

And for those moments, I must thank my friends; Dr. Melanie Weed, Dr. Rayetta and Daniel Henderson, Drs. Dan and Debra Kemp, Dr. Kevin Boyd, Shari and Craig Spero, Kristin Hanley, Debra Reid, and Brooke and Chris Riley.

The most encouragement and understanding has come from those who know me best: my parents have knowingly, or unknowingly, urged me to achieve what at times I thought was unattainable, and for this, I am very grateful. Mom and Dad, your sacrifices throughout life have inspired me and instilled in me the values that have kept me persevering. Josh, Jenn, Allie, and Madelyn, thank you for keeping me grounded and reminding me what is truly most important in life. And last but certainly not least, the one who has stood by me during my most vulnerable times, my husband, Steve. I sincerely believe that together, we can achieve anything.

TABLE OF CONTENTS

LIST OF TABLES	x
LIST OF FIGURES	xi
LIST OF ABBREVIATIONS	xiv
Chapter	
I. BACKGROUND	1
HISTORICAL PERSPECTIVE ON ETHANOL-RELATED BIRTH DEFECTS	1
FETAL ALCOHOL SPECTRUM DISORDERS IN THE HUMAN POPULATION	4
Non-CNS features	4
CNS features	7
Neuropathological studies	7
Neuroimaging	9
Neurocognitive abnormalities associated with FASD	13
ANIMAL MODELS OF FASD	15
ANIMAL MODELS AND IMAGING	20
RATIONALE, HYPOTHESIS, AND SPECIFIC AIMS	22
REFERENCES	33

II. MAGNETIC RESONANCE MICROSCOPY DEFINES ETHANOL-INDUCED BRAIN ABNORMALITIES IN PRENATAL MICE: EFFECTS OF ACUTE INSULT ON GESTATIONAL DAY 7	45
ABSTRACT	47
INTRODUCTION	48
METHODS	52
Animal maintenance	52
Maternal treatment paradigm	52
Fetal specimen selection and preparation	53
Magnetic resonance microscopy	54
Linear measurements	54
Volume measurements	55
Routine histology	56
Statistical analyses	56
RESULTS	57
General features of the study population	57
Holoprosencephaly	57
Cerebral cortical dysplasia/heterotopia	59
Other dysmorphologies	60
Linear and volume assessments	61
DISCUSSION	64
REFERENCES	82

III. DIFFUSION TENSOR IMAGING AND TRACTOGRAPHY DEFINE A SPECTRUM OF FIBER TRACT DYSMORPHOLOGY IN THE BRAINS OF PRENATAL ETHANOL-EXPOSED MICE	90
ABSTRACT	92
INTRODUCTION	93
MATERIALS AND METHODS	94
Animal breeding and maintenance	94
Maternal treatment and animal rearing	95
Specimen collection and preparation for DTI	96
Diffusion tensor imaging (DTI)	97
Image processing and fiber tracking	98
RESULTS	100
General features of ethanol-exposed fetuses	100
Gross and fiber tract anomalies in the brains of HPE fetuses	101
Cortical layers in the fetal mouse	103
Spectrum of ethanol-induced HPE malformations	105
Dysmorphology in non-HPE fetuses	109
Persistence of fiber tract anomalies into the postnatal period	110
DISCUSSION	111
REFERENCES	127
IV. VENTROMEDIAN FOREBRAIN DYSGENESIS FOLLOWS EARLY PRENATAL ETHANOL EXPOSURE IN MICE	136
ABSTRACT	138
INTRODUCTION	139
METHODS	142

Animal husbandry and treatment paradigm	142
Scanning electron microscopy	143
Routine histology	144
<i>In situ</i> hybridization	144
Immunohistochemistry	145
RESULTS	145
DISCUSSION	149
REFERENCES	160
V. GENERAL CONCLUSIONS	171
REFERENCES	179

LIST OF TABLES

Table 1.1	Summary of Autopsy Studies	30
Table 1.2	Summary of Diffusion Tensor Imaging Studies in Humans with FAS and FASD	32
Table 2.1	Linear Brain Measurements	81

LIST OF FIGURES

Figure 1.1	Illustration depicting the facial characteristics of a normal child and a child with FAS.	25
Figure 1.2	Illustrations of two minor anomalies associated with FASD.	26
Figure 1.3	Images showing the similarities in facial dysmorphology between a child with FAS and a fetal mouse that has been exposed to ethanol on GD7 in comparison to a normal fetal mouse.	27
Figure 1.4	Illustrated are three of four distinct signaling centers necessary for telencephalic development	28
Figure 1.5	Diffusion tensor imaging in fetal mice allows for the visualization of fiber tract orientation in the brain, even prior to myelination.	29
Figure 2.1	MRM scans of GD17 mouse fetuses allow for linear measurements, regional segmentation, and 3D reconstruction.	73
Figure 2.2	Shown are the face and reconstructed brain of a control GD 17 mouse along with faces and brains of ethanol-exposed fetuses having semilobar and alobar holoprosencephaly.	74
Figure 2.3	Horizontal MRM scans at two different levels through a control and two affected fetuses illustrate rostro-median tissue loss.	75
Figure 2.4	MRM and routine histology illustrate olfactory nerve abnormality in a holoprosencephalic fetus.	76
Figure 2.5	Shown are the face, brain reconstruction, and histological sections of a control and four dysmorphic GD17 fetal mice.	77
Figure 2.6	Additional light micrographs along with coronal MRM scans and reconstructions and histological sections of the fetus pictured in Fig. 2.5d illustrate its dysmorphic features as compared to control.	78

Figure 2.7	MRM scans and reconstructions illustrate additional dysmorphic features of the fetus pictured in Fig. 2.5c.	79
Figure 2.8	Ethanol-induced volume changes in selected regions of GD 17 fetal mouse brains following acute GD 7 exposure.	80
Figure 3.1:	Illustrated are serial coronal sections of the brain showing fractional anisotropy (FA) and color-coded directional FA maps in a control and a prenatal ethanol-exposed HPE subject.	118
Figure 3.2:	Shown are horizontal scans presented as color-coded anisotropy maps and glyphs overlaid on an FA image of a control and an HPE subject.	120
Figure 3.3:	Illustrated are faces, coronal MRI scans at the level of the anterior commissure, and 3D reconstructed fiber tracts from a control and 6 GD17 mouse fetuses with holoprosencephaly (HPE).	122
Figure 3.4:	Shown are color-coded anisotropy maps and histological sections of a control and prenatal ethanol-exposed HPE mouse fetus.	123
Figure 3.5:	Illustrated are faces, 3D MRM brain reconstructions, and horizontal and midsagittal color-coded FA maps from a control mouse fetus and three that were exposed to ethanol on GD 7.	124
Figure 3.6:	Illustrated are coronal and mid-sagittal color-coded anisotropy maps from a control (a & b) and two ethanol-exposed (c & d; e & f) male mice at postnatal day 45.	126
Figure 4.1:	Scanning electron microscopic analyses of control and two ethanol-exposed GD 13 embryos illustrate that abnormal facial features accompany those of the forebrain.	155
Figure 4.2:	Routine H&E-stained histological sections of a control and 3 ethanol-exposed GD13 embryos illustrate a spectrum of forebrain abnormality.	156
Figure 4.3:	<i>In situ</i> hybridization, to label Nkx2.1 and Fzd8 expression in control and ethanol-exposed GD12.5 embryos illustrates median forebrain deficiency involving the POA and MGEs.	157

- Figure 4.4: Immunohistochemical labeling of Olig2 and GABA illustrates deficiency of these basal forebrain markers in ethanol-exposed GD12.5 mice in comparison to a control. 158
- Figure 4.5: Shown are representative images of somatostatin (Sst)-immunohistochemical staining in the subpallium of GD17 mice. 159

LIST OF ABBREVIATIONS

AC	anterior commissure
ADHD	attention deficit hyperactivity disorder
ANR	anterior neural ridge
BEC	blood ethanol concentration
BTD	bulbo-thalamic distance
CC	corpus callosum
CGE	caudal ganglionic eminence
CNS	central nervous system
CRL	crown-rump length
DT	diffusion tensor
DTI	diffusion tensor imaging
EC	external capsule
EF	executive functioning
F	fornix columns
FA	fractional anisotropy
FAS	fetal alcohol syndrome
FASD	fetal alcohol spectrum disorders
Fim	fimbria
FOV	field of view
FR	fasciculus retroflexus
FTD	fronto-thalamic distance

GABA	γ -Aminobutyric acid
GD	gestational day
GE	ganglionic eminence
H & E	hemotoxylin and eosin
H	hippocampus
HC	hippocampal commissure
HPE	holoprosencephaly
IC	internal capsule
LGE	lateral ganglionic eminence
LV	lateral ventricle
MD	mean diffusivity
MGE	medial ganglionic eminence
MRI	magnetic resonance imaging
MRM	magnetic resonance microscopy
OC	optic chiasm
ON	optic nerve
OT	optic tract
PBS	phosphate buffered saline
PFAS	partial fetal alcohol syndrome
PND	postnatal day
POA	preoptic area
Pv	parvalbumin
ROI	regions of interest

Shh	sonic hedgehog
SN	septal nucleus
Sst	somatostatin
St	striatum
T	tesla
TE	excitation time
TR	relaxation time

CHAPTER I

BACKGROUND

HISTORICAL PERSPECTIVE ON ETHANOL-RELATED BIRTH DEFECTS

Ethanol (alcohol) is a well documented teratogen that causes a wide spectrum of birth defects. There are conflicting opinions as to when ethanol was first mentioned as a teratogen (Abel, 1999; Warren and Hewitt, 2009). It may have been as early as 350 B.C. when Aristotle apparently stated that “foolish, drunken and harebrained women most often bring forth children like unto themselves, morose and languid” (Warren and Hewitt, 2009), though Abel (1999) would argue this statement was misinterpreted by Robert Burton (1621) and that ethanol was not recognized as causing birth defects in 350 B.C. One of the first published scientific studies of ethanol’s effect on embryonic development dates back to 1910 when Charles Stockard noted that fish embryos exposed to ethanol developed gross structural abnormalities of the central nervous system and the eyes (Stockard, 1910). Then, in 1968, Lemoine et al. documented the specific pattern of abnormalities he noticed in children born to alcoholic mothers. These included particular facial characteristics, growth delay, malformations, and psycho-motor retardation (Lemoine et al., 1968; reprinted 2003). Within this study, high rates of

miscarriage and stillbirths were recognized. Seven years later, Jones and Smith coined the term “Fetal Alcohol Syndrome” to describe the defects associated with prenatal ethanol exposure (Jones and Smith, 1975). This, along with the issues discussed at the first NIAAA conference on Fetal Alcohol Syndrome in 1977, led to a government health advisory on ethanol consumption during pregnancy. The advisory recommended a two-drink limit for pregnant women and stated that greater than six drinks per day was dangerous to the developing baby (Department of Health, Education, and Welfare, 1977). A later update in 1981 by the Surgeon General advised that there was no known safe limit of ethanol for pregnant women and recommended abstinence (Koop, 1981). The most recent update in 2005 reinforced the previous advisory on abstinence and added a recommendation that women who may become pregnant also abstain from drinking (Carmona, 2005).

Although it has been well documented for many years that ethanol use during pregnancy can lead to devastating birth defects, pregnant women and non-pregnant women of child bearing age continue to drink. Sadly, a 2009 CDC report showed that the rate of ethanol use among pregnant and non-pregnant women aged 18-44 did not substantially decrease between the years of 1991 to 2005. This information was acquired from a survey that showed that 12.2% of pregnant women reported any ethanol use (defined as having at least 1 drink in the last 30 days), while 1.9% reported binge drinking (defined as having five or more drinks on at least one occasion in the last 30 days). Among non-pregnant women, 53.7% reported any ethanol use while 12.1% had at least one binge episode (CDC, 2009). Ethanol use and abuse is critical in non-pregnant women because most women do not recognize

they are pregnant for the first few weeks and continue to consume ethanol. At these early stages, the developing embryo is already sensitive to ethanol's effects.

Epidemiologic studies of individuals with Fetal Alcohol Syndrome (FAS) and Fetal Alcohol Spectrum Disorders (FASD) report varying statistics depending on the location of the study and population examined. A recent report by May et al. in 2009 states that the prevalence of FAS in a typical mixed-race, mixed socio-economic status population in the US is at least 2 to 7 per 1,000. The prevalence of FASD, which is far more common than FAS, is an alarming 2-5% in the US (May et al., 2009). It is important to recognize that FASD is not just a problem in our country; it is, in fact, a global issue. Studies have been conducted examining FASD in other countries including Canada, Italy, Finland, and South Africa. Some of the highest rates reported are in the Western Cape of South Africa, where the rate for FAS was found in the year 2000 to be between 40.5 and 46.4 per 1,000 births (May, 2000). A more recent study in the Western Cape of South Africa (May, 2007) includes cases of both FAS and partial FAS (PFAS). This study reports that 68.0 to 89.2 per 1,000 births have an alcohol-related birth defect. A recent report regarding a study of 71 children adopted from Eastern Europe states that an alarming 52% of these children have some form of FASD (Landgren et al., 2010).

Caring for individuals with defects resulting from prenatal ethanol exposure is not trivial. Those who are most severely affected will require lifetime health care and support services, as they are not able to care for themselves. Alcohol-related birth defects are expensive. In the US, it has been estimated that we spend \$3.6 billion

annually caring for those with alcohol-related birth defects, and that per individual, there is a lifetime total cost of care of \$2.9 million (Lupton et al., 2004).

FETAL ALCOHOL SPECTRUM DISORDERS IN THE HUMAN POPULATION

Fetal alcohol spectrum disorders (FASD) is an umbrella term used to describe all defects caused by maternal ethanol exposure (Streissguth and O'Malley, 2000). These include, but are not limited to, growth retardation, heart and kidney problems, skeletal defects, vision and hearing problems, abnormal facial features, and structural and functional brain defects. There are many factors involved in the variability of defects caused by ethanol. It is recognized that the extent of defect is dependent upon the dose, pattern, and timing of exposure, as well as maternal factors including nutrition and genetics (Coles et al., 1994).

Non-CNS features

At the most severe end of the alcohol-induced birth defect spectrum is Fetal Alcohol Syndrome (FAS). The characteristic features of FAS include pre- and/or postnatal growth deficiency (below the 10th percentile for both height and weight), a specific facial phenotype, and CNS abnormalities. Individuals with FAS frequently have a decreased head circumference (less than 10th percentile), which is indicative of a small brain. As illustrated in Figure 1.1, there are specific facial features that are characteristic of FAS. These include a relatively flat midface, indistinct philtrum, a thin vermilion border, small palpebral fissures, and a short, upturned nose. Sometimes clefting of the upper lip and/or palate occurs. Unilateral or bilateral cleft

lips are the most common, though median cleft lips have also been reported (Ronen and Andrews, 1991). Other features that can accompany cleft palate include a small tongue (microglossia) or a small mandible (micrognathia). However, micrognathia can also occur without cleft palate. Another structural anomaly of the craniofacies involves the ears. Underdevelopment of the top part of the external ear causes the tissue to fold over parallel to the curve beneath it, giving it a railroad track appearance (see Figure 1.2), hence the name railroad track ears (Wattendorf and Muenke, 2005; Hoyme et al., 2005).

The presence of abnormal craniofacial features frequently accompanies brain damage. In 1964, DeMyer suggested that median facial anomalies predict brain defects, though there are exceptions (DeMyer et al., 1964). This also holds true for ethanol-related craniofacial defects. Importantly, facial features among individuals with FAS are similar to those within the holoprosencephaly spectrum.

Ocular problems occur frequently in individuals with FASD. Stromland (1987) has reported that in her investigations the eyes are abnormal in approximately 90% of affected individuals. The observed ocular abnormalities include microphthalmia, iridial coloboma, cataracts, retinal dysplasia, and more commonly, optic nerve hypoplasia. Strabismus and refractive errors (myopia, hyperopia, and astigmatism) are also common (Stromland et al., 2002; Stromland, 2004). Ocular problems, like facial anomalies, can be indicative of brain defects. Indeed, Jones and colleagues (2009) suggest that short palpebral fissure length (which is a result of reduced globe size) may reflect a defect in forebrain development.

Another sensory function that is impaired in individuals exposed to ethanol prenatally is hearing. Four types of hearing disorders have been described: developmentally delayed auditory function, sensorineural hearing loss, intermittent conductive hearing loss owing to recurrent serous otitis media, and central hearing loss (Church and Abel, 1998; Cohen-Kerem et al., 2007). Hearing problems are often accompanied by speech and language disorders (Church and Gerkin, 1988; Church and Kaltenbach, 1997). Early diagnosis and intervention is critical or problems that could potentially improve with therapy will likely become permanent.

Abnormalities in other organ systems have also been reported in individuals with prenatal ethanol exposure. Included are cardiovascular defects, the most common of which include atrial and ventricular septal defects, stenosis of the pulmonary artery, aberrant great vessels, and tetralogy of Fallot (Burd et al., 2007). Additionally, structural anomalies of the kidneys have been included in a recent update on the diagnostic criteria of FASD. Included are aplastic/hypoplastic/dysplastic or horseshoe kidneys (Hoyme et al., 2005). While liver and gastrointestinal disorders have also been reported in individuals with FASD, no distinctive structural abnormality involving these organs has been determined (Hofer and Burd, 2009).

Ethanol exposure can also impair development of the skeletal system. In one of the first reports by Jones et al. (1973), 6 of the 8 patients examined had some form of limb abnormality. Since then, others have reported joint anomalies including abnormal position and function and shortened fingers and fingernails (Froster and Baird, 1992; Jones and Smith, 1973; Spiegel et al., 1979). An altered palmar crease

which entails a transverse flexion crease between the index and middle finger, forming a “hockey stick” appearance, is another structural anomaly found in individuals with FASD (see Figure 1.2, right) (Wattendorf and Muenke, 2005; Hoyme et al., 2005)

CNS features

Neuropathological Studies

Autopsies of children prenatally exposed to ethanol illustrate the most severe structural end of the spectrum of ethanol’s teratogenic effect on the developing brain (Jones et al., 1973; Jones and Smith, 1975; Clarren et al., 1978; Peiffer et al., 1979; Majewski, 1981; Wisniewski et al., 1983; Ronen and Andrews, 1991; Coulter et al., 1993). These findings are summarized in Table 1.1. The cause of death in those autopsied was commonly associated with cardiac and/or pulmonary dysfunction. The first autopsy study, by Jones and Smith (1973) (also described in Jones and Smith, 1975; Clarren et al., 1978) reported a small brain (micrencephaly) that had extensive developmental anomalies. Grossly, the left hemisphere of the cerebral cortex was covered by an aberrant sheet of tissue. Histologically this tissue resembled a leptomenigeal, neuroglial heterotopia. Beneath the heterotopic tissue layer, the cortex was thin and disorganized. In addition, the lateral ventricles were enlarged and there was agenesis of the corpus callosum (Jones and Smith, 1973).

Other studies have confirmed that prenatal ethanol exposure can affect neuronal migration. Indeed, 14 of the 18 neuropathological evaluations listed in Table 1.1 reported some form of defect in neuronal migration (Jones et al., 1973;

Jones and Smith, 1975; Clarren et al., 1978; Peiffer et al., 1979; Majewski, 1981; Wisniewski et al., 1983; Coulter et al., 1993). These vary from lissencephaly to cerebral and cerebellar heterotopias to microdysplasias. A common finding among the autopsies is leptomeningeal heterotopias, in which clusters of neuronal tissue have migrated beyond the cortex and are associated with the meninges.

Defects in neuronal migration are highly correlated with seizure activity. In fact, Verotti et al. (2009) state that “neuronal migration disorders are considered to be one of the most significant causes of neurological and developmental disabilities and epileptic seizures in childhood.” Seizures have been reported in individuals with FASD (Ioffe and Chernick, 1990; Losub et al., 1981; Jones and Smith, 1975; Majewski, 1981; Marcus, 1987; Murray-Lyon, 1985; Olegard et al., 1979; O’Malley and Barr, 1998; Sun et al., 2008). Majewski (1981) reported abnormal EEG’s in 25% of his study population, which included 61 individuals with varying degrees of ethanol-related birth defects. Generalized convulsions have also been noted in this population (Marcus, 1987; Majewski, 1981). Though it appears the severity of FASD is not a factor that contributes to seizure activity, the timing of ethanol-exposure is critical. Bell and colleagues (2010) found that both first trimester exposure and drinking throughout all three trimesters was associated with a higher prevalence of having a seizure disorder, suggesting that drinking during the first trimester increases the risk of seizures in the offspring.

Characteristics of FASD are consistent with the holoprosencephaly spectrum. Indeed, the first autopsy reported by Jones and Smith (1973) appears to have been a case of ethanol-induced HPE. HPE is a disorder that results from a deficiency in

forebrain development and is characterized by defects in medial forebrain structures. The HPE spectrum is categorized as lobar [least severe], semi-lobar, or alobar [most severe] based on the degree of cerebral hemispheric separation. While the etiology of HPE encompasses multiple genetic and environmental factors, Ronen and Andrews (1991) suggest that first trimester ethanol exposure is one cause of HPE. They reported three infants, all of whose mothers drank heavily during the first trimester that each of whom had a single enlarged lateral ventricle, and fused basal ganglia and thalami. Of these infants, one had typical FAS facial features, one had a median cleft lip and palate, and one had unremarkable facies.

Neuroimaging

While autopsy studies have been informative, they are also incomplete, in that they have only examined a small portion of the FASD spectrum. Recent advances in *in vivo* imaging have allowed a broader population to be studied and have improved our understanding of structure-function relationships involving the CNS. Magnetic resonance imaging (MRI) is a common technique used to create anatomical images of the body. This technique has been used to analyze the size and shape of various brain regions in individuals with FASD (reviewed by Riley et al., 2004; Spadoni et al., 2007; Norman et al., 2009).

Among the most consistent MRI findings in individuals with prenatal ethanol exposure is overall brain volume reduction (Johnson et al., 1996; Swayze et al., 1997; Archibald et al., 2001, Autti-Ramo et al., 2002; Sowell et al., 2002, Astley et al., 2009). Surprisingly, in the same cohort that was shown to have decreased brain

volume (Sowell et al., 2002), Sowell and colleagues (2008) report an increase in cortical thickness in individuals with FASD. The increase in cortical thickness was correlated with measures of reduced verbal recall and visuospatial functioning (Sowell et al., 2008). Another finding is a differential effect on white versus gray matter; Archibald et al. (2001) reported a relative reduction in white matter (in comparison to gray matter) in the cerebrum of individuals with FAS.

The corpus callosum (CC) has been a focus of many imaging studies examining individuals with prenatal ethanol exposure (Autti-Ramo et al., 2002; Johnson et al., 1996; Bhatara et al., 2002; Swayze et al., 1997; Astley et al., 2009; Bookstein et al., 2002a,b, 2007; Sowell, 2000; Riley et al., 1995). A number of investigators have explored regional changes in the CC. Riley et al. (1995) reported decreased volume in the genu, isthmus, and splenium. Sowell and colleagues (2001) confirmed effects on the most posterior regions of the CC, illustrating displacement and volume reductions involving the isthmus and splenium. Variability of CC shape has also been found in individuals with FASD (Bookstein et al., 2002a,b). Bookstein reported that a thick CC is related to deficits in executive functioning, while a thin CC is related to deficits in motor function. One particular shape of the CC that is strongly associated with prenatal ethanol exposure is a “hook”-like angle of the posterior end (Bookstein et al., 2007).

Prenatal alcohol exposure affects the development of the basal ganglia, which are comprised of the caudate, putamen, and globus pallidus. Together, these nuclei are associated with motor control and learning. When analyzed as a whole, Mattson and colleagues (1996) found reduced volumes of the basal ganglia in

individuals with FASD. The Mattson et al. (1996) study found the caudate, but not the putamen, to be affected. Studies by Archibald et al., (2001) and Cortese, et al. (2006) confirmed reductions in the caudate in individuals with FAS. A recent study by Astley et al., (2009) reported reductions in both the caudate and putamen in FAS subjects.

The hippocampus, a part of the limbic system that plays a role in long-term memory and spatial navigation, may be affected by prenatal alcohol exposure. While Autti-Ramo and colleagues (2002) found small hippocampi in 3 (2 FASD, 1 FAS) of 17 total participants in his study, Archibald et al. (2001) reported a “disproportionate sparing of the hippocampal volume” in the otherwise hypoplastic brains of individuals with FAS. A recent study by Astley and colleagues (2009) examined a larger cohort of subjects subdivided into three ethanol-exposed groups and found a reduction in the mean absolute hippocampal volume that increased in accordance with severity across groups.

Another region of the brain that is sensitive to ethanol's teratogenic effects is the cerebellum. This region of the brain is important in motor control, attention and language, and possibly some emotional regulation. In neuropathological studies examining individuals heavily exposed to ethanol, the cerebellum and the cerebellar vermis was found to be hypoplastic (Peiffer et al., 1979; Majewski, 1981; Wisniewski et al., 1983). More recently, imaging studies have confirmed that some individuals with FASD have smaller cerebellar regions (Autti-Ramo et al., 2002; Sowell et al., 1996; O'Hare et al., 2005; Astley et al., 2009). In accordance with the neuropathology studies, a specific effect on the vermal region was found (Autti-

Ramo et al., 2002; Astley et al., 2009). When the vermis was subdivided in two regions, the anterior, but not the posterior vermis was found to be smaller in individuals with FASD (Sowell et al., 1996; O'Hare et al., 2005).

Diffusion tensor imaging (DTI) is an MRI modality that allows for the study of fiber tracts in the brain both *in vivo* and *ex vivo*. This technique measures the diffusivity of water molecules and the orientation of their movement within a defined tissue (Mori and Zhang, 2006). Anisotropy is a term used to define the directionality of the diffusion. If the diffusion is not restricted, and is uniform in all directions, it is referred to as isotropic diffusion. In the brain, water should move more easily along axonal fibers, giving the diffusion directionality. This information can be used to evaluate the organization of the fiber tracts in the brain. Although there are several measurements that can be derived from DTI analyses, the most common are Fractional Anisotropy (FA) and Mean Diffusivity (MD). FA and MD are scalar values between 0 and 1 that indicate how anisotropic a given voxel or fiber is in one direction and the average diffusivity across all directions, respectively. Higher values of FA and lower values of MD are indicative of more organized fiber tracts in the adult brain. A method used to analyze the morphology of white matter fibers is fiber tracking. For this, computer-based programs use measures of anisotropy to “track” white matter fibers in the brain, yielding three-dimensional images that detail the connectivity of the brain (Mori and van Zijl, 2002).

DTI has only recently been applied to the examination of the brains of individuals with FASD. The main focus of the majority of these studies has been the CC. As previously mentioned, as shown in early autopsy studies (Jones and Smith,

1973; Jones and Smith, 1975; Clarren et al., 1978; Peiffer et al., 1979; Majewski et al., 1981; Wisniewski, 1983) and recent neuroimaging analyses (Autti-Ramo et al., 2002; Bhatara et al., 2002; Bookstein et al., 2002a,b; Johnson et al., 1996; Riley et al., 1995; Sowell et al., 2001), the CC is affected in individuals prenatally exposed to ethanol. DTI studies conducted on individuals with FAS or FASD have shown decreased organization in various regions of the corpus callosum (Table 1.2; Ma et al., 2005; Wozniak et al., 2006; Sowell et al., 2008; Lebel et al., 2008; Fryer et al., 2009; Li et al., 2009; Wozniak et al., 2009). Abnormalities of fiber tracts within the posterior regions have been the most consistently reported, with decreased FA in the splenium (Ma et al., 2005; Sowell et al., 2008; Lebel et al., 2008; Wozniak et al., 2009) and isthmus (Li et al., 2009; Wozniak et al., 2009), and increased MD in the isthmus (Wozniak et al., 2006). Abnormalities in other fiber tracts, including the cingulum, corticospinal tract, inferior fronto-occipital fasciculus, and inferior and superior longitudinal fasciculus have been reported as well (Lebel et al., 2008).

Neurocognitive abnormalities associated with FASD

Along with structural brain defects, individuals with FASD have a range of neurocognitive and behavioral problems. A consistent finding regards intellectual ability. The intellectual quotient (IQ) of individuals with FASD has been a focus of many studies (reviewed in Mattson and Riley, 1998). A recent Canadian report states that the average IQ among individuals with FASD is between 75 and 85, with the full range being between 20 and 140 (Lutke and Antrobus, 2004).

Many individuals with FASD have been diagnosed with attention deficit hyperactivity disorder (ADHD), as they have attention problems, restlessness, and impulsivity (Mattson and Riley, 1998). In fact, ADHD is the most common comorbidity in FASD (Fryer et al., 2007; Herman et al., 2008). There are five factors of attention that are studied in attention disorders; the ability to focus attention, shift attention, sustain attention, encode information, and stabilize attention. While both ethanol-exposed and non-exposed ADHD individuals show deficits in attention, the degree and pattern appear to differ between groups (Vaurio et al., 2008). Coles et al. (1997) compared individuals with FASD to individuals with ADHD (no known exposure) and found that those with FASD had greater deficits in two of the factors of attention (Encode and Shift) while those with ADHD alone had deficits in the two other factors (Focus and Sustain). A study from Greenbaum et al. (2009) reported that individuals with FASD have difficulties in social cognition and emotion processing in comparison to those with ADHD alone.

Executive functioning (EF) encompasses a range of abilities involved in goal-oriented behavior, including many cognitive processes such as planning, inhibition, working memory, set shifting, and organization (Rasmussen, 2005). EF is impaired in individuals prenatally exposed to ethanol and also in individuals with ADHD (alone). Similar to findings regarding patterns of attention, research shows that there are specific patterns of EF deficit in individuals with FASD versus those with ADHD (alone) (Vaurio et al., 2008). Frontal-subcortical circuitry, which is associated with EF, is altered in individuals with FASD. This is in keeping with structural

imaging studies showing volumetric changes in both the caudate (Archibald et al., 2001) and frontal cortex (Sowell et al., 2002) of ethanol-exposed individuals.

Multiple mental health problems have been reported in individuals with FASD (reviewed by O'Connor and Paley, 2009). These include depression, anxiety, and ethanol and drug use disorders. Unfortunately, the cognitive and mental health problems that result from prenatal ethanol exposure also contribute to the overall behavior of these individuals. Many individuals with FASD have trouble in school, problems with the law, and inappropriate sexual behaviors (Kodituwakku, 2007).

ANIMAL MODELS OF FASD

The pathogenesis of FASD has been difficult to study in humans for many reasons. First, it is not commonly a fatal disease and autopsy reports only describe a portion of exposed individuals. While recent *in vivo* imaging techniques have allowed for a more comprehensive analysis of structural and functional deficits than previously possible, these studies still have not answered the many questions regarding the pathogenesis of ethanol's teratogenicity. In human populations confounding factors (maternal, genetic, and environmental) pose a significant problem in characterizing FASD. Temporal patterns of ethanol use during pregnancy vary from case to case, making it nearly impossible to relate the adverse effect to the developmental stage of exposure. Another concern is the dosage of ethanol, and the resulting blood alcohol concentration (BAC), both of which vary considerably when evaluating humans. The use of animal models allows for the control of these factors.

Various animal models have been used to examine the dysmorphologies and mechanisms of action associated with prenatal ethanol exposure. In 1910, Charles Stockard used fish as a model system to illustrate the effect of ethanol on the developing organism. He noted that ethanol exposure during a specific time in development caused cyclopia and brain abnormalities. Other animal models used to study prenatal ethanol exposure have included non-human primates, rodents, chicks, fish, and large mammals (i.e. sheep and pigs) (reviewed by Cudd, 2005). The most common animal model employed for FASD research is the rodent. Both rats and mice have been used extensively to study third-trimester equivalent structural and functional deficits resulting from prenatal ethanol exposure. Unfortunately, the brain growth spurt occurs during the third trimester in humans, a time that corresponds to the early postnatal period in rodents. For third trimester equivalent analyses in rodents, West and colleagues (1993) developed a “pup in a cup” model system where the newborn pup was artificially reared and received adequate nutrition, even during periods of intoxication.

Acute early pregnancy (first trimester equivalent) exposures have not been examined as thoroughly as the late exposures (third trimester equivalent). In 1980, Webster and colleagues found that an acute ethanol exposure during critical times of pregnancy in both inbred and outbred mice was highly teratogenic. An acute ethanol exposure on gestational day (GD) 7 resulted in fetuses with exencephaly, cyclopia, cleft lip, and mandibular hypoplasia. The GD7 exposure paradigm is important because it corresponds to the middle of the third week of human gestation

(approximately day 17 post fertilization), a time when most women do not recognize they are pregnant.

In 1981, Sulik et al. utilized Webster's dosing regimen to examine the embryogenesis of the defects that result from an early acute prenatal ethanol exposure. The dosing regimen entailed two maternal intraperitoneal doses of 2.9 g/kg ethanol four hours apart on GD 7 and resulted in peak blood ethanol concentrations (BEC) between 400 – 500 mg/dl. A comparable acute high dose may result from an alcoholic's binge drinking episode. Sulik et al. (1981) reported that the facial malformations resulting from this mouse GD7 ethanol exposure were remarkably similar to those of a child with the FAS facial phenotype (small head circumference, short palpebral fissures, small nose, and deficient philtrum) (shown in Figure 1.3). Further examination of the ethanol-exposed fetuses demonstrated that the eyes and brains of these mice were also affected (Sulik et al., 1984; Cook et al., 1987). Schambra et al. (1990) found that an acute ethanol exposure on GD 7 affected the forebrain (specifically septal nuclei), but not the midbrain or hindbrain. Neurons located in the forebrain (cholinergic) were reduced, but those located in the midbrain (catecholaminergic) and hindbrain (serotonergic) were not. Other forebrain areas that are affected by a GD7 ethanol exposure include the corpus callosum, basal ganglia, hippocampus, and anterior cingulate cortex (reviewed by Sulik, 2005).

Though the cellular mechanisms of prenatal ethanol exposure are not fully defined, some of those proposed include disrupted cellular energetics, impaired cell cycle, altered regulation of gene expression and signaling, disrupted cell-cell

interactions, and cell damage/cell death (reviewed by Goodlett and Horn, 2001; Goodlett et al., 2005). Identification of multiple mechanisms of action is likely due to differences in the various tissues targeted by ethanol, the developmental stage of exposure, and the concentration of ethanol exposure.

Of those mentioned above, a mechanism that is of particular interest for this work is ethanol-mediated alteration in Sonic hedgehog (Shh) signaling (Blader and Strahle 1998; Ahlgren et al., 2002; Yamada et al., 2005; Higashiyama et al., 2007; Li et al., 2007; Loucks et al., 2007; Aoto et al., 2008; Loucks and Ahlgren, 2009). Early in development, just after neural induction is initiated, Shh is expressed at one of four distinct signaling centers necessary for regional telencephalic development (reviewed in Hoch et al., 2009). The three other spatially regulated centers express a variety of secretory factors including Fgfs (fibroblast growth factors), BMPs (bone morphogenetic proteins), and Wnts (wingless/ints), among others (see Figure 1.4). Notably, 1) Shh is required for normal forebrain and craniofacial development (Chiang, 1996), 2) disruptions in Shh signaling result in craniofacial dysmorphologies (Marcucio et al., 2005) similar to those seen following exposure to ethanol prenatally (Ahlgren et al., 2002), 3) Shh is necessary in order to maintain the expression of Fgf8, which is expressed in the anterior neural ridge (ANR) and other organizing centers of the brain, and 4) Fgf8 knockout mice have CNS dysmorphologies similar to those of the FAS mouse model, with a loss of midline structures including the septal nuclei and ganglionic eminences (Storm et al., 2006).

Another teratogenic mechanism of action described for ethanol is the induction of cell death. Early studies that have examined ethanol-induced cell death

include those conducted in the chick by Sandor (1968), and those in mouse embryos by Bannigan and co-workers (Bannigan and Burke, 1982; Bannigan and Cottell, 1984). More recently, Dunty et al. (2001) reported that ethanol causes a highly specific pattern of cell death, depending on the time of exposure. Twelve hours after a GD 7 ethanol exposure, excessive cell death was found along the ANR. The ANR is important in development because it is known to act as an organizer of the prosencephalon (forebrain).

As previously noted, CNS dysmorphologies in the *Fgf8* knockout mouse are similar to those of FAS. Importantly, the ganglionic eminences (GEs) are affected in both cases (Storm et al., 2006). Among the cell populations that originate in the GEs are oligodendrocytes, which are neuroglial. These cells originate specifically from the medial GE (MGE), anterior entopeduncular area (AEP) and preoptic area (POA) (Kessaris et al., 2006) and require *Shh* expression for normal development (Nery et al., 2001). Regarding FAS, a study, by Ozer and colleagues (2000), shows a significant reduction in oligodendroglial expression of myelin basic protein in GD17 mouse fetuses after a maternal dietary ethanol exposure lasting from GD6 through GD17.

A second GE-derived cell population is inhibitory (GABAergic) interneurons. These interneurons migrate from the GEs to either the cortex or the hippocampus. Some of these inhibitory interneurons originate from the MGE and bind parvalbumin or somatostatin, while others are specific to the caudal GE (CGE) and bind calretinin (Butt et al., 2007; Wichterle et al., 2001; Xu et al., 2003). Previous studies from Moore et al., using a dietary maternal ethanol exposure in rats, show reduced

expression of parvalbumin interneurons in the medial septum (Moore et al., 1997) and cingulate cortex (Moore et al., 1998) of the offspring. Another study employing a postnatal ethanol exposure paradigm reports differential effects on interneuron subtypes, with an increase in numbers of calretinin-expressing interneurons and a decrease in calbindin-expressing interneurons (Granato, 2006). While informative, these studies examine the effects of ethanol exposures over relatively long periods of time.

ANIMAL MODELS AND IMAGING

The application of new imaging technologies, including high resolution magnetic resonance imaging (MRI; aka magnetic resonance microscopy, MRM), to basic research provides unprecedented opportunities to explore normal and abnormal morphology. Regarding normal morphology, it is notable that adult mouse MRI-based atlases are now available (for example, Mouse Imaging Centre - http://www.mouseimaging.ca/research/mouse_atlas.html; Mouse Atlas Project - <http://map.loni.ucla.edu/atlas/>; Caltech Atlas of Mouse Development - <http://mouseatlas.caltech.edu/>). Recent advances, including the use of contrast agents (e.g. gadolinium/ Prohance) to aid in improved resolution (e.g. down to 21.5 μm isotropic resolution) and accurate regional segmentation have facilitated the creation of such atlases (Badea et al., 2007; Dorr et al., 2008). Segmentation provides for analysis of area, volume, and shape of regions of interest. Regarding disease states, MRI has been a useful tool in characterizing animal models of neurological disorders including degenerative disease, inflammatory disease,

cerebral ischemia and stroke, tumors, infectious disease, and traumatic brain and/or spinal cord injury (reviewed by Anderson and Frank, 2007).

More recently, imaging has been applied to the study of prenatal and early postnatal development. Petiet et al. (2007) employed MRM in creating a 4-dimensional atlas of gestational day (GD) 10.5 to postnatal day (PN) 32 mice (available at <http://www.civm.duhs.duke.edu/devatlas/index.htm>). In this atlas, over 200 structures have been labeled. The optimization of both contrast and signal-to-noise allow for all major organs to be identified, making it possible to appreciate the development of various organ systems, specifically the heart.

Another imaging technique that has recently been applied to animal models is diffusion tensor imaging (DTI). As previously mentioned, DTI is a method that can delineate fiber tracts within the brain and that is based on the diffusion of water molecules. The use of DTI in the postnatal mouse brain provides for analysis of myelinated fibers (Jiang and Johnson, 2010), including examination of fiber tract development over time (Zhang et al., 2005). Mori and colleagues were the first to utilize DTI to examine mouse brains at embryonic and fetal stages, that is at a time in development when myelination has not yet occurred (Zhang et al., 2003). In this work, fixed specimens were imaged on GDs 12 through 18 with the resulting color-coded anisotropy maps and fiber tracking illustrating the orientation of migrating neurons and the conformation of (unmyelinated) fiber tracts including the hippocampal commissure, anterior commissure, and corpus callosum (See Figure 1.5) (Zhang et al., 2003). DTI has also been employed for studies of mutant mouse models (Andrews et al., 2006; Ren et al., 2007). Exemplary are studies of the

Robo1 knockout mouse which has a deficient CC, as shown in color-coded anisotropy maps (Ren et al., 2007). In another genetically altered mouse model, Probst bundles, which form in the absence of a CC, are apparent in both color-coded maps and fiber tracked images (Andrews et al., 2006). While immensely promising, these advanced imaging technologies had not yet been applied to the field of developmental toxicology.

RATIONALE, HYPOTHESES, AND SPECIFIC AIMS

Previous studies employing FASD models have shown that prenatal exposure to ethanol occurring as early as GD7 in the mouse can result in severe brain defects.

The objective of the work described in this thesis was to better characterize the spectrum of morphologic and cellular changes in the brain that result from acute maternal ethanol treatment during this early stage of development. The overall hypothesis tested was that the pioneering application of magnetic resonance-based imaging (MRM and DTI) to examination of brain morphology, regional volumes and fiber tracts in fetal mice would facilitate discovery of ethanol-induced CNS damage. For this research, the following specific aims were addressed:

SPECIFIC AIM 1: To apply MRM-based analyses to the definition of fetal mouse brain dysmorphology resulting from GD7 ethanol exposure.

The ethanol exposure paradigm entailed administration of two intraperitoneal injections of ethanol (2.9g/kg) to C57Bl/6J dams on their seventh day of pregnancy. Fetuses were harvested on GD17 and immersion-fixed in a Bouins solution containing a contrast agent (Prohance). Ethanol-exposed fetuses with varying

degrees of affect (based on craniofacial and ocular morphology) along with stage-matched control fetuses were selected and imaged employing a 7.0 or 9.4 Tesla (T) small bore magnet. Linear and volumetric brain measures, the latter of which were acquired from 21 manually segmented regions of interest, were made and compared between groups. Routine histology was utilized to verify the MRI-based results.

SPECIFIC AIM 2: To apply DTI-based analyses for definition of fiber tract dysmorphology resulting from GD7 ethanol exposure.

For this, the ethanol treatment paradigm, specimen selection and preparation were the same as in Aim 1. GD17 fetuses were imaged at 9.4 T in either 6 or 12 directions. Resulting 39 or 43 micron images were processed, registered, and aligned to a template. DTI Studio was employed to reconstruct and compare selected forebrain fiber tracts including the anterior commissure, corpus callosum, and fornix/fimbria/hippocampal commissure.

SPECIFIC AIM 3: To define the affect of ethanol-induced ventromedian forebrain deficiency on medial ganglionic eminence (MGE)-derived cell populations.

Routine histology was employed to examine the dysmorphology of the forebrain resulting from a GD7 ethanol exposure. *In situ* hybridization was utilized to distinguish cells of the MGEs and POA (*Nkx2.1*) from those of the lateral ganglionic eminences (LGE) (*Fzd8*) in GD12.5 embryos exposed to either ethanol or saline on GD7. Antibodies for *Olig2*, a transcription factor necessary for the specification of oligodendrocytes, and GABA, an inhibitory neurotransmitter, were used to further examine ethanol's effect on the ventral forebrain. Somatostatin (Sst)-expressing

cells were examined in GD17 control and ethanol-exposed fetal brains to investigate later consequences resulting from early loss of the ventromedian forebrain. The results of this work were expected to extend the current knowledge and highlight possible implications of ethanol-induced median forebrain loss.

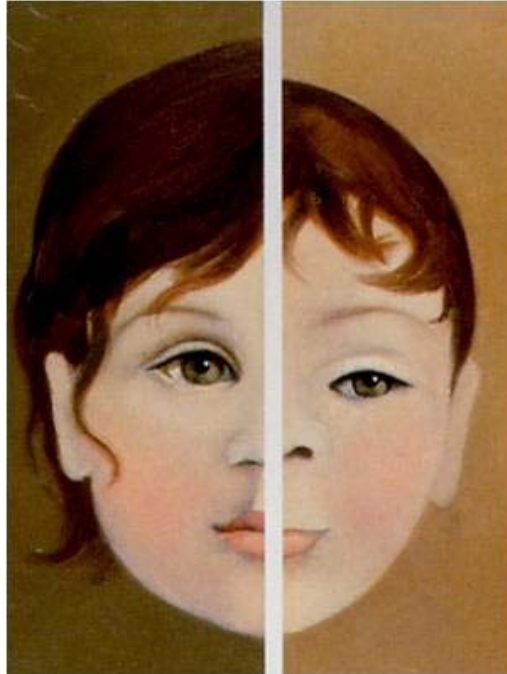


Figure 1.1: Illustration depicting the facial characteristics of a normal child (left) and a child with FAS (right). Individuals with FAS typically have small head circumference, short palpebral fissures, long thin upper lip, indistinct philtrum, and short, upturned nose.

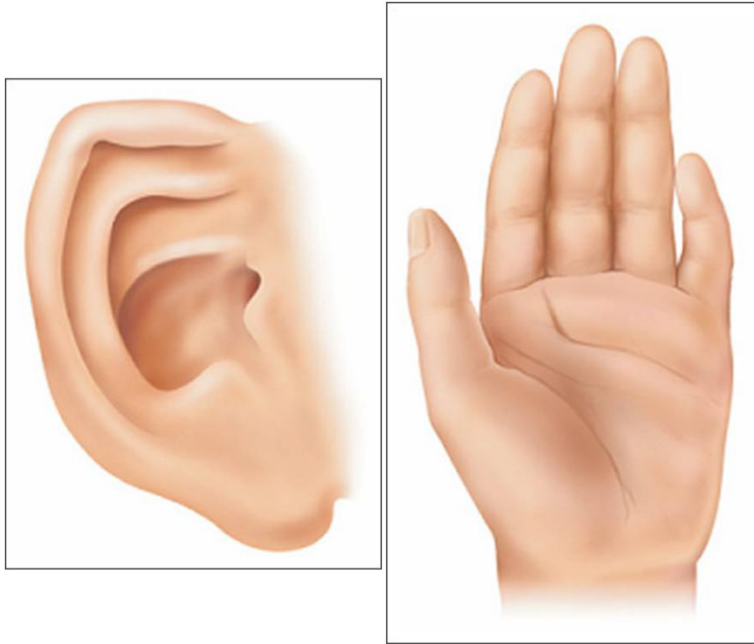


Figure 1.2: Illustrations of two minor anomalies associated with FASD. Railroad track ears (left) and a “hockey stick” palmar crease (right) are included in the diagnostic criteria for FASD. Adapted from Wattendorf and Muenke, 2005

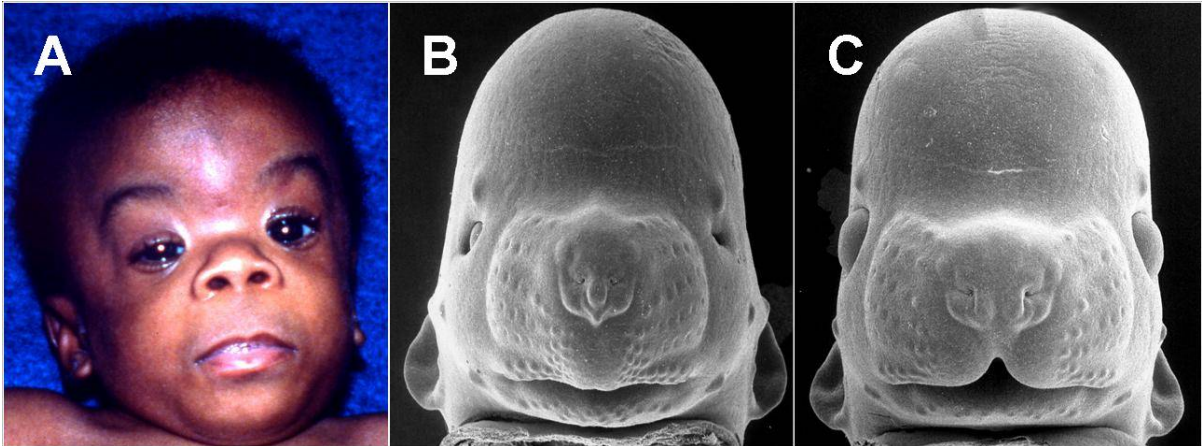


Figure 1.3: Images showing the similarities in facial dysmorphology between a child with FAS (A) and a fetal mouse that has been exposed to ethanol on GD7 (B) in comparison to a normal fetal mouse (C). Note the small head circumference, long upper lip, and small palpebral fissures in both A and B. Adapted from Sulik et al., 1981

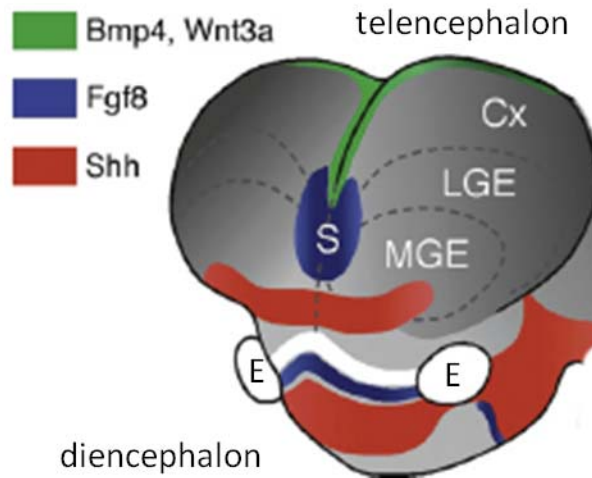


Figure 1.4: Illustrated are three of four distinct signaling centers necessary for telencephalic development, including a ventrally located center (red) that secretes Shh, a rostral patterning center (blue) which secretes Fgf8, and a caudodorsal center (green) that secretes Bmp4 and Wnt3a. E = eye, Cx = cortex, S = septum, LGE = lateral ganglionic eminence, MGE = medial ganglionic eminence. Adapted from Hoch et al., 2009

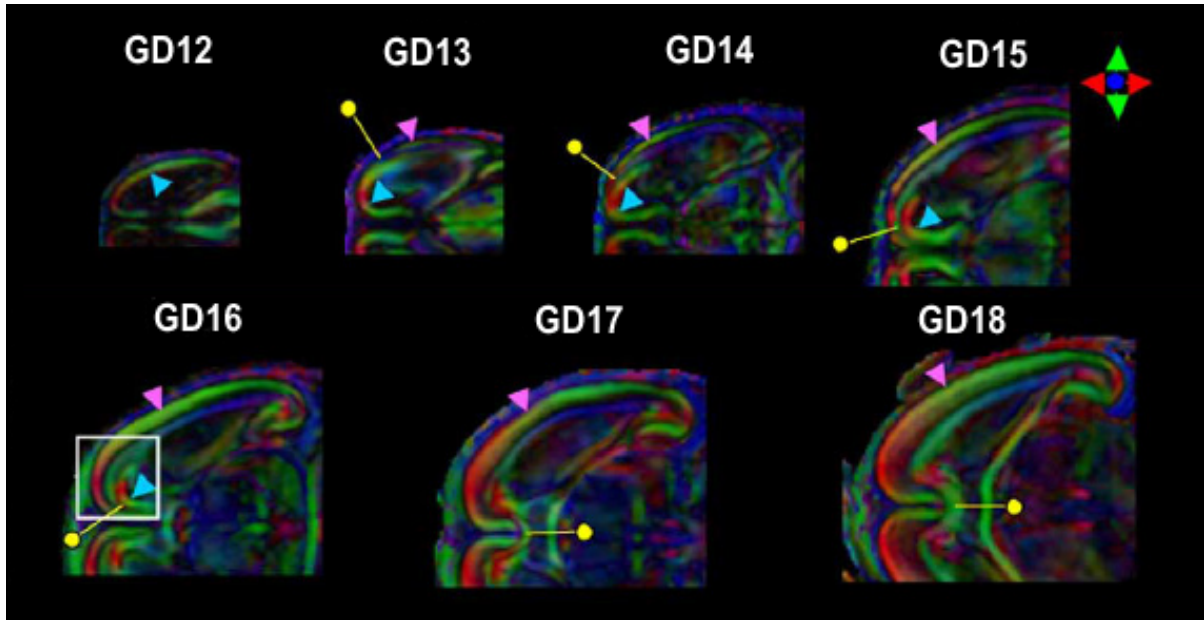


Figure 1.5: Diffusion tensor imaging in fetal mice allows for the visualization of fiber tract orientation in the brain, even prior to myelination. Color-coded fractional anisotropy maps of GD12 through GD18 mice illustrate that cellular orientation in the brain can be visualized as early as GD 12. Colors represent preferential directionality of the fibers in the brain (i.e. green = left to right; red = anterior/posterior; blue = dorsal/ventral). Adapted from Zhang et al., 2003

TABLE 1.1: Summary of Autopsy Studies

	Case #	Age	Malformations
Jones and Smith, 1973 Jones and Smith, 1975 Clarren, et al., 1978	1	5 days	Micrencephaly leptomeningeal heterotopias Lissencephaly thin cortex and enlarged ventricles CC and AC agenesis
Clarren, et al., 1978	2	10 weeks	Hydrocephaly enlarged ventricles lack pons and medulla leptomeningeal heterotopias
	3	29 gw stillborn	Hydrocephaly rudimentary brain stem and cerebellum
	4	3 days	cerebellar heterotopias
Peiffer, et al., 1979 Majewski, 1981	5	4.5 years	Microdysplasias spongiform in optic nerve and hypothalamus
	6	6 months	Hydrocephaly cerebellar heterotopias lumbar spina bifida occulta
	7	9 months	arhinencephaly with CC and AC agenesis Porencephaly Hydrocephaly Polymicrogyria Syringomyelia hypoplastic cerebellum and agenesis of vermis
	8	20 gw terminated	Hydrancephaly
	9	18 gw terminated	microdysplasias in dentate nuclei spongy state in thalamus heterotopias of choroid plexus in leptomeninges
	10	17 gw terminated	microdysplasias of brainstem spongy state in thalamus

	Case #	Age	Malformations
Majewski, 1981	11	17-20 gw	no malformations
Wisniewski et al., 1983	12	8 months	small cortex CC agenesis Cerebellar vermis hypoplasia leptomeningeal heterotopias
	13	4 months	Micrencephaly leptomeningeal heterotopias
	14	2 days	submeningeal heterotopias
	15	17 days	Micrencephaly leptomeningeal heterotopias
	16	4 days	Micrencephaly heterotopia in temporal lobe
Ronen and Andrews, 1991	17	8 days	alobar holoprosencephaly
Coulter et al., 1993	18	2.5 months	Arhinencephaly glial heterotopias in temporal lobes hypothalamic dysfunction absence of septum pellucidum fusion of cerebral hemispheres

gw = gestational week

TABLE 1.2: Summary of Diffusion Tensor Imaging Studies in Humans with FAS and FASD

	Subjects	Age	Corpus Callosum Findings	Other CNS Findings
Ma et al., 2005	9 FAS, 7 Cont	18-25 yo	↓FA in genu and splenium	
Wozniak et al., 2006	13 FASD, 13 Cont	10-13 yo	↑MD in isthmus	↓gray matter volume, CSF
Sowell et al., 2008	17 FASD, 19 Cont	7-15 yo	↓FA in lateral splenium	↓FA in posterior cingulate, deep white matter of temporal lobe, right internal capsule, brainstem
Lebel et al., 2008	24 FASD, 95 Cont	5-13 yo	↓FA in splenium, ↓MD genu	↓gray matter, white matter and total brain volume ↓FA cingulum, ILF, SLF, thalamus; ↑FA gp; ↑MD CS tract, IFOF, ILF, gp, putamen, thalamus
Fryer et al., 2009	15 FASD, 12 Cont	8-18 yo	↓FA in body	↓FA in bilateral portions of frontal, parietal, and occipital lobes
Li et al., 2009	28 FAS, 29 FASD, 25 Cont	19-27 yo	↓FA, MD in isthmus (FAS vs Cont)	
Wozniak et al., 2009	33 FASD, 19 Cont	10-17 yo	↓FA in posterior mid-body, isthmus, and splenium	

FA = fractional anisotropy

MD = mean diffusivity

CSF = cerebral spinal fluid

ILF = inferior longitudinal fasciculus

SLF = superior longitudinal fasciculus

IFOF = inferior fronto-occipital fasciculus

CS = corticospinal tract

gp = globus pallidus

REFERENCES

Andrews W, Liapi A, Plachez C, Camurri L, Zhang J, Mori S, Murakami F, Parnavelas JG, Sundaresan V, Richards LJ (2006) Robo1 regulates the development of major axon tracts and interneuron migration in the forebrain. *Development* 133(11):2243-52.

Aoto K, Shikata Y, Higashiyama D, Shiota K, Motoyama J (2008) Fetal ethanol exposure activates protein kinase A and impairs Shh expression in prechordal mesendoderm cells in the pathogenesis of holoprosencephaly. *Birth Defects Res A Clin Mol Teratol* 82(4):224-31.

Archibald SL, Fennema-Notestine C, Gamst A, Riley EP, Mattson SN, Jernigan TL (2001) Brain dysmorphology in individuals with severe prenatal alcohol exposure. *Dev Med Child Neurol* 43(3):148-54.

Astley SJ, Aylward EH, Olson HC, Kerns K, Brooks A, Coggins TE, Davies J, Dorn S, Gendler B, Jirikowic T, Kraegel P, Maravilla K, Richards T (2009) Magnetic resonance imaging outcomes from a comprehensive magnetic resonance study of children with fetal alcohol spectrum disorders. *Alcohol Clin Exp Res* 33(10):1671-89.

Autti-Ramo I, Autti T, Korkman M, Kettunen S, Salonen O, Valanne L (2002) MRI findings in children with school problems who had been exposed prenatally to alcohol. *Dev Med Child Neurol* 44(2):98-106.

Badea A, Ali-Sharief AA, Johnson GA (2007) Morphometric analysis of the C57BL/6J mouse brain. *Neuroimage* 37(3):683-93.

Bannigan J, Burke P (1982) Ethanol teratogenicity in mice: a light microscopic study. *Teratology* 26(3):247-54.

Bannigan J, Cottell D (1984) Ethanol teratogenicity in mice: an electron microscopic study. *Teratology* 30(2):281-90.

Bell SH, Stade B, Reynolds JN, Rasmussen C, Andrew G, Hwang PA, Carlen PL (2010) The Remarkably High Prevalence of Epilepsy and Seizure History in Fetal Alcohol Spectrum Disorders. *Alcohol Clin Exp Res* 34(6):1084-9

Bhatara VS, Lovrein F, Kirkeby J, Swayze V, 2nd, Unruh E, Johnson V (2002) Brain function in fetal alcohol syndrome assessed by single photon emission computed tomography. *S D J Med* 55(2):59-62.

Blader P, Strahle U (1998) Ethanol impairs migration of the prechordal plate in the zebrafish embryo. *Dev Biol* 201(2):185-201.

Bookstein FL, Connor PD, Huggins JE, Barr HM, Pimentel KD, Streissguth AP (2007) Many infants prenatally exposed to high levels of alcohol show one particular anomaly of the corpus callosum. *Alcohol Clin Exp Res* 31(5):868-79.

Bookstein FL, Sampson PD, Connor PD, Streissguth AP (2002) Midline corpus callosum is a neuroanatomical focus of fetal alcohol damage. *Anat Rec* 269(3):162-74.

Bookstein FL, Streissguth AP, Sampson PD, Connor PD, Barr HM (2002) Corpus callosum shape and neuropsychological deficits in adult males with heavy fetal alcohol exposure. *Neuroimage* 15(1):233-51.

Burd L, Deal E, Rios R, Adickes E, Wynne J, Klug MG (2007) Congenital heart defects and fetal alcohol spectrum disorders. *Congenit Heart Dis* 2(4):250-5.

Butt SJ, Cobos I, Golden J, Kessar N, Pachnis V, Anderson S (2007) Transcriptional regulation of cortical interneuron development. *J Neurosci* 27(44):11847-50.

Carmona RH (2005) Alcohol warning for pregnant women. *FDA Consumer* 39(4).

CDC (2009) Alcohol Use Among Pregnant and Nonpregnant Women of Childbearing Age - United States, 1991 - 2005. *MMWR* 28(19):529-532.

Chiang C, Litingtung Y, Lee E, Young KE, Corden JL, Westphal H, Beachy PA (1996) Cyclopia and defective axial patterning in mice lacking Sonic hedgehog gene function. *Nature* 383(6599):407-13.

Church MW, Abel EL (1998) Fetal alcohol syndrome. Hearing, speech, language, and vestibular disorders. *Obstet Gynecol Clin North Am* 25(1):85-97.

Church MW, Gerkin KP (1988) Hearing disorders in children with fetal alcohol syndrome: findings from case reports. *Pediatrics* 82(2):147-54.

- Church MW, Kaltenbach JA (1997) Hearing, speech, language, and vestibular disorders in the fetal alcohol syndrome: a literature review. *Alcohol Clin Exp Res* 21(3):495-512.
- Clarren SK, Alvord EC, Jr., Sumi SM, Streissguth AP, Smith DW (1978) Brain malformations related to prenatal exposure to ethanol. *J Pediatr* 92(1):64-7.
- Cohen-Kerem R, Bar-Oz B, Nulman I, Papaioannou VA, Koren G (2007) Hearing in children with fetal alcohol spectrum disorder (FASD). *Can J Clin Pharmacol* 14(3):e307-12.
- Coles CD (1994) Critical periods for prenatal alcohol exposure: evidence from animal and human studies. *Alcohol Health and Research World* 18(1):22.
- Coles CD, Platzman KA, Raskind-Hood CL, Brown RT, Falek A, Smith IE (1997) A comparison of children affected by prenatal alcohol exposure and attention deficit, hyperactivity disorder. *Alcohol Clin Exp Res* 21(1):150-61.
- Cook CS, Nowotny AZ, Sulik KK (1987) Fetal alcohol syndrome. Eye malformations in a mouse model. *Arch Ophthalmol* 105(11):1576-81.
- Coulter CL, Leech RW, Schaefer GB, Scheithauer BW, Brumback RA (1993) Midline cerebral dysgenesis, dysfunction of the hypothalamic-pituitary axis, and fetal alcohol effects. *Arch Neurol* 50(7):771-5.
- Cudd TA (2005) Animal model systems for the study of alcohol teratology. *Exp Biol Med (Maywood)* 230(6):389-93.
- DeMyer W, Zeman W, Palmer CG (1964) The Face Predicts the Brain: Diagnostic Significance of Median Facial Anomalies for Holoprosencephaly (Arhinencephaly). *Pediatrics* 34:256-63.
- Department of Health E, and Welfare, Public Health Service (1977) Fetal Alcohol Syndrome. *FDA Drug Bulletin* 7(4):18.
- Dorr AE, Lerch JP, Spring S, Kabani N, Henkelman RM (2008) High resolution three-dimensional brain atlas using an average magnetic resonance image of 40 adult C57Bl/6J mice. *Neuroimage* 42(1):60-9.

Dunty WC, Jr., Chen SY, Zucker RM, Dehart DB, Sulik KK (2001) Selective vulnerability of embryonic cell populations to ethanol-induced apoptosis: implications for alcohol-related birth defects and neurodevelopmental disorder. *Alcohol Clin Exp Res* 25(10):1523-35.

Froster UG, Baird PA (1992) Congenital defects of the limbs and alcohol exposure in pregnancy: data from a population based study. *Am J Med Genet* 44(6):782-5.

Fryer SL, McGee CL, Matt GE, Riley EP, Mattson SN (2007) Evaluation of psychopathological conditions in children with heavy prenatal alcohol exposure. *Pediatrics* 119(3):e733-41.

Fryer SL, Schweinsburg BC, Bjorkquist OA, Frank LR, Mattson SN, Spadoni AD, Riley EP (2009) Characterization of white matter microstructure in fetal alcohol spectrum disorders. *Alcohol Clin Exp Res* 33(3):514-21.

Goodlett CR, Horn KH (2001) Mechanisms of alcohol-induced damage to the developing nervous system. *Alcohol Res Health* 25(3):175-84.

Goodlett CR, Horn KH, Zhou FC (2005) Alcohol teratogenesis: mechanisms of damage and strategies for intervention. *Exp Biol Med (Maywood)* 230(6):394-406.

Granato A (2006) Altered organization of cortical interneurons in rats exposed to ethanol during neonatal life. *Brain Res* 1069(1):23-30.

Greenbaum RL, Stevens SA, Nash K, Koren G, Rovet J (2009) Social cognitive and emotion processing abilities of children with fetal alcohol spectrum disorders: a comparison with attention deficit hyperactivity disorder. *Alcohol Clin Exp Res* 33(10):1656-70.

Herman LE, Acosta MC, Chang PN (2008) Gender and attention deficits in children diagnosed with a Fetal Alcohol Spectrum Disorder. *Can J Clin Pharmacol* 15(3):e411-9.

Higashiyama D, Saitsu H, Komada M, Takigawa T, Ishibashi M, Shiota K (2007) Sequential developmental changes in holoprosencephalic mouse embryos exposed to ethanol during the gastrulation period. *Birth Defects Res A Clin Mol Teratol* 79(7):513-23.

Hofer R, Burd L (2009) Review of published studies of kidney, liver, and gastrointestinal birth defects in fetal alcohol spectrum disorders. *Birth Defects Res A Clin Mol Teratol* 85(3):179-83.

Hoyme HE, May PA, Kalberg WO, Kodituwakku P, Gossage JP, Trujillo PM, Buckley DG, Miller JH, Aragon AS, Khaole N, Viljoen DL, Jones KL, Robinson LK (2005) A practical clinical approach to diagnosis of fetal alcohol spectrum disorders: clarification of the 1996 institute of medicine criteria. *Pediatrics* 115(1):39-47.

Ioffe S, Chernick V (1990) Prediction of subsequent motor and mental retardation in newborn infants exposed to alcohol in utero by computerized EEG analysis. *Neuropediatrics* 21(1):11-7.

Iosub S, Fuchs M, Bingol N, Gromisch DS (1981) Fetal alcohol syndrome revisited. *Pediatrics* 68(4):475-9.

Jiang Y, Johnson GA (2010) Microscopic diffusion tensor imaging of the mouse brain. *Neuroimage* 50(2):465-71.

Johnson VP, Swayze VW, II, Sato Y, Andreasen NC (1996) Fetal alcohol syndrome: craniofacial and central nervous system manifestations. *Am J Med Genet* 61(4):329-39.

Jones KL, Hoyme HE, Robinson LK, del Campo M, Manning MA, Bakhireva LN, Prewitt LM, Chambers CD (2009) Developmental pathogenesis of short palpebral fissure length in children with fetal alcohol syndrome. *Birth Defects Res A Clin Mol Teratol* 85(8):695-9.

Jones KL, Smith DW (1973) Recognition of the fetal alcohol syndrome in early infancy. *Lancet* 302(7836):999-1001.

Jones KL, Smith DW (1975) The fetal alcohol syndrome. *Teratology* 12(1):1-10.

Jones KL, Smith DW, Ulleland CN, Streissguth P (1973) Pattern of malformation in offspring of chronic alcoholic mothers. *Lancet* 1(7815):1267-71.

Kessarlis N, Fogarty M, Iannarelli P, Grist M, Wegner M, Richardson WD (2006) Competing waves of oligodendrocytes in the forebrain and postnatal elimination of an embryonic lineage. *Nat Neurosci* 9(2):173-9.

Kodituwakku PW (2007) Defining the behavioral phenotype in children with fetal alcohol spectrum disorders: a review. *Neurosci Biobehav Rev* 31(2):192-201.

Koop C (1981) Warning on alcohol and pregnancy. *FDA Bulletin*.

Landgren M, Svensson L, Stromland K, Gronlund MA (2010) Prenatal Alcohol Exposure and Neurodevelopmental Disorders in Children Adopted From Eastern Europe. *Pediatrics*.

Lebel C, Rasmussen C, Wyper K, Walker L, Andrew G, Yager J, Beaulieu C (2008) Brain diffusion abnormalities in children with fetal alcohol spectrum disorder. *Alcohol Clin Exp Res* 32(10):1732-40.

Lemoine P, Harousseau H, Borteyru JP, Menuet JC (2003) Children of alcoholic parents--observed anomalies: discussion of 127 cases. *Ther Drug Monit* 25(2):132-6.

Li L, Coles CD, Lynch ME, Hu X (2009) Voxelwise and skeleton-based region of interest analysis of fetal alcohol syndrome and fetal alcohol spectrum disorders in young adults. *Hum Brain Mapp* 30(10):3265-74.

Li YX, Yang HT, Zdanowicz M, Sicklick JK, Qi Y, Camp TJ, Diehl AM (2007) Fetal alcohol exposure impairs Hedgehog cholesterol modification and signaling. *Lab Invest* 87(3):231-40.

Loucks EJ, Ahlgren SC (2009) Deciphering the role of Shh signaling in axial defects produced by ethanol exposure. *Birth Defects Res A Clin Mol Teratol* 85(6):556-67.

Loucks EJ, Schwend T, Ahlgren SC (2007) Molecular changes associated with teratogen-induced cyclopia. *Birth Defects Res A Clin Mol Teratol* 79(9):642-51.

Lupton C, Burd L, Harwood R (2004) Cost of fetal alcohol spectrum disorders. *Am J Med Genet C Semin Med Genet* 127C(1):42-50.

Lutke J, Antrobus T (2004) Fighting for a Future: FASD and "the system": adolescents, adults, and their families and the state of affairs, in *FASD Connections*, Surrey, British Columbia.

Ma X, Coles CD, Lynch ME, Laconte SM, Zurkiya O, Wang D, Hu X (2005) Evaluation of corpus callosum anisotropy in young adults with fetal alcohol syndrome according to diffusion tensor imaging. *Alcohol Clin Exp Res* 29(7):1214-22.

Majewski F (1981) Alcohol embryopathy: some facts and speculations about pathogenesis. *Neurobehav Toxicol Teratol* 3(2):129-44.

Marcucio RS, Cordero DR, Hu D, Helms JA (2005) Molecular interactions coordinating the development of the forebrain and face. *Dev Biol* 284(1):48-61.

Marcus JC (1987) Neurological findings in the fetal alcohol syndrome. *Neuropediatrics* 18(3):158-60.

Mattson SN, Riley EP (1998) A review of the neurobehavioral deficits in children with fetal alcohol syndrome or prenatal exposure to alcohol. *Alcohol Clin Exp Res* 22(2):279-94.

Mattson SN, Riley EP, Sowell ER, Jernigan TL, Sobel DF, Jones KL (1996) A decrease in the size of the basal ganglia in children with fetal alcohol syndrome. *Alcohol Clin Exp Res* 20(6):1088-93.

May PA, Brooke L, Gossage JP, Croxford J, Adnams C, Jones KL, Robinson L, Viljoen D (2000) Epidemiology of fetal alcohol syndrome in a South African community in the Western Cape Province. *Am J Public Health* 90(12):1905-12.

May PA, Gossage JP, Kalberg WO, Robinson LK, Buckley D, Manning M, Hoyme HE (2009) Prevalence and epidemiologic characteristics of FASD from various research methods with an emphasis on recent in-school studies. *Dev Disabil Res Rev* 15(3):176-92.

May PA, Gossage JP, Marais AS, Adnams CM, Hoyme HE, Jones KL, Robinson LK, Khaole NC, Snell C, Kalberg WO, Hendricks L, Brooke L, Stellavato C, Viljoen DL (2007) The epidemiology of fetal alcohol syndrome and partial FAS in a South African community. *Drug Alcohol Depend* 88(2-3):259-71.

Moore DB, Quintero MA, Ruygrok AC, Walker DW, Heaton MB (1998) Prenatal ethanol exposure reduces parvalbumin-immunoreactive GABAergic neuronal number in the adult rat cingulate cortex. *Neurosci Lett* 249(1):25-8.

Moore DB, Ruygrok AC, Walker DW, Heaton MB (1997) Effects of prenatal ethanol exposure on parvalbumin-expressing GABAergic neurons in the adult rat medial septum. *Alcohol Clin Exp Res* 21(5):849-56.

Mori S, van Zijl PC (2002) Fiber tracking: principles and strategies - a technical review. *NMR Biomed* 15(7-8):468-80.

Mori S, Zhang J (2006) Principles of diffusion tensor imaging and its applications to basic neuroscience research. *Neuron* 51(5):527-39.

Murray-Lyon IM (1985) Alcohol and foetal damage. *Alcohol Alcohol* 20(2):185-8.

Nery S, Wichterle H, Fishell G (2001) Sonic hedgehog contributes to oligodendrocyte specification in the mammalian forebrain. *Development* 128(4):527-40.

Norman AL, Crocker N, Mattson SN, Riley EP (2009) Neuroimaging and fetal alcohol spectrum disorders. *Dev Disabil Res Rev* 15(3):209-17.

O'Connor MJ, Paley B (2009) Psychiatric conditions associated with prenatal alcohol exposure. *Dev Disabil Res Rev* 15(3):225-34.

O'Hare ED, Kan E, Yoshii J, Mattson SN, Riley EP, Thompson PM, Toga AW, Sowell ER (2005) Mapping cerebellar vermal morphology and cognitive correlates in prenatal alcohol exposure. *Neuroreport* 16(12):1285-90.

Olegard R, Sabel KG, Aronsson M, Sandin B, Johansson PR, Carlsson C, Kyllerman M, Iversen K, Hrbek A (1979) Effects on the child of alcohol abuse during pregnancy. Retrospective and prospective studies. *Acta Paediatr Scand Suppl* 275:112-21.

O'Malley KD, Barr H (1998) Fetal alcohol syndrome and seizure disorder. *Can J Psychiatry* 43(10):1051.

Ozer E, Sarioglu S, Gure A (2000) Effects of prenatal ethanol exposure on neuronal migration, neuronogenesis and brain myelination in the mice brain. *Clin Neuropathol* 19(1):21-5.

Peiffer J, Majewski F, Fischbach H, Bierich JR, Volk B (1979) Alcohol embryo- and fetopathy. Neuropathology of 3 children and 3 fetuses. *J Neurol Sci* 41(2):125-37.

Petiet A, Hedlund L, Johnson GA (2007) Staining methods for magnetic resonance microscopy of the rat fetus. *J Magn Reson Imaging* 25(6):1192-8.

Rasmussen C (2005) Executive functioning and working memory in fetal alcohol spectrum disorder. *Alcohol Clin Exp Res* 29(8):1359-67.

Ren T, Zhang J, Plachez C, Mori S, Richards LJ (2007) Diffusion tensor magnetic resonance imaging and tract-tracing analysis of Probst bundle structure in Netrin1- and DCC-deficient mice. *J Neurosci* 27(39):10345-9.

Riley EP, McGee CL, Sowell ER (2004) Teratogenic effects of alcohol: a decade of brain imaging. *Am J Med Genet C Semin Med Genet* 127(1):35-41.

Ronen GM, Andrews WL (1991) Holoprosencephaly as a possible embryonic alcohol effect. *Am J Med Genet* 40(2):151-4.

Sandor S (1968) The influence of ethyl alcohol on the developing chick embryo, II. *Rev Roum Embryol Cytol Ser Embryol* 5(167).

Schambra UB, Lauder JM, Petrusz P, Sulik KK (1990) Development of neurotransmitter systems in the mouse embryo following acute ethanol exposure: a histological and immunocytochemical study. *Int J Dev Neurosci* 8(5):507-22.

Sowell ER, Jernigan TL, Mattson SN, Riley EP, Sobel DF, Jones KL (1996) Abnormal development of the cerebellar vermis in children prenatally exposed to alcohol: size reduction in lobules I-V. *Alcohol Clin Exp Res* 20(1):31-4.

Sowell ER, Johnson A, Kan E, Lu LH, Van Horn JD, Toga AW, O'Connor MJ, Bookheimer SY (2008) Mapping white matter integrity and neurobehavioral correlates in children with fetal alcohol spectrum disorders. *J Neurosci* 28(6):1313-9.

Sowell ER, Mattson SN, Kan E, Thompson PM, Riley EP, Toga AW (2008) Abnormal cortical thickness and brain-behavior correlation patterns in individuals with heavy prenatal alcohol exposure. *Cereb Cortex* 18(1):136-44.

Sowell ER, Thompson PM, Mattson SN, Tessner KD, Jernigan TL, Riley EP, Toga AW (2002) Regional brain shape abnormalities persist into adolescence after heavy prenatal alcohol exposure. *Cereb Cortex* 12(8):856-65.

Spadoni AD, McGee CL, Fryer SL, Riley EP (2007) Neuroimaging and fetal alcohol spectrum disorders. *Neurosci Biobehav Rev* 31(2):239-45.

Spiegel PG, Pekman WM, Rich BH, Versteeg CN, Nelson V, Dudnikov M (1979) The orthopedic aspects of the fetal alcohol syndrome. *Clin Orthop Relat Res* (139):58-63.

Stockard CR (1910) The influence of alcohol and other anaesthetics on embryonic development. *Am J Anat* 10:369-392.

Storm EE, Garel S, Borello U, Hebert JM, Martinez S, McConnell SK, Martin GR, Rubenstein JL (2006) Dose-dependent functions of Fgf8 in regulating telencephalic patterning centers. *Development* 133(9):1831-44.

Streissguth AP, O'Malley K (2000) Neuropsychiatric implications and long-term consequences of fetal alcohol spectrum disorders. *Semin Clin Neuropsychiatry* 5(3):177-90.

Stromland K (1987) Ocular involvement in the fetal alcohol syndrome. *Surv Ophthalmol* 31(4):277-84.

Stromland K (2004) Visual impairment and ocular abnormalities in children with fetal alcohol syndrome. *Addict Biol* 9(2):153-7; discussion 159-60.

Stromland K, Pinazo-Duran MD (2002) Ophthalmic involvement in the fetal alcohol syndrome: clinical and animal model studies. *Alcohol Alcohol* 37(1):2-8.

Sulik KK (2005) Genesis of alcohol-induced craniofacial dysmorphism. *Exp Biol Med (Maywood)* 230(6):366-75.

Sulik KK, Johnston MC, Webb MA (1981) Fetal alcohol syndrome: embryogenesis in a mouse model. *Science* 214(4523):936-8.

Sulik KK, Lauder JM, Dehart DB (1984) Brain Malformations in Prenatal Mice Following Acute Maternal Ethanol Administration. *Int J Dev Neurosci* 2(3):203-214.

Sun Y, Strandberg-Larsen K, Vestergaard M, Christensen J, Nybo Andersen AM, Gronbaek M, Olsen J (2009) Binge drinking during pregnancy and risk of seizures in childhood: a study based on the Danish National Birth Cohort. *Am J Epidemiol* 169(3):313-22.

Swayze VW, 2nd, Johnson VP, Hanson JW, Piven J, Sato Y, Giedd JN, Mosnik D, Andreasen NC (1997) Magnetic resonance imaging of brain anomalies in fetal alcohol syndrome. *Pediatrics* 99(2):232-40.

Vaurio L, Riley EP, Mattson SN (2008) Differences in executive functioning in children with heavy prenatal alcohol exposure or attention-deficit/hyperactivity disorder. *J Int Neuropsychol Soc* 14(1):119-29.

Warren KR, Hewitt BG (2009) Fetal alcohol spectrum disorders: when science, medicine, public policy, and laws collide. *Dev Disabil Res Rev* 15(3):170-5.

Wattendorf DJ, Muenke M (2005) Fetal alcohol spectrum disorders. *Am Fam Physician* 72(2):279-82, 285.

Webster WS, Walsh DA, Lipson AH, McEwen SE (1980) Teratogenesis after acute alcohol exposure in inbred and outbred mice. *Neurobehav Teratol* 2:227-234.

West JR (1993) Use of pup in a cup model to study brain development. *J Nutr* 123(2 Suppl):382-5.

Wichterle H, Turnbull DH, Nery S, Fishell G, Alvarez-Buylla A (2001) In utero fate mapping reveals distinct migratory pathways and fates of neurons born in the mammalian basal forebrain. *Development* 128(19):3759-71.

Wisniewski K, Dambaska M, Sher JH, Qazi Q (1983) A clinical neuropathological study of the fetal alcohol syndrome. *Neuropediatrics* 14(4):197-201.

Wozniak JR, Mueller BA, Chang PN, Muetzel RL, Caros L, Lim KO (2006) Diffusion tensor imaging in children with fetal alcohol spectrum disorders. *Alcohol Clin Exp Res* 30(10):1799-806.

Wozniak JR, Muetzel RL, Mueller BA, McGee CL, Freerks MA, Ward EE, Nelson ML, Chang PN, Lim KO (2009) Microstructural corpus callosum anomalies in children with prenatal alcohol exposure: an extension of previous diffusion tensor imaging findings. *Alcohol Clin Exp Res* 33(10):1825-35.

Xu Q, de la Cruz E, Anderson SA (2003) Cortical interneuron fate determination: diverse sources for distinct subtypes? *Cereb Cortex* 13(6):670-6.

Yamada Y, Nagase T, Nagase M, Koshima I (2005) Gene expression changes of sonic hedgehog signaling cascade in a mouse embryonic model of fetal alcohol syndrome. *J Craniofac Surg* 16(6):1055-61; discussion 1062-3.

Zhang J, Miller MI, Plachez C, Richards LJ, Yarowsky P, van Zijl P, Mori S (2005) Mapping postnatal mouse brain development with diffusion tensor microimaging. *Neuroimage* 26(4):1042-51.

Zhang J, Richards LJ, Yarowsky P, Huang H, van Zijl PC, Mori S (2003) Three-dimensional anatomical characterization of the developing mouse brain by diffusion tensor microimaging. *Neuroimage* 20(3):1639-48.

CHAPTER II

MAGNETIC RESONANCE MICROSCOPY DEFINES ETHANOL-INDUCED BRAIN ABNORMALITIES IN PRENATAL MICE: EFFECTS OF ACUTE INSULT ON GESTATIONAL DAY 7

Alcohol Clin Exp Res (2010) 34:98-111.

Abbreviated title: Ethanol-induced brain defects in prenatal mice

Elizabeth A. Godin, B.S., Shonagh K. O’Leary-Moore, Ph.D., Amber A. Khan, B.S.,
Scott E. Parnell, Ph.D., Jacob J. Ament, B.S., Deborah B. Dehart, Brice W. Johnson,
G. Allan Johnson, Ph.D., Martin A. Styner, Ph.D., and Kathleen K. Sulik, Ph.D.

Bowles Center for Alcohol Studies (EAG, SOM, AAK, SEP, JJA, DBD, KKS) and
Department of Psychiatry (MAS), University of North Carolina, Chapel Hill, NC
27599

Center for *In Vivo* Microscopy, Duke University, Durham NC (BWJ, GAJ)

Corresponding author: E.A. Godin, Bowles Center for Alcohol Studies,
University of North Carolina at Chapel Hill, CB# 7178, Chapel Hill, NC 27599-7178;
Fax: (919) 966-5679; Phone: (919) 966-3208. Email: eamyers@med.unc.edu

Number of figures/tables: 9

Number of pages: 45

Key words: magnetic resonance microscopy, fetal alcohol spectrum disorder, holoprosencephaly, cortical dysplasia, leptomeningeal heterotopia

Sources of Support: This work was supported by NIH/NIAAA grants AA007573, AA11605, AA017124; NCI/NCRR grants P41 05959 and U24 CA092656; and the UNC Neurodevelopmental Disorders Research Center HD 03110; and was done in conjunction with the Collaborative Initiative on Fetal Alcohol Spectrum Disorders (CIFASD). Additional information about CIFASD can be found at www.cifasd.org.

ABSTRACT

Background: This magnetic resonance microscopy (MRM)-based report is the 2nd in a series designed to illustrate the spectrum of craniofacial and central nervous system (CNS) dysmorphia resulting from single- and multiple-day maternal ethanol treatment. The study described in this report examined the consequences of ethanol exposure on gestational day (GD) 7 in mice, a time in development when gastrulation and neural plate development begins; corresponding to the mid- to late 3rd week post-fertilization in humans. Acute GD 7 ethanol exposure in mice has previously been shown to result in CNS defects consistent with holoprosencephaly (HPE) and craniofacial anomalies typical of those in Fetal Alcohol Syndrome (FAS). MRM has facilitated further definition of the range of GD 7 ethanol-induced defects.

Methods: C57Bl/6J female mice were intraperitoneally administered vehicle or 2 injections of 2.9 g/kg ethanol on day 7 of pregnancy. Stage-matched control and ethanol-exposed GD 17 fetuses selected for imaging were immersion fixed in a Bouins/Prohance solution. MRM was conducted at either 7.0 Tesla (T) or 9.4 T. Resulting 29 μm isotropic spatial resolution scans were segmented and reconstructed to provide 3D images. Linear and volumetric brain measures, as well as morphological features, were compared for control and ethanol-exposed fetuses. Following MRM, selected specimens were processed for routine histology and light microscopic examination.

Results: GD 7 ethanol exposure resulted in a spectrum of median facial and forebrain deficiencies, as expected. This range of abnormalities falls within the HPE spectrum; a spectrum for which facial dysmorphology is consistent with and typically

is predictive of that of the forebrain. In addition, other defects including median facial cleft, cleft palate, micrognathia, pituitary agenesis and third ventricular dilatation were identified. MRM analyses also revealed cerebral cortical dysplasia/heterotopias resulting from this acute, early insult and facilitated a subsequent focused histological investigation of these defects.

Conclusions: Individual MRM scans and 3D reconstructions of fetal mouse brains have facilitated demonstration of a broad range of GD 7 ethanol-induced morphological abnormality. These results, including the discovery of cerebral cortical heterotopias, elucidate the teratogenic potential of ethanol insult during the 3rd week of human prenatal development.

INTRODUCTION

This is one in a series of reports (published as well as in preparation) describing developmental stage-dependent structural brain abnormalities in a mouse model of Fetal Alcohol Spectrum Disorder [FASD, the umbrella term encompassing the spectrum of prenatal ethanol exposure-induced defects, including Fetal Alcohol Syndrome (FAS)]. As for the 1st publication in this series (Parnell et al., 2009a), magnetic resonance microscopy (MRM, magnetic resonance imaging at microscopic levels) has been employed, readily allowing comprehensive structural analyses. The ethanol exposure time that is the focus of the current report is gestational day (GD) 7, a time in mouse development when gastrulation begins and neural plate formation is initiated.

That ethanol insult limited to early gastrulation stages results in a range of defects involving both the face and brain was first reported by Stockard in 1910 (Stockard, 1910). As in Stockard's investigation, which employed fish as the model system, more recently Blader and Strahl (Blader and Strahle, 1998) have reported that the ethanol-induced brain defects fall within a spectrum termed holoprosencephaly (HPE) and that in fish, there is a very narrow (3 hour) window of sensitivity during the beginning of gastrulation that is associated with this endpoint. Using a mouse model to examine ethanol teratogenesis, Sulik and Johnston (1982) also illustrated HPE resulting from acute ethanol insult during early gastrulation stages; i.e. during GD 7 in mice.

The HPE spectrum includes phenotypes ranging from the most severe, alobar form, which is characterized by a single forebrain holosphere in which there is broad communication of the lateral ventricles with each other and the third ventricle, accompanied by agenesis of the corpus callosum and olfactory bulbs; to semilobar, an intermediate form characterized by cerebral hemispheres that are most deficient rostrally and are only entirely separate through approximately their caudal half; to a least severe, lobar, form in which there is a distinct interhemispheric fissure that may or may not be interrupted anteriorly and in which the corpus callosum may be absent, hypoplastic, or normal and the olfactory bulbs may or may not be present (DeMyer and Zeman, 1963). Accompanying holoprosencephalic brains are varying degrees of ocular and midfacial dysmorphology (DeMyer et al., 1964; reviewed by Muenke and Cohen, 2000; Sulik and Johnston, 1982). Examining this spectrum of defects in humans, DeMyer and colleagues (1964) noted that frequently (though not

always) the face "predicts" the brain; i.e. that the severity of craniofacial and brain dysmorphology are often directly correlated. HPE is not rare. This spectrum of abnormalities is now recognized as the most commonly occurring type of birth defect, being present in as many as 1/250 human conceptuses (Matsunaga and Shiota, 1977). However, most of those affected are lost prenatally, resulting in only a 1/10,000 live birth incidence (Croen et al., 1996; reviewed in Leoncini et al., 2008; Rasmussen et al., 1996).

Study of the genesis of ethanol-induced facial and brain defects in mice (Sulik et al., 1981; Sulik and Johnston, 1982; Webster et al., 1983) led to the hypothesis that those individuals who present with the characteristic facies of full blown FAS will have brain dysmorphology falling within the HPE spectrum (Sulik and Johnston, 1982). Indeed, histological analyses of fetal mice that had FAS-like facies and had been acutely exposed to ethanol on their 7th GD have illustrated the presence of forebrain deficiencies including hypoplasia or aplasia of the corpus callosum and septal nuclei (Schambra et al., 1990; Sulik et al., 1984). Importantly, in a non-human primate model, ethanol exposure early in pregnancy, specifically on GD 19 and 20, corresponding to the early gastrulation stage, also yielded HPE (Astley et al., 1999; Siebert et al., 1991). Features of HPE have been reported in human FAS. Indeed, in the first autopsy case-report, Jones and Smith (1975) described corpus callosum agenesis. Other autopsies revealed olfactory bulb deficiencies and pituitary abnormalities (Majewski, 1981; Peiffer et al., 1979; Shiota et al., 2007).

The advent of clinical magnetic resonance imaging (MRI) has made structural analyses of the brains in live patients with FASD possible. Initial MRI studies

illustrated deficiencies in the cerebellar vermis, basal ganglia and corpus callosum in individuals with FAS (Archibald et al., 2001; Mattson et al., 1996; Riley et al., 1995). More recently, the corpus callosum has been the focus of detailed FASD imaging studies. Variability in its shape, size, and microstructure among individuals exposed to alcohol prenatally has been described (Bookstein et al., 2002; Fryer et al., 2009; Lebel et al., 2008; Ma et al., 2005; Sowell et al., 2001; Spadoni et al., 2007; Wozniak et al., 2006). While its protracted development is expected to make the corpus callosum vulnerable to teratogenic insult during many prenatal stages, when found in combination with the typical facies of FAS, it is most likely that the dysmorphology is, indeed, the result of ethanol exposure during gastrulation.

Employing a mouse FASD model, the current investigation is directed toward further defining and documenting the types and range of brain and facial defects that prenatal ethanol exposure can cause and, thus, to informing improved pre- and postnatal FASD clinical recognition and diagnosis. The acute GD7 ethanol exposure time used for this study corresponds to the mid- to late 3rd week post-fertilization in humans and is the earliest of a number of times during embryogenesis from which MRM-based data is currently being collected and compared. Since most human pregnancies remain unrecognized at this early stage, for education-based FASD prevention efforts clear illustration of the vulnerability of the brain to ethanol-mediated damage at this time is particularly important.

METHODS

Animal maintenance

C57Bl/6J mice, purchased from The Jackson Laboratory (Bar Harbor, ME), were housed in a temperature and humidity-controlled AAALAC-approved environment. They were maintained on an *ad libitum* diet of standard laboratory chow and water. For mating, 2 females were placed with 1 male for 2 hours early in the light portion of a 12/12 hours light/dark cycle. The beginning of the breeding period in which a copulation plug was detected was defined as gestational day (GD) 0, 0 hours (h).

Maternal treatment paradigm

On day 7 of pregnancy, mice in the experimental group were administered two intraperitoneal doses of 25% (v/v) ethanol in lactated Ringer's solution at a dosage of 2.9 g/kg maternal body weight. The injections were given 4 h apart, with the first administered at GD 7, 0 h. Control animals were injected with an equivalent volume of lactated Ringer's solution according to the above treatment paradigm. To determine the peak blood ethanol concentration (BEC), a separate group of mice were administered ethanol, utilizing the previously described paradigm (Webster et al., 1983). Thirty minutes after the second injection, 35 μ l of tail blood were obtained from each dam and analyzed using an Analox Alcohol Analyser (Model AM1, Analox Instruments USA Inc, Lunenburg, MA). All animal treatment protocols were approved by the University of North Carolina at Chapel Hill, Institutional Animal Care and Use Committee (IACUC).

Fetal specimen selection and preparation

At the beginning of their 17th day of pregnancy, dams were anesthetized via CO₂ inhalation, followed by cervical dislocation. Following laparotomy, the uteri were removed and the fetuses were immediately dissected free of decidua in ice-cold phosphate buffered-saline (PBS). The GD 17 fetuses were examined for the presence of gross abnormalities. For the control group, 7 fetuses (from 4 litters) were selected for MRM scanning based on normal morphology and developmental stage-matching with the ethanol-exposed fetuses. Staging was based on degree of limb, skin, and hair follicle development (Theiler, 1989). For the ethanol group, 19 fetuses (from 8 litters) were selected for MRM scanning. As for the Parnell et al. (2009a) MRM study, selection of the ethanol-exposed fetuses was based on the presence of grossly-observable dysmorphology; an approach that is not unlike selection of children with known physical features of FAS for subsequent CNS analyses. For this investigation, all of the ethanol-exposed fetuses selected had ocular defects and among these, some had apparently normal facies, while others had obvious facial dysmorphia. To account for the entire spectrum of effect, fetuses with apparently normal, subtly affected and severely-affected facies were included. Following photography to document ocular and facial abnormalities, the fetuses were immersion fixed for 9 hours in a 20:1 solution of Bouin's fixative (Sigma-Aldrich, St. Louis, MO) containing Prohance[®] (Bracco Diagnostics Inc., Princeton, NJ) (Petiet et al., 2007). The specimens were then immersed in a storage solution of 200:1 PBS:Prohance in which they were held until imaged.

Magnetic resonance microscopy

MRM images were acquired at either 7.0Tesla (T) or 9.4T using a GE EXCITE console modified for MRM. To provide full resolution at the Nyquist frequency, a 3D rf refocused spin echo sequence (7.0T: TR = 100 ms, TE = 6.2 ms; 9.4T: TR = 75 ms, TE = 5.2 ms) with asymmetric partial Fourier sampling was used (Johnson et al., 2007). For all MRM scans acquired, the matrix size was 1024 X 512 X 512 and the FOV was 30 X 15 X 15 mm³, which yielded an isotropic spatial resolution of 29 µm. The total scan time was approximately 4 hrs for each specimen. During scanning, specimens were immersed in fomblin, a perfluorocarbon used to limit dehydration and reduce susceptibility artifacts.

Linear measurements

In order to ensure accurate orientation, each MRM scan was aligned in the horizontal, coronal and sagittal plane using ImageJ (Version 1.38x, NIH; <http://rsbweb.nih.gov/ij/>). This program was also used to obtain linear measurements. For each fetus, the following were determined: crown rump length (CRL), mid-sagittal brain length, frontothalamic distance (FTD) (excluding olfactory bulbs), bulbothalamic distance (BTD) (including olfactory bulbs), brain width (biparietal distance), third ventricle width and transverse cerebellar distance (Fig. 2.1a). All measurements were taken at the level of the anterior commissure, except the transverse cerebellar distance which was measured at its widest level and are reported in Table 2.1.

Volume measurements

Total body (including the head) and brain volume, as well as regional brain volumes for each fetus were computed using ITK-Snap, a software program originally developed at the University of North Carolina, Chapel Hill (Yushkevich et al., 2006; www.itksnap.org). Total body volume was ascertained using the automatic segmentation feature of this program. Total brain volume was determined by adding the volumes of 17 brain regions that were each manually segmented, allowing subsequent 3D reconstruction of each region (Fig. 2.1c). The manually segmented regions were the right and left cortex, right and left olfactory bulb, right and left striatum, right and left hippocampus, septal region, diencephalon, mesencephalon, pons/medulla, cerebellum, pituitary gland, lateral ventricles, third ventricle, mesencephalic (cerebral aqueduct) and fourth ventricle. In addition, for the eyes, each globe and lens was segmented. Segmentation entailed tracing each MRM slice (Fig. 2.1b) via a computer mouse or a pen tablet. Tracings were performed by only one individual for each selected region, for every fetus examined. Intra-rater reliability was assessed following a blind repeated segmentation of each of the selected structures in one control and one non-HPE ethanol-exposed fetus. Regional boundaries were determined based on existing fetal mouse atlases (Kaufman, 1992; Schambra et al., 1992; Schambra, 2008). Coronal, sagittal, and horizontal planes of section were used to ensure anatomical accuracy. In addition to volumetric analyses, 3D reconstructions allowed visual assessment of shape changes in ethanol-exposed versus control brains.

Routine histology

Following imaging, each fetus was held in a 70% ethanol solution to clear the residual Bouin's fixative and to prepare the specimens for subsequent routine histological analyses. The latter was performed on selected specimens to confirm and extend MRM findings. Prior to processing, the fixed fetuses were photographed to further document facial dysmorphology. Fetal heads were removed and processed routinely for paraffin embedding using a tissue processor. Sections were cut at 10 μm , mounted on glass slides, stained with aqueous hemotoxylin and eosin (H & E), cover-slipped and viewed with a light microscope.

Statistical analyses

Group comparisons were made between stage-matched control fetuses [control] (n=7), ethanol-exposed fetuses with two distinctly separate cerebral hemispheres [non-HPE] (n=14), and ethanol-exposed fetuses with features of semilobar or alobar HPE [HPE] (n=5). Group differences among regional brain volumes, ocular measurements and linear measurements were assessed using Multivariate Analyses of Variance (MANOVAs). Crown-rump length, whole brain volume and whole body volume (including head) were analyzed using one-way ANOVAs. When applicable, post-hoc analyses were performed using Student-Newman-Keuls (SNK). An alpha value of 0.05 was maintained for all analyses.

To assess the reliability of manual segmentation of regional brain and ocular volumes, intra-rater reliability was analyzed using coefficients of variation (CV). The

average CV was 3.8% (range: 0.5% - 11.8%), thus, demonstrating high reliability for manual brain segmentation.

RESULTS

General features of the study population

With a research goal of accomplishing detailed MRM-based analyses of a broad spectrum of structural brain abnormalities resulting from acute GD 7 ethanol exposure, this work employed a previously-published ethanol exposure paradigm known to yield sufficient numbers of viable fetuses having a range of effect.

Consistent with previous reports, the ethanol treatment yielded peak maternal BECs (30 minutes after the second dose) averaging 440 mg/dl (range: 400 to 466 mg/dl).

The 19 ethanol-exposed GD 17 fetuses that underwent detailed MRM analyses were selected based, in part, on the presence of defects involving one or both eyes, and in part, based on facial morphology. The eye defects ranged from apparently slight microphthalmia, to iridial coloboma, to apparent anophthalmia. The facial appearance in the ethanol-exposed fetuses ranged from apparently normal to severely dysmorphic. The facial characteristics, along with MRM-based brain findings, provided for distinction and comparison between subgroups of ethanol-exposed fetuses, as described below.

Holoprosencephaly

Illustrated in Fig. 2.2 are light micrographs of the faces and the respective brain and ventricle reconstructions of a control GD 17 fetus and of 5 ethanol-

exposed fetuses that presented with varying degrees of facial dysmorphia. The facial abnormalities are consistent with those in the HPE spectrum. In the affected animals, notable features of the upper midface include a long upper lip and closely spaced nostrils. Additionally, the lower jaw is slightly to severely reduced in size (micrognathic), appearing narrow from a frontal view.

Frontal views of the reconstructed brains of the affected fetuses (Fig. 2.2 h-l) clearly show a spectrum of rostral union of the cerebral hemispheres along with olfactory bulb reduction to agenesis. These rostro-medial telencephalic deficiencies are consistent with HPE and grade in severity from semilobar (h) to lobar (l). From a dorsal view (Fig. 2.2 m-r), the varying degrees of forebrain reduction/dysmorphology are readily appreciated in the ethanol-exposed fetuses as compared to the control. Also apparent in 2 of the affected fetuses are asymmetries involving the olfactory bulbs. The animal shown in Fig. 2.2 h & n is more severely affected on its right, while that in i & o is more severely affected on its left. As expected, and notable in regional reconstructions and in individual MRM scans as shown in Fig. 2.3, are reductions in the septal region with union of the striatum across the midline. Also illustrated in Figs. 2.2 and 2.3 are the overall size reduction in the brains and the remarkably normal morphology of the brain segments caudal to the forebrain of the ethanol-exposed versus the control fetuses.

Overall, the morphology of the ventricles reflects the median forebrain deficiency in the holoprosencephalic fetuses. Most notably, rather than being continuous with the third ventricle via the narrow passages at the foramina of Monro, the lateral ventricles are broadly united with each other in the rostral midline.

Accompanying the very dysmorphic lateral ventricles are third ventricles that appear relatively normal. From a dorsal view, while the ventricular space of the mesencephalon and the fourth ventricle appear normally-shaped, the aqueductal isthmus was found to be abnormally narrow in the 2 fetuses whose faces are shown in Fig. 2.2 e & f. The isthmus appears normal in the 3 less severely-affected fetuses in this group.

Of interest, MRM scans of all of the ethanol-exposed specimens shown in Fig. 2.2 revealed an aberrant tissue mass located between the base of the rostral forebrain and the nasal septum (Fig. 2.4 b). In some, the mass was continuous with the forebrain and in others it was not. Typically, a single mass was found to occupy a median position. However, in the animal shown in Fig. 2.2 c, there were two similar, more laterally-positioned masses. Subsequent routine histological coronal sections illustrate that the tissue is continuous, through the cribriform plate, with the nasal epithelium (Fig. 2.4 c & d; from the fetus shown in Fig. 2.2 d). The control counterpart is represented by olfactory nerves that extend from the nasal epithelium to the olfactory bulbs.

Cerebral cortical dysplasia/heterotopia

MRM and subsequent routine histology revealed cerebral cortical dysplasia/heterotopias in ethanol-exposed fetuses whose brains were not overtly holoprosencephalic (i.e. they did not present with semilobar or alobar HPE) (Fig. 2.5). These cortical defects were observed in animals having faces that were apparently normal, presented with a long upper lip and severe micrognathia,

foreshortened, or cleft in the midline (Fig. 2.5 b-e, respectively). In all of these animals, the cerebral hemispheres were completely separate and slightly widely spaced as evidenced by the ability to visualize deep brain structures (septal region and diencephalon) from a frontal view. Additionally, both olfactory bulbs, though in some cases small and widely-spaced, were present. Initially observed in the reconstructed brain images (Fig. 2.5 g and j) of the fetuses shown in Fig. 2.5 b and e, the cortical defects present as focal protrusions on the otherwise smooth cerebral surfaces. Histological sections of these two fetuses (Fig. 2.5 l, q and o, t), along with sections from the other ethanol-exposed fetuses pictured in Fig. 2.5 (m, r and n, s) reveal relatively large and numerous, to minute and isolated irregularities in the cerebral cortex. Typically, the dysplastic/heterotopic cortical tissue was adherent to the associated leptomeninges. In the fetus with the median facial cleft (Fig. 2.5 e) the dysplastic cortex is localized to the medial aspect of both cerebral hemispheres, with cortical layers I through IV being involved. Subsequent to the MRM-based discovery of ethanol-induced cerebral cortical dysplasia/heterotopia, careful examination of histological sections of the brains of the fetuses with semilobar and alobar HPE revealed a small heterotopia in the frontal cortex of the most severely affected animal; the fetus shown in Fig. 2.2 f. No heterotopias were found in any of the control animals or any of the other ethanol-exposed fetuses.

Other dysmorphologies

A profile view (Fig. 2.6 b) of the fetus that is also shown in Fig. 2.5 d illustrates that in addition to being anophthalmic, its snout is abnormally short. MRM

revealed that the nasal cavities of this fetus are very small; the turbinates are absent; and along its entire length, the nasal septum is short in the dorso-ventral direction (Fig. 2.6 d). Additionally, 3D reconstruction of the ventricular spaces illustrated dysmorphology involving the third ventricle presenting as excessive width and extension ventrally beyond the normal boundaries (Fig. 2.6 f). Both a frontal (Fig. 2.5 i) and a ventral view (Fig. 2.6 h), of the reconstructed brain of this fetus show that the olfactory bulbs are small and widely-spaced. Remarkable is the complete absence of the pituitary gland. Subsequent to MRM, examination of H & E-stained coronal histological sections of this animal revealed that the corpus callosum, while identifiable in control fetuses, was not apparent (Fig. 2.6 j). With the concurrent small olfactory bulbs and pituitary absence/deficiency, the dysmorphology of this brain appears to be consistent with lobar HPE.

Severe micrognathia was noted in 3 of the ethanol-exposed fetuses; those pictured in Fig. 2.2 b and f and in Fig. 2.5 c. MRM scans revealed severe micro- or aglossia in all of these animals and clefting of the secondary palate in the Fig. 2.2 b and 2.5 c fetuses. These features in the latter specimen are shown in Fig. 2.7, as is the reconstructed mesencephalic and fourth ventricle. Marked narrowing of the aqueductal isthmus is apparent in this fetus and is also present in 2 others (fetuses in 2.2 e and f; described above).

Linear and volume assessments

Due to the marked morphological differences in the brains of ethanol-exposed animals that presented with overt HPE versus the remainder that had two entirely

separate cerebral hemispheres (non-HPE), measurements made for these two groups of ethanol-exposed fetuses were separately compared to controls and to each other. In spite of developmental stage-matching, there were significant differences in CRL [$F(2,22) = 5.44, p < 0.05$], total body volume [$F(2,23) = 4.065, p < 0.05$], and total brain volume [$F(2,23) = 4.51, p < 0.05$] between the three groups examined. Post hoc tests revealed that HPE subjects were significantly smaller than controls in terms of CRL (~9% reduction) but neither group differed from non-HPE ethanol-exposed subjects [control: 17.27 (± 0.23) mm (mean \pm SEM)], non-HPE: 16.38 (± 0.23) mm; HPE: 15.74 (± 0.31) mm]. In addition, the HPE group also had a significantly smaller total brain volume (~20% reduction) compared to controls but non-HPE ethanol-exposed animals did not differ from either HPE subjects or controls [control: 52.86 (± 2.58) mm³, non-HPE: 47.75 (± 1.52) mm³, HPE: 42.38 (± 2.50) mm³]. Finally, whole body volume measures for the non-HPE and HPE ethanol-exposed fetuses were decreased by 15% and 16%, respectively, as compared to controls, but SNK post-hoc tests only approached significance ($p = 0.06$) [control: 679.15 (± 25.95) mm³, non-HPE: 537.09 (± 22.17) mm³, HPE: 576.81 (± 45.93) mm³].

Linear brain measurements are shown in Table 2.1. A MANOVA indicated significant group differences in linear brain measurements [$F(14,34) = 4.197, p < 0.05$] with significant between group effects for brain length, bulbothalamic distance (BTD), frontothalamic distance (FTD), brain width and third ventricle width (all p 's < 0.05). Post hoc tests indicated that the HPE group had significantly smaller brain length, BTD and third ventricle widths compared to non-HPE subjects and controls

($p < 0.05$). FTD in HPE subjects differed only compared to controls (p 's < 0.05). Brain widths were significantly smaller in HPE subjects compared to the non-HPE subjects and both ethanol-exposed groups had smaller brain widths compared to controls ($p < 0.05$). There were no differences between groups in transverse cerebellar distance ($p > 0.05$).

In spite of the overall decrease in brain volume in the HPE subjects, analyses of the regional volume measurements indicated that the overall brain volume reductions is largely the result of insult to the rostral brain structures with a remarkable sparing of more caudal regions. As expected, MANOVAs illustrated significant group differences in regional brain volumes [$F(34,16) = 3.68, p < 0.05$] and ocular volumes [$F(8,42) = 5.65, p < 0.05$] between HPE, non-HPE and control groups (Fig. 2.8). Significant between group effects were seen for the following brain measurements: left and right cortex, left and right olfactory bulbs, left and right striatum, septal region, diencephalon, lateral and third ventricles (all p 's < 0.05). Consistent with visual inspection of the 3D reconstruction data, post hoc tests illustrated that HPE subjects had significantly smaller cortices, olfactory bulbs, striata and septal regions (which were non-existent in all HPE subjects) compared to controls and non-HPE ethanol-exposed subjects (p 's < 0.05). In addition, lateral ventricles were significantly larger in HPE subjects than non-HPE and controls while the third ventricle was significantly larger in the non-HPE ethanol exposed group compared to HPE and control groups (p 's < 0.05). Reductions in volumes of both the left and right globe and lens of the eyes were apparent in both ethanol exposed groups (HPE and non-HPE) compared to controls (p 's < 0.05). Remarkably, despite

significant dysmorphology accompanied with volumetric reductions in ethanol-exposed animals, no group differences were evident in the hippocampus, pituitary or hindbrain regions (mesencephalon, pons/medulla, cerebellum, mesencephalic and fourth ventricle) (p 's > 0.05) illustrating the regional specificity of defects following exposure at this time.

In Figure 2.8, volumetric data is expressed to illustrate the broad range of insult. Specifically, mean control values from 7 fetuses are indicated by a black dot and the bars indicate the 95% confidence interval for the control mean. Individual data points for each ethanol-exposed subject are plotted for each region in order to convey the range of volumetric data ascertained. Values for the 5 ethanol-exposed animals with overt HPE are expressed as X's; and for all of the other ethanol-exposed animals (non-HPE, $n=14$) a grey circle is employed.

DISCUSSION

This report describes MRM-based discovery and documentation of structural abnormalities resulting from early gastrulation stage ethanol insult in mice. In addition to providing a 3D perspective of ethanol-induced HPE, with its range of median forebrain deficiencies, other CNS and craniofacial abnormalities were also identified. As discussed below, these findings extend our understanding of the spectrum of ethanol-induced birth defects and of the critical periods for their induction.

It is clear that, as with other teratogens, both dosage and timing (developmental stage) dictate the consequences of prenatal ethanol exposure.

Regarding the former, with the objective of identifying even the most severe of ethanol's dysmorphogenic effects, a previously-reported maternal ethanol dose high enough to yield abnormalities without substantially increasing resorption rates was selected. This dosage was somewhat higher (yielding peak maternal BECs of approx. 380 vs. $440 \pm$ mg/dl) than utilized for an MRM-based GD 8 ethanol exposure study by Parnell et al., 2009a (the 1st publication in a series of which this is a part). On GD 8, exposure to the higher ethanol dose typically yields severe heart defects and substantial embryo lethality. As shown in previous studies that employed the same treatment paradigm as for the current investigation, peaking within 30 minutes of the last dose, the maternal BEC remains above 100 mg/dl for a total of approximately 9 hours and reaches 0 within a few more hours (Kotch et al., 1992; Webster et al., 1983). Thus, exposure to ethanol totals less than 12 hours, including a period for which the concentration is expected to be less than teratogenic. An intraperitoneal (ip) route of maternal ethanol administration was employed for both the GD 8 and the GD 7 studies. As compared to maternal dietary ethanol intake, ip administration provides interlitter outcomes that are more consistent. It is recognized that with the ip treatment, embryos may experience a higher peak ethanol concentration than occurs in the maternal blood (Clarke et al., 1985). However, it is notable that abnormalities consistent with those described herein also occur following a dietary exposure paradigm that yields maternal BECs comparable to those in the current study (Webster et al., 1983).

Regarding timing, it is clear that ethanol is teratogenic at virtually every post-implantation stage. Remarkable is that ethanol exposure occurring within a relatively

narrow window in 2 hr. time-mated inbred animals can yield not only a range of defects within a single spectrum, but also defects that appear to be virtual opposites. This is exemplified by the occurrence of median forebrain and facial deficiencies typical of semilobar and alobar HPE (a narrow snout and forebrain) in some fetuses and median split face accompanied by widely spaced cerebral hemispheres and olfactory bulbs in others; all following acute insult on GD 7. Undoubtedly, the fact that in C57Bl/6J mice there is significant intra-litter variation, representing as much as 12 hours difference in developmental staging among littermates, plays an important role in this variability (Parnell et al., 2009b). HPE has been the most commonly-reported dysmorphology following GD 7 ethanol exposure in mice (Higashiyama et al., 2007, Myers et al., 2008; Schambra et al., 1990; Sulik and Johnston, 1982; Sulik et al., 1984; Webster et al., 1983), and was also observed in the current study population. GD 8 has previously been identified as the time in mouse development when median facial clefts and excessive brain width are induced by ethanol (Kotch and Sulik 1992; Parnell et al., 2009a; Webster et al., 1983), while HPE is not a typical result of GD 8 ethanol treatment. Thus, it appears that among the dysmorphic fetuses described herein, those without HPE were more developmentally advanced at the time of ethanol insult than those with HPE. While insult on each individual day of mouse development is expected to yield a specific pattern of dysmorphology, it is also expected that, due to inter- and intra- litter variability in developmental stages, there will be some overlap.

With respect to HPE, via individual scans and 3D reconstructions, MRM has made it possible to readily show the range and severity of median forebrain

deficiency that occurs in the absence of overt hindbrain dysmorphology. In those cases with semilobar and alobar forms of HPE, the severity of brain effect is consistent with that of the upper midface as evidenced, to a large extent, by the proximity of the nostrils. In all of the mouse fetuses whose nostrils are too closely positioned the median portion of the upper lip is too long (from nose to oral cavity). Notable was one fetus in which an effect on nostril positioning was subtle (if present), and that still had an unmistakably long upper lip. In this fetus the cerebrum had a complete interhemispheric fissure. It is expected that this phenotype is consistent with lobar HPE. Ongoing studies employing diffusion tensor imaging (DTI) and 3D facial analyses based on MRM reconstructions (Hammond et al., 2005) are designed to enable identification of subtle changes in facial morphology and to better define the brain fiber tracts in fetuses such as this.

The genesis of the HPE-related facial dysmorphology has previously been described as resulting from ethanol-induced loss of medial nasal prominence tissue (i.e. the progenitor of both the nasal tip and the intermaxillary segment, the latter of which becomes the philtrum of the lip and the primary palate) and subsequent overconvergence of the maxillary prominences, yielding the excessively long upper lip (Sulik and Johnston, 1983). DeMyer (1975) recognized hypoplasia of the intermaxillary segment as being pathognomonic of brain malformation; the greater the deficiency of intermaxillary tissue, the greater the likelihood of a malformed brain. In the HPE spectrum, the human face presents with an absent or indistinct philtrum accompanied by a thin (vermillion) upper lip border; a phenotype that

undoubtedly results from medial nasal prominence deficiency. These facial features are also characteristic of FAS.

In addition to ethanol exposure, other environmental agents (e.g. retinoic acid, cyclopamine, cholesterol biosynthesis inhibitors) and mutations in a number of different genes including sonic hedgehog (SHH), ZIC2, SIX3, and TGIF β can cause HPE and the associated facial abnormalities (Cohen, 2006; Monuki, 2007; reviewed by Muenke and Cohen, 2000). Of particular note is interference with sonic hedgehog signaling (Shh-s) as a basis for these defects. Shh-s is a primary event in neural plate induction. Studies by Ahlgren and her co-workers in chicken (2002) and fish embryos (Loucks and Ahlgren, 2009) and also by Li et al. in the latter species (2007), have illustrated that ethanol interferes with this signaling. Strongly supporting this as a key mechanism underlying ethanol-induced defects is that enhancing Shh-s can diminish the teratogenesis (Loucks and Ahlgren, 2009). The prevalence of alcohol (ethanol) use and abuse and the multiple genes involved in the genesis of HPE contribute to the likelihood that via gene-environment interactions ethanol significantly factors into the high (1/250) incidence of HPE among human conceptuses (Matsunaga and Shiota, 1974).

Along with the forebrain and upper midfacial defects that characterize HPE, other defects that are associated with this spectrum were noted in this study. Micrognathia commonly occurs both in human HPE and in FASD (Ades and Sillence, 1992; Blaas et al., 2002; Cohen, 1989; Jones and Smith, 1975; Lemoine et al., 1968; Majewski, 1981; Pauli et al., 1981; 1983), and was clearly evident in a third of the 19 ethanol-exposed mouse fetuses. 3D facial analyses are expected to also

identify more subtle mandibular deficiencies resulting from ethanol exposure on GD 7. Severe micrognathia was accompanied by narrowing of the cerebral aqueduct in some specimens. The latter abnormality is commonly and causally associated with hydrocephalus, a condition that co-occurs with human HPE (Barr and Cohen, 1999; Dickinson et al., 2006) and that was previously noted to result from GD 7 ethanol treatment in mice (Sulik and Johnston, 1983). Micro/aglossia and cleft palate, as seen in this study, also co-occur with HPE (Cohen, 1989; Pauli et al., 1981; 1983; Porteous et al., 1993). In part, due to the relatively long period of genesis of the secondary palate, clefting of this structure (a recognized feature of FASD) is expected to also result from ethanol insult at later developmental stages. Of these (“other”) defects, for the fetuses in this study, certainly aqueductal stenosis, and probably cleft palate would not have been readily recognized without MRM.

Also with MRM, tissue that appears to correspond to misplaced olfactory nerves was found in the overtly holoprosencephalic animals. Normally, the olfactory nerves should project from the nasal epithelium, through the cribriform plate, to synapse in the olfactory bulbs. In the absence of olfactory bulbs, these nerves still extend upward, but lacking a target, form an intracranial mass that remains unattached to the brain. Recent analyses of holoprosencephalic mouse fetuses whose defects resulted from Shh-inhibition via *in utero* exposure to a potent cycloamine analog revealed comparable olfactory nerve masses (R.J. Lipinski, personal communication).

Two of the ethanol-exposed fetuses in this study have small, widely spaced olfactory bulbs. Of these, one is anophthalmic and has an enlarged third ventricle

(indicating hypothalamic deficiency), no pituitary, apparent absence of the corpus callosum, and markedly small/stenotic nasal cavities. The other has a median facial cleft. The collection of defects in these mice is consistent with the following recognized human syndromes/associations: 1) median cleft face syndrome; a condition for which agenesis of the corpus callosum and anomalies of the pituitary gland have been reported (DeMyer, 1967), 2) septo-optic dysplasia; a syndrome characterized by absence of the septum pellucidum, pituitary hormone deficiency, and optic nerve hypoplasia; features of which a clinical report by Coulter et al. (1993) attributed to prenatal ethanol exposure, and 3) CHARGE association which includes nasal cavity narrowing, growth and mental retardation, along with a variety of structural brain abnormalities including absence/hypoplasia of the olfactory bulbs and tracts, dysgenesis /hypoplasia of the frontal lobes and optic nerves, and agenesis of the corpus callosum and septum pellucidum. CHARGE association was highlighted in the Parnell et al. (2009a) report as resulting from GD 8 ethanol exposure in mice. Indeed, although each has its own key features, there is significant overlap between HPE and these 3 clinical conditions (Bomelburg et al., 1987; de Toni et al., 1985; Fitz, 1994; Lin et al., 1990; Polizzi et al., 2005). This is also true for the dysmorphology resulting from GD 7 versus GD 8 ethanol exposure in mice.

The MRM-based discovery of cerebral cortical dysplasia/heterotopias resulting from acute GD 7 ethanol exposure is novel and is expected to be of significant clinical importance. Nearly 35 years ago the first autopsy report by Jones and Smith (1975) of a newborn with FAS described a large heterotopia

encompassing the left cerebral hemisphere. Under this mass of tissue, the cortex was thin and disorganized and the lateral ventricles were enlarged. In more recent studies of rodent FASD models, one of which was conducted utilizing cultured GD17 fetal rat cortical slices (Mooney et al., 2004) and one which employed maternal dietary ethanol exposure on days 10 through 21 in the rat (Komatsu et al., 2001; Sakata-Haga et al., 2004), cortical heterotopias have also been found. The cortical defects noted in the current study ranged from extremely small and isolated, to involving the medial aspect of both cerebral hemispheres. In most cases, the morphology is consistent with leptomeningeal heterotopia, though a more accurate descriptor for the most extensive defects is probably cortical dysplasia. Cortical heterotopias are generally considered as resulting from neuronal migration errors (Verotti et al., 2009). It is remarkable that they can result from an acute teratogenic insult occurring as early as the time of neural plate induction.

The presence of cortical heterotopias is highly correlated with seizure activity. Indeed, Verotti et al. (2009) state that “neuronal migration disorders are considered to be one of the most significant causes of neurological and developmental disabilities and epileptic seizures in childhood”. Among individuals with FAS the prevalence of epilepsy is higher than in the general population (1%), with estimates varying from 3-21% (Dorris, 1989; Ioffe and Chernick, 1990; Jones et al., 1973; Majewski, 1981; Marcus, 1987; Murray-Lyon, 1985; Olegard et al., 1979; O’Malley and Barr, 1998; Streissguth et al., 1978). Work directed toward identifying pathologic changes that may underlie alcohol-induced seizure threshold reduction has shown an association with hippocampal abnormalities induced during the

human 3rd trimester equivalent (Bonthius et al., 2001 a,b). These studies employed a rat FASD model in which both behavioral and electrographic seizure thresholds were examined. Similar testing of postnatal animals following acute ethanol exposure during early gastrulation is needed.

Linear and volume measurements made in this study from MRM scans and 3D reconstructions are consistent with the visually-assessed dysmorphology. Notable in the ethanol-exposed animals are reduced frontothalamic and brain width measures and lateral ventricular enlargement; features that can be readily assessed in human fetal ultrasounds. Work by Kfir et al. (2009) showing that both 2nd and 3rd trimester ultrasound can detect frontothalamic reductions in the fetuses of moderate to heavy alcohol users, is consistent with the mouse data (Sulik et al., 2009). Together, the human and experimental studies illustrate the diagnostic potential of early (prenatal) forebrain measures.

In conclusion, this work contributes significantly to defining the CNS dysmorphology that results from ethanol insult at times corresponding to the middle through the end of the 3rd week of human development. Individual MRM scans and 3D reconstructions of fetal mouse brains have facilitated this effort, allowing documentation and discovery of ethanol-induced CNS defects and appreciation of their relationship to co-occurring facial abnormalities. These results promise to aid in clinical recognition, diagnosis, and prevention of FASD.

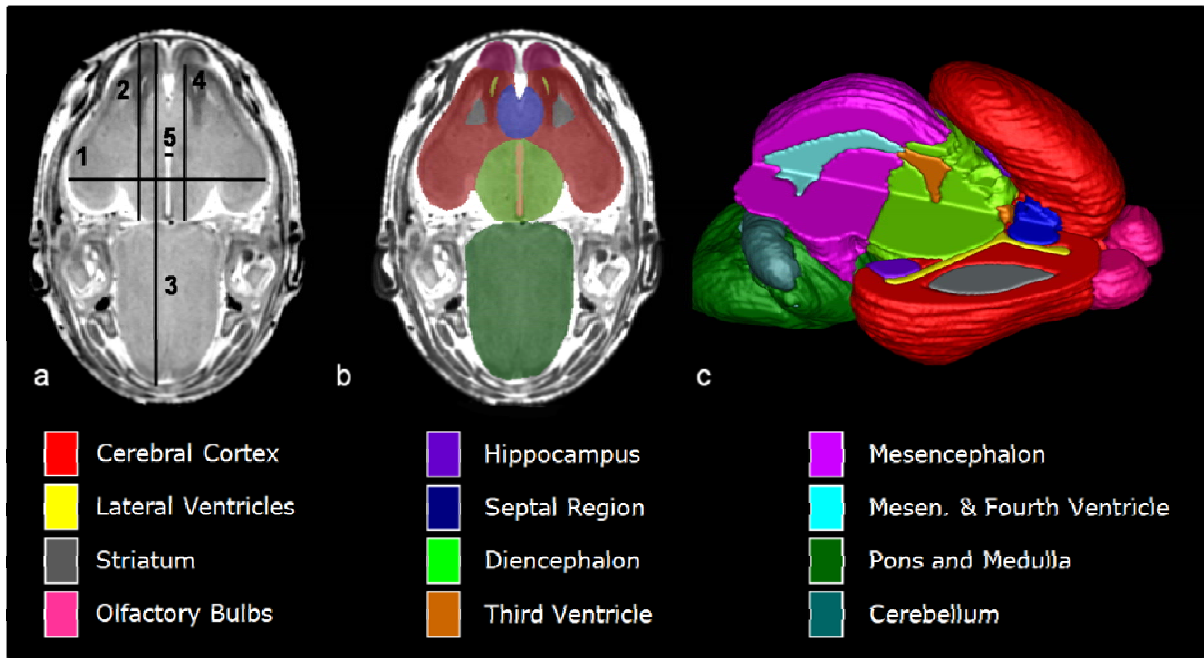


Figure 2.1: MRM scans of GD 17 mouse fetuses allow for linear measurements, regional segmentation, and 3D reconstruction. Illustrated in (a) is a horizontal scan with lines depicting sites of linear measurement as follows: brain width (biparietal distance), line 1; bulbothalamic distance, line 2; mid-sagittal brain length, line 3; frontothalamic distance, line 4; third ventricle width, line 5. [Cerebellar width (transverse cerebellar distance, not included) was measured at its greatest dimension.] Manual segmentation, as depicted by the color-coded regions in (b) allowed for subsequent 3D reconstruction (c) and analyses of selected brain regions. In (c), the upper right quadrant of the brain has been removed to allow for visualization of the interior structures. Color-codes for the segmented brain regions shown are at the bottom of the Figure. Other regions that were also examined for each of the animals in this study, but are not shown in this illustration, are the pituitary and the ocular globe and lens of each eye. (modified from Figs. 1 & 2, Parnell et al., 2009a)

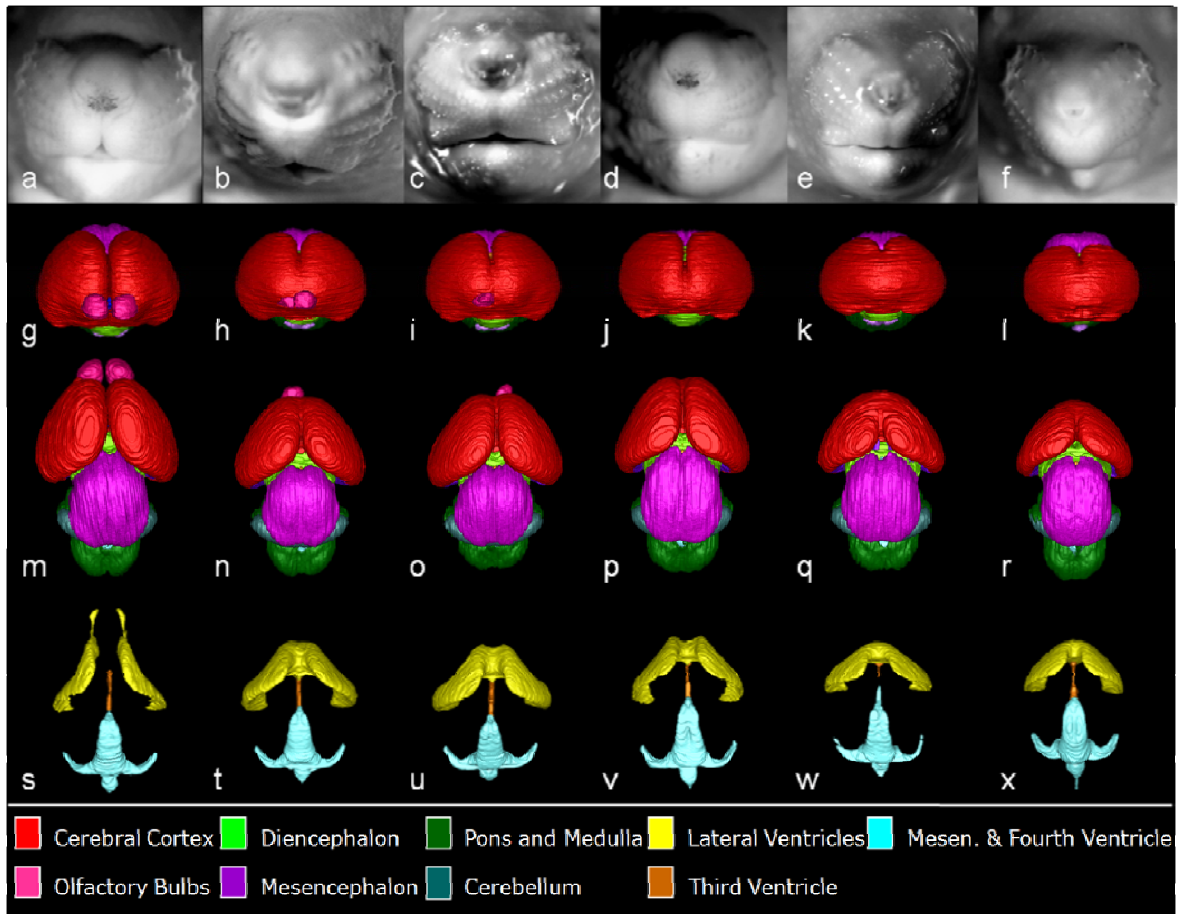


Figure 2.2: Shown are the face and reconstructed brain of a control GD 17 fetal mouse along with the faces and brains of ethanol-exposed fetuses having semilobar and alobar holoprosencephaly (HPE). As compared to the control face (a), those fetuses with HPE (b-f) have varying degrees of midfacial abnormality; each presenting with a long (from nose to mouth) upper lip, a small nose with closely-set nostrils, and micrognathia (narrow, pointed chin), the latter of which is severe in the specimens shown in (b) and (f). Segmented MRM scans of control (g, m, s) and ethanol-exposed fetuses (h-l, n-r, t-x) were reconstructed to yield whole brain (frontal view, g-l; dorsal view, m-r) and ventricular system (s-x) images. Notable forebrain abnormalities include varying degrees of olfactory bulb deficiency and rostral union of the cerebral hemispheres, accompanied by dysmorphic lateral ventricles. From a dorsal view, the mid- and hindbrain and their ventricles appear relatively normal in all of the affected fetuses. Color codes for the segmented brain regions are shown at the bottom of the Figure.

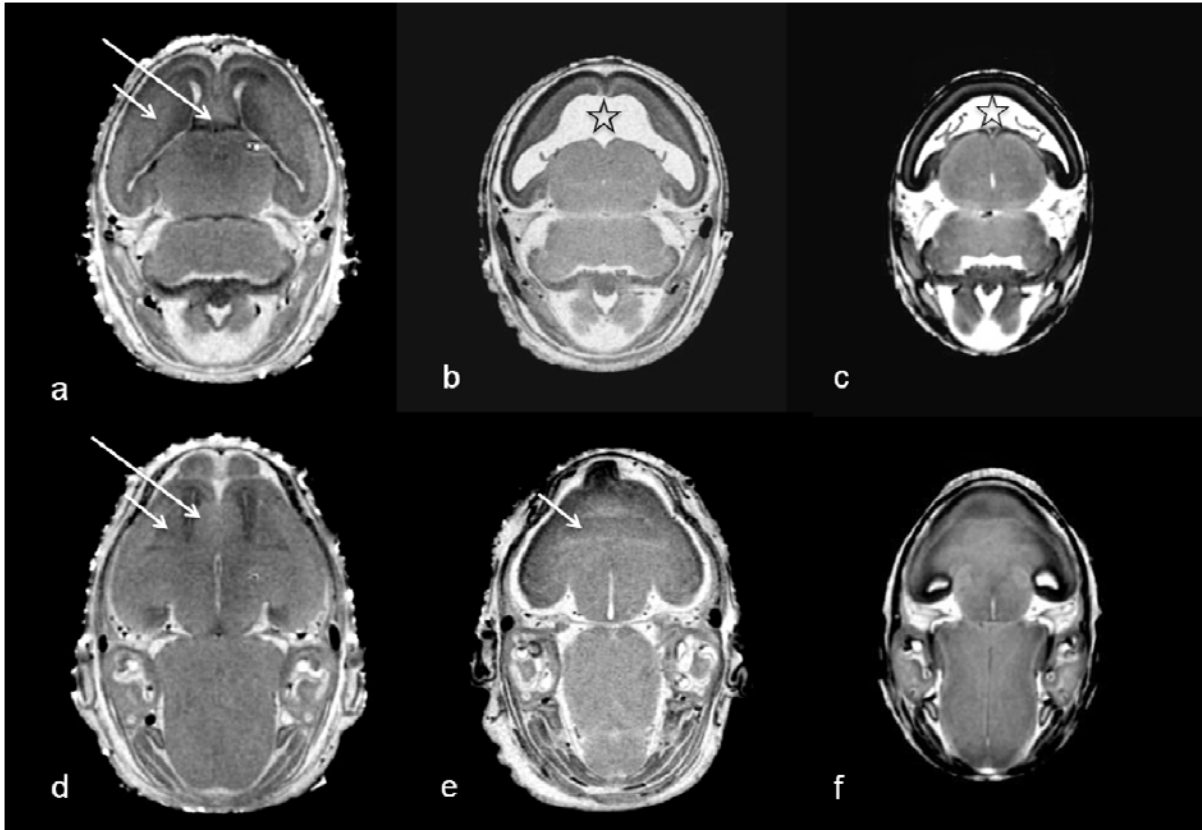


Figure 2.3: Horizontal MRM scans at two different levels through a control (a, d) and two affected fetuses (b, e with semilobar HPE & c, f with alobar HPE; shown in Fig. 2.2 b, f, respectively) illustrate rostro-median tissue loss. The septal region (long arrow), which is apparent in the rostral midline of the control, is absent in the affected fetuses. In the more mildly affected fetus (b, e), the striatal tissue (short arrow) can be defined and, in the absence of the septal region, is united across the midline. In the more severely affected fetus (c, f), MRM does not allow clear identification of the striatal boundaries. Notable in both affected fetuses is the vastly enlarged and rostro-medially fused lateral ventricles (☆).

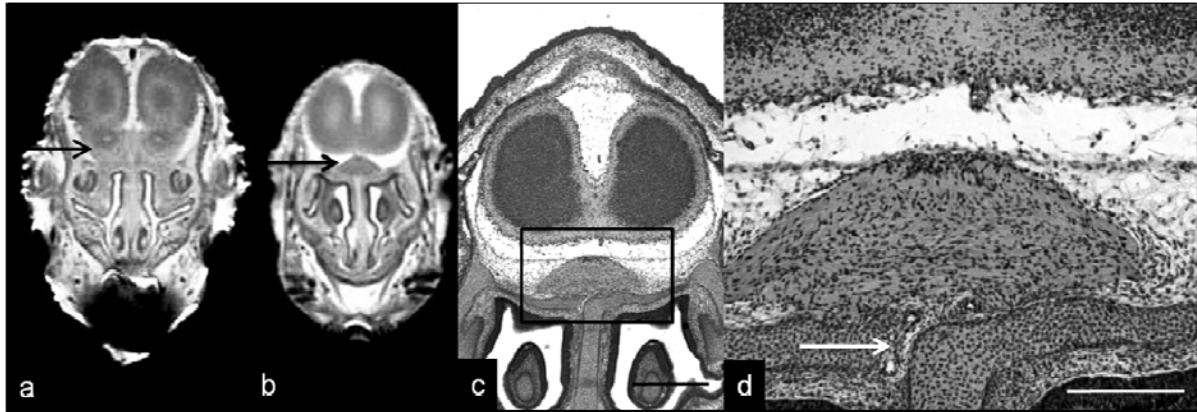


Figure 2.4: MRM and routine histology illustrate olfactory nerve abnormality in a holoprosencephalic fetus. As compared to an MRM image of a normal coronal scan (a; arrow indicates olfactory bulb) that from an ethanol-exposed fetus (b; fetus also shown in Fig. 2.2 d), reveals absence of the olfactory bulbs and the presence of an aberrant intracranial median mass that is located dorsal to the nasal septum (boxed area). Subsequent examination of histological sections through this region revealed that the tissue is continuous, through the cribriform plate, with the nasal epithelium (arrow in d). Bar in c = 0.5 mm, in d = 0.2 mm

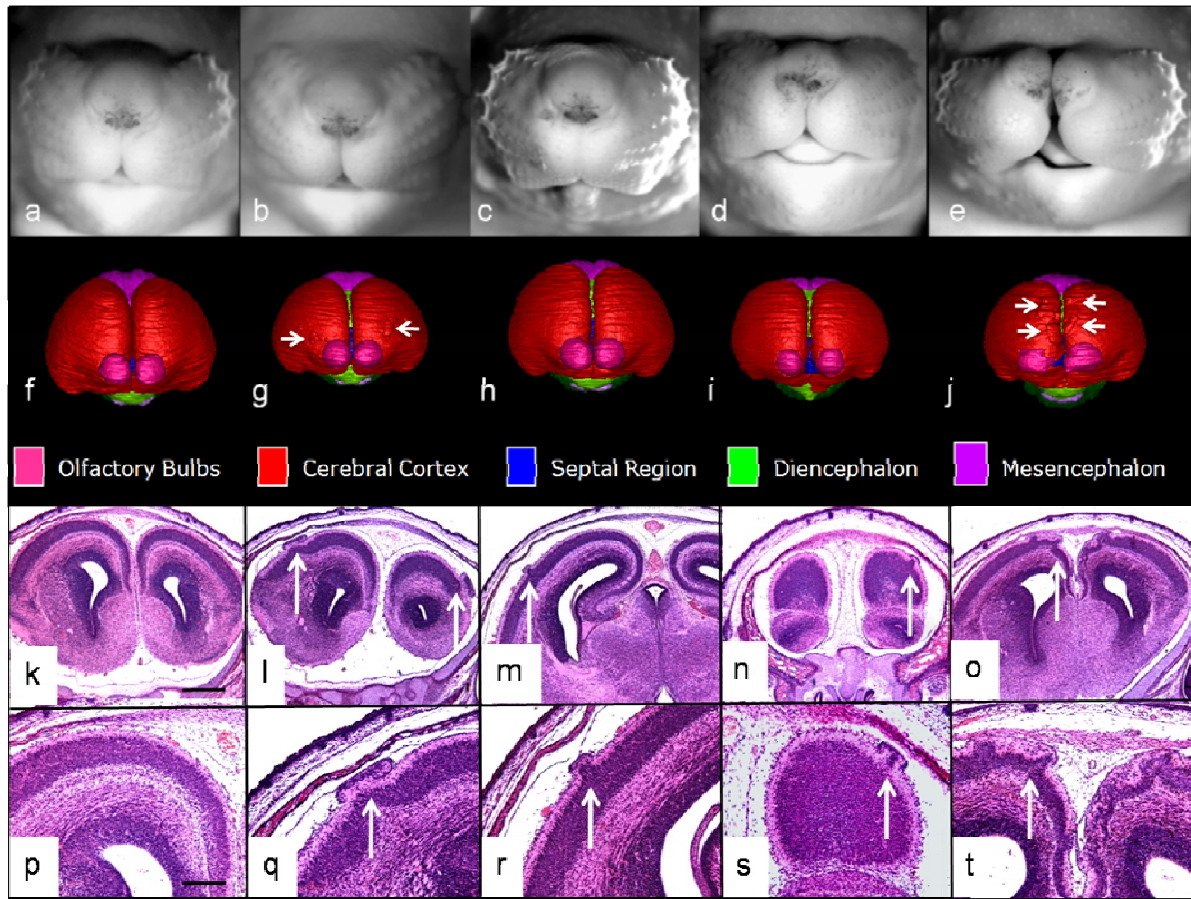


Figure 2.5: Shown are the face, brain reconstruction, and histological sections of a control and four dysmorphic GD 17 fetal mice. A common feature among the ethanol-exposed animals is cortical dysplasia/heterotopia in the absence of overt HPE. As compared to the control (a), the affected fetuses have faces that appear relatively normal (b), or that present with a long upper lip along with severe micrognathia (c), or foreshortening (d; also note Fig. 2.6 b) or median cleft of the snout (e). As viewed from the front, reconstructed MRM scans illustrate a slight widening of the space between the cerebral hemispheres (as evidenced by visibility of the septal region and diencephalon) in the affected fetuses (g-j) as compared to control (f). (Color codes for the segmented brain regions are shown beneath the 3D reconstructions.) Also evident in (g) and (j) are irregularities on the cerebral cortical surface (arrows). Subsequent histological analyses of these and the other 2 fetuses shown in this Figure identified these structures as cortical dysplasia/heterotopias (arrows in l-o, 4X; q-t, 10X). Bar in k = 0.5mm, in p = 0.2 mm

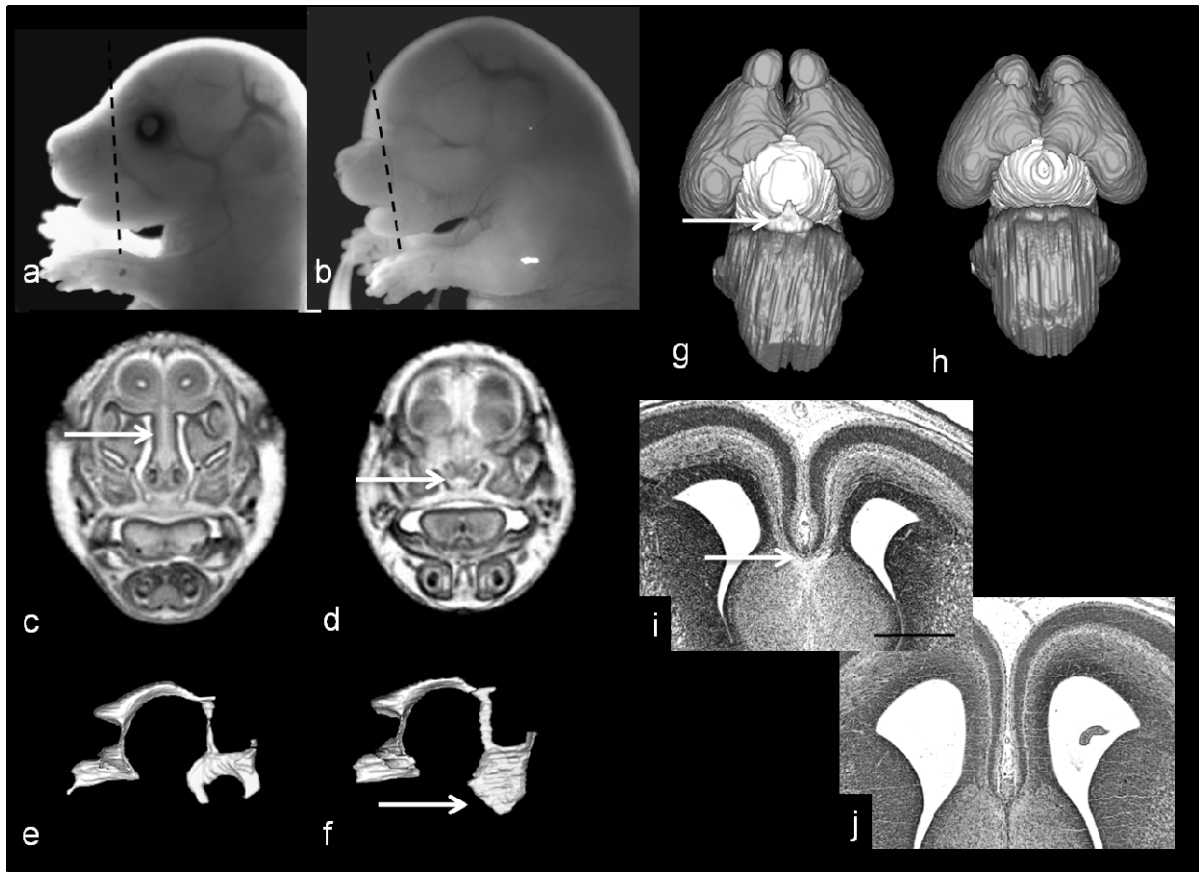


Figure 2.6: Additional light micrographs along with coronal MRM scans and reconstructions and histological sections of the fetus pictured in Fig. 2.5 d illustrate its dysmorphic features as compared to control (a, c, e, g, i). Included are anophthalmia and snout foreshortening (evident in b), short nasal septum and small nasal cavity (arrow in d) [scan made at the level of the line in (b)], third ventricular enlargement (arrow in f), pituitary agenesis (h; compare to control, arrow in g), and apparent absence of the corpus callosum (j; compare to control, arrow in i). Bar in i = 0.5 mm

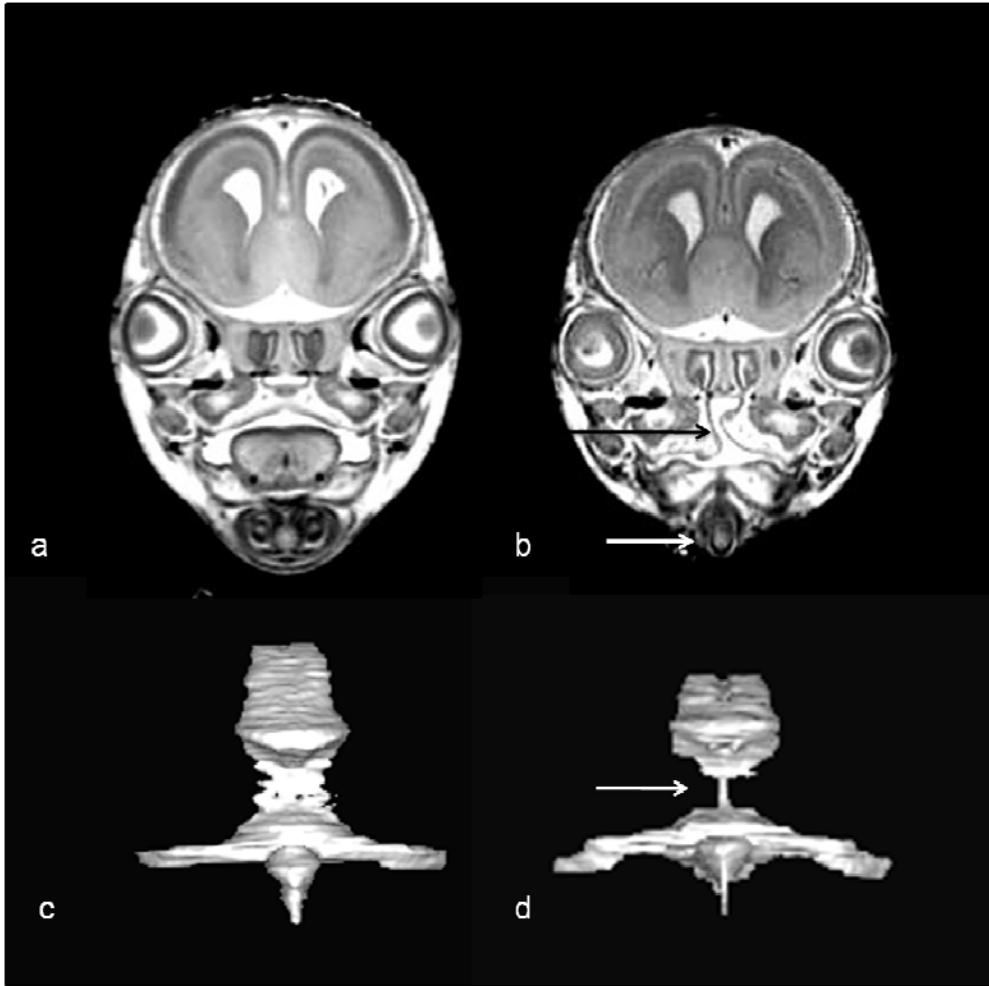


Figure 2.7: MRM scans and reconstructions illustrate additional dysmorphic features of the fetus pictured in Fig. 2.5 c. Coronal scans made at the level of the eyes illustrate clefting of the secondary palate (black arrow in b), no apparent tongue, and this fetus's very narrow mandible (white arrow in b). A posterior view of the reconstructed mesencephalic and fourth ventricle show stenosis (narrowing) at the level of the aqueductal isthmus (arrow in d). Shown in (a & c) are comparable views of a control fetus.

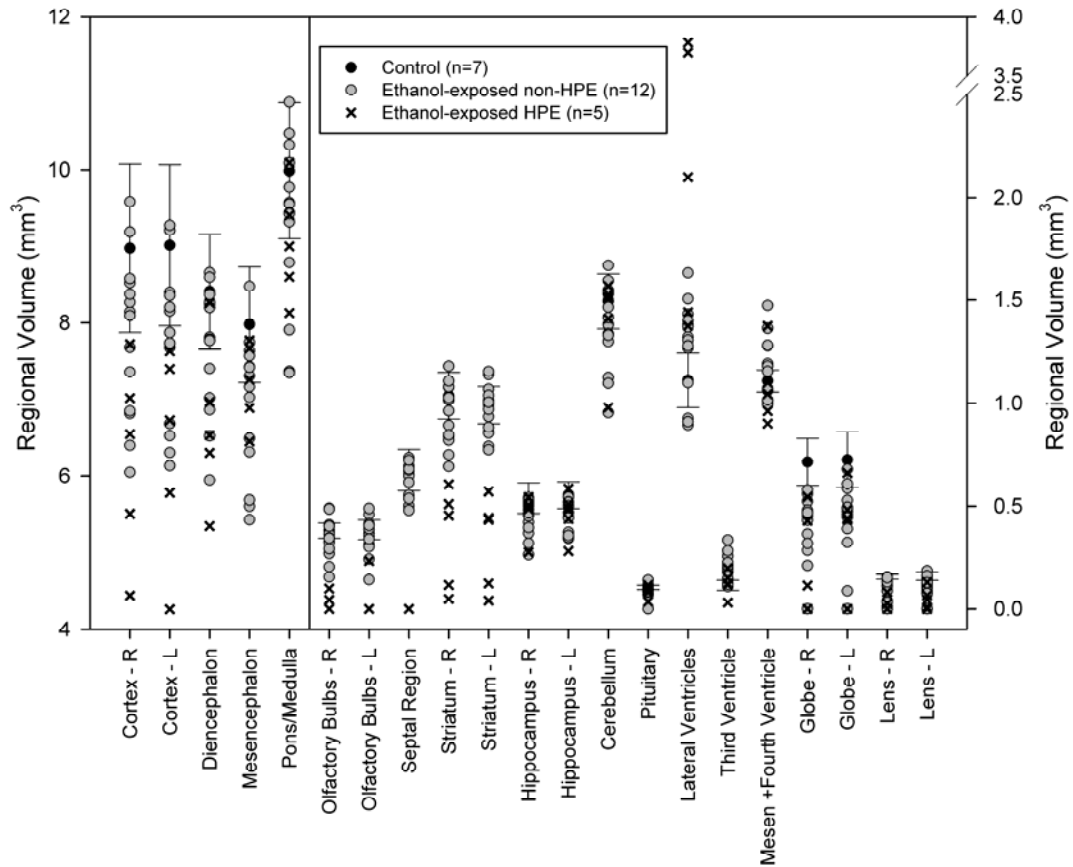


Figure 2.8: Ethanol-induced volume changes in selected regions of GD 17 fetal mouse brains following acute GD 7 exposure. Data is expressed to illustrate the broad range of insult. Mean values from 7 control fetuses are indicated by a black dot, with a bar indicating the 95% confidence interval of the control mean. Values for the 5 ethanol-exposed animals with overt HPE are expressed as x's; and for all of the other ethanol-exposed animals (n=14) a grey circle is employed. Please note differing scales on the right and left, as needed to facilitate representation of the data.

Table 1: Linear Brain Measurements

Measurement	Control	non-HPE	HPE
Mid-sagittal brain length	7.46 ± 0.08 mm (7.21 - 7.84)	7.21 ± 0.09 mm (6.77 - 7.64)	6.75 ± 0.18 mm (6.28 - 7.11) #,†
Brain width	4.76 ± 0.09 mm (4.52 - 5.22)	4.44 ± 0.04 mm (4.16 - 4.64) #	4.07 ± 0.19 mm (3.52 - 4.35) #,†
Bulbothalamic distance	3.99 ± 0.06 mm (3.79 - 4.23)	3.78 ± 0.06 mm (3.36 - 4.12)	3.27 ± 0.15 mm (2.90 - 3.60) #,†
Frontothalamic distance	3.45 ± 0.05 mm (3.25 - 3.62)	3.32 ± 0.04 mm (3.11 - 3.52)	3.17 ± 0.10 mm (2.90 - 3.39) #
Third Ventricle Width	0.22 ± 0.02 mm (0.15 - 0.30)	0.23 ± 0.01 mm (0.17 - 0.29)	0.10 ± 0.01 mm (0.08 - 0.13) #,†
Transverse Cerebellar Distance	3.46 ± 0.05 mm (3.31 - 3.71)	3.34 ± 0.04 mm (3.15 - 3.64)	3.37 ± 0.14 mm (2.96 - 3.58)

Table 2.1: Linear brain measurements are represented as the mean ± the standard error of the mean. Range of measurements in each region and group are indicated in parentheses. # denotes a significant difference from controls, while † denotes a significant difference from the non-HPE group. For controls, n=7; non-HPE, n=14; HPE, n=4.

REFERENCES

Ades LC, Sillence DO (1992) Agnathia-holoprosencephaly with tetramelia. *Clin Dysmorphol* 1(3):182-4.

Ahlgren SC, Thakur V, Bronner-Fraser M (2002) Sonic hedgehog rescues cranial neural crest from cell death induced by ethanol exposure. *Proc Natl Acad Sci U S A* 99(16):10476-81.

Archibald SL, Fennema-Notestine C, Gamst A, Riley EP, Mattson SN, Jernigan TL (2001) Brain dysmorphology in individuals with severe prenatal alcohol exposure. *Dev Med Child Neurol* 43(3):148-54.

Astley SJ, Magnuson SI, Omnell LM, Clarren SK (1999) Fetal alcohol syndrome: changes in craniofacial form with age, cognition, and timing of ethanol exposure in the macaque. *Teratology* 59(3):163-72.

Barr M, Jr., Cohen MM, Jr. (1999) Holoprosencephaly survival and performance. *Am J Med Genet* 89(2):116-20.

Blaas HG, Eriksson AG, Salvesen KA, Isaksen CV, Christensen B, Mollerlokken G, Eik-Nes SH (2002) Brains and faces in holoprosencephaly: pre- and postnatal description of 30 cases. *Ultrasound Obstet Gynecol* 19(1):24-38.

Blader P, Strahle U (1998) Ethanol impairs migration of the prechordal plate in the zebrafish embryo. *Dev Biol* 201(2):185-201.

Bomelburg T, Lenz W, Eusterbrock T (1987) Median cleft face syndrome in association with hydrocephalus, agenesis of the corpus callosum, holoprosencephaly and choanal atresia. *Eur J Pediatr* 146(3):301-2.

Bonthius DJ, Woodhouse J, Bonthius NE, Taggard DA, Lothman EW (2001a) Reduced seizure threshold and hippocampal cell loss in rats exposed to alcohol during the brain growth spurt. *Alcohol Clin Exp Res* 25(1):70-82.

Bonthius DJ, Pantazis NJ, Karacay B, Bonthius NE, Taggard, Da, Lothman EW (2001b) Alcohol exposure during the brain growth spurt promotes hippocampal seizures, rapid kindling, and spreading depression. *Alcohol Clin Exp Res* 25(5):734-45.

Bookstein FL, Sampson PD, Connor PD, Streissguth AP (2002) Midline corpus callosum is a neuroanatomical focus of fetal alcohol damage. *Anat Rec* 269(3):162-74.

Clarke DW, Steenaart NA, Breedon TH, Brien JF (1985) Differential pharmacokinetics for oral and intraperitoneal administration of ethanol to the pregnant guinea pig. *Can J Physiol Pharmacol* 63(2):169-72.

Cohen MM, Jr. (1989) Perspectives on holoprosencephaly: Part I. Epidemiology, genetics, and syndromology. *Teratology* 40(3):211-35.

Cohen MM, Jr. (2006) Holoprosencephaly: clinical, anatomic, and molecular dimensions. *Birth Defects Res A Clin Mol Teratol* 76(9):658-73.

Coulter CL, Leech RW, Schaefer GB, Scheithauer BW, Brumback RA (1993) Midline cerebral dysgenesis, dysfunction of the hypothalamic-pituitary axis, and fetal alcohol effects. *Arch Neurol* 50(7):771-5.

Croen LA, Shaw GM, Lammer EJ (1996) Holoprosencephaly: epidemiologic and clinical characteristics of a California population. *Am J Med Genet* 64(3):465-72.

DeMyer W, Zeman W (1963) Alobar holoprosencephaly (arhinencephaly) with median cleft lip and palate: clinical, electroencephalographic and nosologic considerations. *Confin Neurol* 23:1-36.

DeMyer W, Zeman W, Palmer CG (1964) The Face Predicts the Brain: Diagnostic Significance of Median Facial Anomalies for Holoprosencephaly (Arhinencephaly). *Pediatrics* 34:256-63.

DeMyer W (1967) The median cleft face syndrome. Differential diagnosis of cranium bifidum occultum, hypertelorism, and median cleft nose, lip, and palate. *Neurology* 17(10):961-71.

DeMyer W (1975) Median facial malformations and their implications for brain malformations. *Birth Defects Orig Artic Ser* 11(7):155-81.

Dickinson BP, Spoon DB, Cordray TL, Lazareff J, Wasson K, Bradley JP (2006) Correction of massive hydrocephalus and brain wound in holoprosencephaly. *J Craniofac Surg* 17(4):707-13.

Dorris M (1989) *The Broken Cord*. Harper and Row Publishers Inc., New York.

Fitz CR (1994) Holoprosencephaly and septo-optic dysplasia. *Neuroimaging Clin N Am* 4(2):263-81.

Fryer SL, Schweinsburg BC, Bjorkquist OA, Frank LR, Mattson SN, Spadoni AD, Riley EP (2009) Characterization of white matter microstructure in fetal alcohol spectrum disorders. *Alcohol Clin Exp Res* 33(3):514-21.

Hammond P, Hutton TJ, Allanson JE, Buxton B, Campbell LE, Clayton-Smith J, Donnai D, Karmiloff-Smith A, Metcalfe K, Murphy KC, Patton M, Pober B, Prescott K, Scambler P, Shaw A, Smith AC, Stevens AF, Temple IK, Hennekam R, Tassabehji M (2005) Discriminating power of localized three-dimensional facial morphology. *Am J Hum Genet* 77(6):999-1010.

Higashiyama D, Saito H, Komada M, Takigawa T, Ishibashi M, Shiota K (2007) Sequential developmental changes in holoprosencephalic mouse embryos exposed to ethanol during the gastrulation period. *Birth Defects Res A Clin Mol Teratol* 79(7):513-23.

Ioffe S, Chernick V (1990) Prediction of subsequent motor and mental retardation in newborn infants exposed to alcohol in utero by computerized EEG analysis. *Neuropediatrics* 21(1):11-7.

Johnson GA, Ali-Sharief A, Badea A, Brandenburg J, Cofer G, Fubara B, Gewalt S, Hedlund LW, Upchurch L (2007) High-throughput morphologic phenotyping of the mouse brain with magnetic resonance histology. *Neuroimage* 37(1):82-9.

Jones KL, Smith DW, Ulleland CN, Streissguth P (1973) Pattern of malformation in offspring of chronic alcoholic mothers. *Lancet* 1(7815):1267-71.

Jones KL, Smith DW (1975) The fetal alcohol syndrome. *Teratology* 12(1):1-10.

Kaufman MH (1992) *The Atlas of Mouse Development*. Academic Press, San Diego.

Kfir M, Yevtushok L, Onishchenko S, Wertelecki W, Bakhireva L, Chambers CD, Jones KL, Hull AD (2009) Can prenatal ultrasound detect the effects of in-utero alcohol exposure? A pilot study. *Ultrasound Obstet Gynecol* 33(6):683-9.

Komatsu S, Sakata-Haga H, Sawada K, Hisano S, Fukui Y (2001) Prenatal exposure to ethanol induces leptomenigeal heterotopia in the cerebral cortex of the rat fetus. *Acta Neuropathol* 101(1):22-6.

Kotch LE, Dehart DB, Alles AJ, Chernoff N, Sulik KK (1992) Pathogenesis of ethanol-induced limb reduction defects in mice. *Teratology* 46(4):323-32.

Kotch LE, Sulik KK (1992) Experimental fetal alcohol syndrome: proposed pathogenic basis for a variety of associated facial and brain anomalies. *Am J Med Genet* 44(2):168-76.

Lebel C, Rasmussen C, Wyper K, Walker L, Andrew G, Yager J, Beaulieu C (2008) Brain diffusion abnormalities in children with fetal alcohol spectrum disorder. *Alcohol Clin Exp Res* 32(10):1732-40.

Lemoine P, Harousseau H, Borteyru JP, Menuet J (1968) Les enfants de parents alcooliques: anomalies observees. *Quest Med* 25:476-482

Leoncini E, Baranello G, Orioli IM, Anneren G, Bakker M, Bianchi F, Bower C, Canfield MA, Castilla EE, Cocchi G, Correa A, De Vigan C, Doray B, Feldkamp ML, Gatt M, Irgens LM, Lowry RB, Maraschini A, Mc Donnell R, Morgan M, Mutchinick O, Poetzsch S, Riley M, Ritvanen A, Gnansia ER, Scarano G, Sipek A, Tenconi R, Mastroiacovo P (2008) Frequency of holoprosencephaly in the International Clearinghouse Birth Defects Surveillance Systems: searching for population variations. *Birth Defects Res A Clin Mol Teratol* 82(8):585-91.

Li YX, Yang HT, Zdanowicz M, Sicklick JK, Qi Y, Camp TJ, Diehl AM (2007) Fetal alcohol exposure impairs Hedgehog cholesterol modification and signaling. *Lab Invest* 87(3):231-40.

Lin AE, Siebert JR, Graham JM, Jr. (1990) Central nervous system malformations in the CHARGE association. *Am J Med Genet* 37(3):304-10.

Loucks EJ, Ahlgren SC (2009) Deciphering the role of Shh signaling in axial defects produced by ethanol exposure. *Birth Defects Res A Clin Mol Teratol.* 85(6):556-67.

- Ma X, Coles CD, Lynch ME, Laconte SM, Zurkiya O, Wang D, Hu X (2005) Evaluation of corpus callosum anisotropy in young adults with fetal alcohol syndrome according to diffusion tensor imaging. *Alcohol Clin Exp Res* 29(7):1214-22.
- Majewski F (1981) Alcohol embryopathy: some facts and speculations about pathogenesis. *Neurobehav Toxicol Teratol* 3(2):129-44.
- Marcus JC (1987) Neurological findings in the fetal alcohol syndrome. *Neuropediatrics* 18(3):158-60.
- Matsunaga E, Shiota K (1977) Holoprosencephaly in human embryos: epidemiologic studies of 150 cases. *Teratology* 16(3):261-72.
- Mattson SN, Riley EP, Sowell ER, Jernigan TL, Sobel DF, Jones KL (1996) A decrease in the size of the basal ganglia in children with fetal alcohol syndrome. *Alcohol Clin Exp Res* 20(6):1088-93.
- Monuki ES (2007) The morphogen signaling network in forebrain development and holoprosencephaly. *J Neuropathol Exp Neurol* 66(7):566-75.
- Mooney SM, Siegenthaler JA, Miller MW (2004) Ethanol induces heterotopias in organotypic cultures of rat cerebral cortex. *Cereb Cortex* 14(10):1071-80.
- Muenke M, Cohen MM, Jr. (2000) Genetic approaches to understanding brain development: holoprosencephaly as a model. *Ment Retard Dev Disabil Res Rev* 6(1):15-21.
- Murray-Lyon IM (1985) Alcohol and foetal damage. *Alcohol Alcohol* 20(2):185-8.
- Myers EA, Parnell SE, Dehart DB, Johnson GA, Sulik KK (2008) Analysis of Ethanol-Induced Abnormalities in the Medial Forebrain of Fetal Mice. *Toxicologist CD - An official J Soc Toxicol* 102:1530.
- O'Malley KD, Barr H (1998) Fetal alcohol syndrome and seizure disorder. *Can J Psychiatry* 43(10):1051.
- Olegard R, Sabel KG, Aronsson M, Sandin B, Johansson PR, Carlsson C, Kyllerman M, Iversen K, Hrbek A (1979) Effects on the child of alcohol abuse during pregnancy. Retrospective and prospective studies. *Acta Paediatr Scand Suppl* 275:112-21.

Parnell SE, O'Leary-Moore SK, Godin EA, Dehart DB, Johnson BW, Allan Johnson G, Styner MA, Sulik KK (2009a) Magnetic Resonance Microscopy Defines Ethanol-Induced Brain Abnormalities in Prenatal Mice: Effects of Acute Insult on Gestational Day 8. *Alcohol Clin Exp Res* 33(6):1001-1011.

Parnell SE, Dehart DB, Zhou FC, Sulik KK (2009b) Sub-strain-dependent variability in susceptibility to ethanol-induced teratogenesis. *Alcohol Clin Exp Res* 33(S1): 132A

Pauli RM, Graham JM, Jr., Barr M, Jr. (1981) Agnathia, situs inversus, and associated malformations. *Teratology* 23(1):85-93.

Pauli RM, Pettersen JC, Arya S, Gilbert EF (1983) Familial agnathia-holoprosencephaly. *Am J Med Genet* 14(4):677-98.

Peiffer J, Majewski F, Fischbach H, Bierich JR, Volk B (1979) Alcohol embryo- and fetopathy. Neuropathology of 3 children and 3 fetuses. *J Neurol Sci* 41(2):125-37.

Petiet A, Hedlund L, Johnson GA (2007) Staining methods for magnetic resonance microscopy of the rat fetus. *J Magn Reson Imaging* 25(6):1192-8.

Polizzi A, Pavone P, Iannetti P, Gambardella A, Ruggieri M (2005) CNS findings in three cases of septo-optic dysplasia, including one with semilobar holoprosencephaly. *Am J Med Genet A* 136A(4):357.

Porteous ME, Wright C, Smith D, Burn J (1993) Agnathia-holoprosencephaly: a new recessive syndrome? *Clin Dysmorphol* 2(2):161-4.

Rasmussen SA, Moore CA, Khoury MJ, Cordero JF (1996) Descriptive epidemiology of holoprosencephaly and arhinencephaly in metropolitan Atlanta, 1968-1992. *Am J Med Genet* 66(3):320-33.

Riley EP, Mattson SN, Sowell ER, Jernigan TL, Sobel DF, Jones KL (1995) Abnormalities of the corpus callosum in children prenatally exposed to alcohol. *Alcohol Clin Exp Res* 19(5):1198-202.

Sakata-Haga H, Sawada K, Ohnishi T, Fukui Y (2004) Hydrocephalus following prenatal exposure to ethanol. *Acta Neuropathol* 108(5):393-8.

Schambra UB, Lauder JM, Petrusz P, Sulik KK (1990) Development of neurotransmitter systems in the mouse embryo following acute ethanol exposure: a histological and immunocytochemical study. *Int J Dev Neurosci* 8(5):507-22.

Schambra UB, Lauder JM, Silver J (1992) *Atlas of Prenatal Mouse Brain*. Academic Press, San Diego.

Schambra UB (2008) *Prenatal Mouse Brain Atlas*. Springer Science + Business Media, New York.

Shiota K, Yamada S, Komada M, Ishibashi M (2007) Embryogenesis of holoprosencephaly. *Am J Med Genet A* 143A(24):3079-87.

Siebert JR, Astley SJ, Clarren SK (1991) Holoprosencephaly in a fetal macaque (*Macaca nemestrina*) following weekly exposure to ethanol. *Teratology* 44(1):29-36.

Sowell ER, Mattson SN, Thompson PM, Jernigan TL, Riley EP, Toga AW (2001) Mapping callosal morphology and cognitive correlates: effects of heavy prenatal alcohol exposure. *Neurology* 57(2):235-44.

Spadoni AD, McGee CL, Fryer SL, Riley EP (2007) Neuroimaging and fetal alcohol spectrum disorders. *Neurosci Biobehav Rev* 31(2):239-45.

Stockard CR (1910) The influence of alcohol and other anaesthetics on embryonic development. *Am J Anat* 10:369-392.

Streissguth AP, Herman CS, Smith DW (1978) Intelligence, behavior, and dysmorphogenesis in the fetal alcohol syndrome: a report on 20 patients. *J Pediatr* 92(3):363-7.

Sulik KK, Johnston MC (1982) Embryonic origin of holoprosencephaly: interrelationship of the developing brain and face. *Scan Electron Microsc (Pt 1)*:309-22.

Sulik KK, Johnston MC (1983) Sequence of developmental alterations following acute ethanol exposure in mice: craniofacial features of the fetal alcohol syndrome. *Am J Anat* 166(3):257-69.

Sulik KK, Johnston MC, Webb MA (1981) Fetal alcohol syndrome: embryogenesis in a mouse model. *Science* 214(4523):936-8.

Sulik KK, Lauder JM, Dehart DB (1984) Brain Malformations in Prenatal Mice Following Acute Maternal Ethanol Administration. *Int J Dev Neurosci* 2(3):203-214.

Sulik KK, O'Leary-Moore SK, Parnell SE, Myers EA, Dehart DB, Johnson GA, Chambers CD, Hull AD (2009) High resolution magnetic resonance imaging of alcohol-exposed fetal mice confirms and informs human prenatal ultrasound studies. *Proceedings of the Greenwood Genetic Center 28: in press.*

Theiler K (1989) *The House Mouse: Atlas of Embryonic Development*. Springer-Verlag, New York.

de Toni T, Lazzaroni-Fossati F, Gastaldi R, Taccone A, Pesce F, Piccotti E, Balzarini C, Tarateta A (1985) [Median cleft face syndrome associated with holoprosencephaly. Description of a case]. *Minerva Pediatr* 37(21-22):875-82.

Verrotti A, Spalice A, Ursitti F, Papetti L, Mariani R, Castronovo A, Mastrangelo M, Iannetti P (2009) New trends in neuronal migration disorders. *Eur J Paediatr Neurol. In press*

Webster WS, Walsh DA, McEwen SE, Lipson AH (1983) Some teratogenic properties of ethanol and acetaldehyde in C57BL/6J mice: implications for the study of the fetal alcohol syndrome. *Teratology* 27(2):231-43.

Wozniak JR, Mueller BA, Chang PN, Muetzel RL, Caros L, Lim KO (2006) Diffusion tensor imaging in children with fetal alcohol spectrum disorders. *Alcohol Clin Exp Res* 30(10):1799-806.

Yushkevich PA, Piven J, Hazlett HC, Smith RG, Ho S, Gee JC, Gerig G (2006) User-guided 3D active contour segmentation of anatomical structures: significantly improved efficiency and reliability. *Neuroimage* 31(3):1116-28.

CHAPTER III

DIFFUSION TENSOR IMAGING AND TRACTOGRAPHY DEFINE A SPECTRUM OF FIBER TRACT DYSMORPHOLOGY IN THE BRAINS OF PRENATAL ETHANOL-EXPOSED MICE

Abbreviated title: DTI defines ethanol-induced CNS damage

Shonagh K. O'Leary-Moore, Elizabeth A. Godin, Yi Jiang, Francois Budin, Scott E. Parnell, Deborah B. Dehart, Martin A. Styner, G. Allan Johnson, Ipek Oguz, Kathleen K. Sulik

Bowles Center for Alcohol Studies (SOM, EAG, SEP, DBD, KKS) and
Department of Psychiatry (IO, FB, MAS), University of North Carolina, Chapel
Hill, NC 27599

Center for *In Vivo* Microscopy, Duke University Medical Center, Durham NC (YJ,
GAJ)

Corresponding author: Dr. S.K. O'Leary-Moore, Fetal Toxicology Division,
Bowles Center for Alcohol Studies, University of North Carolina at Chapel Hill,
CB #7178 Thurston Bowles Building Chapel Hill, NC 27599-7178; (919) 966-
3208. Email: somoore@med.unc.edu

Number of figures/tables: 6

Number of pages: 45

Key words: alcohol; diffusion tensor imaging; holoprosencephaly; mouse; fetal

Sources of Support: This work was supported by NIH/NIAAA grants AA007573, AA011605, AA017124; NCRR/NCI grants P41 05959 and U24 CA092656; and the UNC Intellectual and Developmental Disability Research Center HD 031110; and was conducted in conjunction with the Collaborative Initiative on Fetal Alcohol Spectrum Disorders (CIFASD). Additional information about CIFASD can be found at www.cifasd.org.

ABSTRACT

Within the spectrum of disorders that prenatal ethanol exposure causes are alterations in brain white matter microstructure. Diffusion tensor imaging (DTI) of human subjects has illustrated that the corpus callosum (CC) is particularly sensitive to ethanol's teratogenic effects. In this study, DTI was applied to an established Fetal Alcohol Spectrum Disorders (FASD) mouse model in order to examine patterns of white matter/fiber tract dysmorphology. Both gestational day (GD) 17 and postnatal day (PND) 45 C57Bl/6J mice that had been acutely exposed to ethanol (2 x 2.9 g/kg doses) on their 7th gestational day, as well as comparably staged control mice were selected for DTI analyses. The embryonic stage at the time of ethanol exposure corresponds to that in the 3rd week of human pregnancy. Of the 13 ethanol-exposed fetuses that were imaged, 6 presented with facial and CNS dysmorphology consistent with holoprosencephaly (HPE). Among these, fiber tract alterations including agenesis of the CC, thickened fimbria/fornices, absence of fornix columns, and anterior commissure dysmorphology were found. Probst bundles were also evident in an HPE subject. Additionally, DTI facilitated the identification of CC agenesis in ethanol-exposed fetuses that did not have overt HPE features. In PND 45 subjects DTI also revealed significant CC dysmorphology. This novel application of DTI to examination of an FASD model has confirmed and extended clinical findings and has highlighted the vulnerability of the brain at very early stages of its development to ethanol insult.

INTRODUCTION

Ethanol's teratogenic effects in humans have been recognized for decades (Jones & Smith, 1973; Lemoine, 1968) and are collectively referred to as Fetal Alcohol Spectrum Disorders (FASD) (reviewed by Riley & McGee, 2005). Resulting from heavy maternal drinking during pregnancy, and at the severe end of the alcohol-induced birth defects spectrum, is Fetal Alcohol Syndrome (FAS) which is characterized by pre- and/or post-natal growth retardation, craniofacial anomalies and central nervous system (CNS) dysfunction (Jones & Smith, 1973). Aided by the development of magnetic resonance imaging (MRI)-based approaches [including diffusion tensor imaging (DTI)], specific brain regions that are particularly vulnerable to ethanol's insult have begun to be identified and include major white matter tracts such as the corpus callosum (CC) (reviewed by Norman et al., 2009; Riley et al., 2004).

Modeling FASD in rodents allows precise control of the dose, timing and pattern of ethanol exposure, all of which influence the range of teratogenic insult (eg; Goodlett, et al., 1998; Bonthius & West, 1990; Maier et al., 1999; Thomas, et al., 1996). Previous work from our laboratories has shown that exposure of mice to ethanol on their 7th gestational day (GD 7) results in a spectrum of birth defects (eg. Sulik, 2005; Godin et al., 2010). At this time in gestation, mice are at a stage of development that occurs during the human 3rd week of pregnancy. Recently, magnetic resonance microscopy (MRM) has been applied to the study of this mouse model and has facilitated illustration and discovery of a range of

ethanol-induced structural brain abnormalities including holoprosencephaly (HPE) at the most severe end of the spectrum (Godin et al., 2010).

As shown by Mori and colleagues (eg. Mori et al., 2001; Zhang et al., 2003; Zhang et al., 2006), in the developing mouse brain, diffusion tensor imaging (DTI) affords more detailed examination of brain morphology than allowed by traditional imaging techniques and can be applied to fiber tract analyses even prior to the time that myelination occurs. Extending our previous MRM-based report, the current study employs DTI to characterize brain and fiber tract abnormalities resulting from ethanol exposure on GD 7 in mice. For this, examination of non-diffusion weighted anatomical scans, color-coded anisotropy maps, and 3D fiber tract reconstructions from ethanol-exposed and control fetuses and a selected number of postnatal animals were conducted. Based on previous data, it was anticipated that fiber tract changes typical of HPE would be identified in ethanol-exposed animals having facial dysmorphology. Additionally, in ethanol-exposed mice having no apparent facial defects, more subtle changes in fiber tract morphology were expected.

MATERIALS AND METHODS

Animal breeding and maintenance

C57Bl/6J mice were purchased from The Jackson Laboratory (Bar Harbor, ME) and housed in a temperature and light-controlled (12/12 hr light/dark) environment approved by AAALAC. Standard laboratory chow and water was available *ad libitum*. For breeding, 1-2 females were placed with one male for 2

hours. Detection of a copulation plug marked the beginning of gestational day (GD) 0.

Maternal treatment and animal rearing

On the beginning of GD 7, pregnant dams were assigned to either an ethanol or control group, weighed, and administered either an intraperitoneal (ip) dose of 25% ethanol (2.9 g/kg) or an equivalent dose of Ringer's solution. Four hrs later a second ethanol or Ringer's solution dose of equal volume and concentration was administered to each of the dams in the respective groups. This ethanol administration paradigm has previously been employed, yielding a mean peak blood ethanol concentration (BEC) of 440 mg/dl and inducing a range of CNS abnormalities including HPE (eg. Godin et al., 2010). Following ethanol administration, dams were left undisturbed until GD 17 or were allowed to give birth.

For those dams that were to provide subjects for postnatal imaging, beginning on GD 20, cages were checked daily and the date of birth was recorded and designated as postnatal day (PND) 0. If necessary, litters were culled to 8 (retaining 4 males and 4 females when possible) on PND 2 and were left undisturbed until weaning on PND 28. All procedures involving animals were approved by an Institutional Animal Care and Use Committee (IACUC) at the University of North Carolina at Chapel Hill.

Specimen collection and preparation for DTI

To provide subjects for fetal DTI, on their 17th day of pregnancy, following CO₂ anesthesia, dams were killed by cervical dislocation. Following laparotomy, the uteri were removed and fetuses were dissected free of decidua under a dissecting microscope and placed on ice in phosphate buffered saline (PBS). Fetuses were then examined for any gross abnormalities. As in our previous study (Godin et al., 2010), in order to characterize the most severe end of the spectrum of ethanol-induced dysmorphogenesis, the selection of ethanol-exposed subjects to be scanned was based on the presence of grossly-observable dysmorphology; including facial anomalies commonly associated with HPE (eg. elongated philtrum, closely spaced nostrils) and the presence of ocular defects. For this investigation, all of the fetuses selected had ocular abnormalities (ranging from mild to severe), and among these, some had normal faces while others had varying degrees of facial dysmorphology.

In preparation for DTI, the fetuses were drop-fixed in a solution of Bouin's fixative (Sigma-Aldrich, St. Louis, MO) and ProHance (Bracco Diagnostics Inc. Princeton, NJ) (20:1 v:v) for 9 hours (Petiet et al., 2008; 2010). This was followed by a brief PBS rinse and placement in a storage solution containing PBS and ProHance (200:1 v:v). Fetuses were typically imaged within 72 hrs of fixation. Using no more than 2 subjects from each litter, a total of 21 fetuses (13 ethanol-exposed and 8 control fetuses from 9 and 5 litters, respectively) were imaged.

For postnatal DTI analysis, on PND 45, male offspring of ethanol-exposed dams were deeply anesthetized using 250 mg/kg tribromoethanol (Sigma Aldrich) and were perfused using an active staining protocol adapted from Jiang and Johnson (2010). Briefly, a catheter was inserted into the left ventricle and a solution of saline and ProHance (10:1 v:v) (Bracco Diagnostics, Inc, Princeton, NJ) was pumped at a flow rate of 4.5 ml/min for 3 minutes. This was followed by 6 minutes of fixation using a solution of formalin and ProHance (10:1 v:v). Once perfused, the heads were stored in formalin for 72 hours followed by removal of the tissue surrounding the skull. Specimens were then placed into a holding solution of PBS and ProHance (100:1 v:v) for approximately 2-3 days prior to imaging.

Diffusion tensor imaging (DTI)

DTI is a powerful imaging technique that exploits the local diffusion characteristics of water in various regions of the brain, allowing detailed examination of white matter morphology. In regions of the CNS where there is fibrous tissue, such as in the white matter tracts of the brain, water diffusion is anisotropic. That is, diffusion is restricted and preferential along the axis of the fiber and will move more rapidly in the direction aligned with the fiber. This is in contrast to isotropic diffusion where diffusion is homogeneous in all directions. DTI takes advantage of these diffusion properties and allows the quantification of diffusion anisotropy in the brain (eg. FA) (Basser et al., 1996; Pierpaoli et al., 1996a,b) and also provides information regarding the preferential direction of

diffusion which can be expressed as color coded maps (see figure 3.1).

Importantly, in the developing mouse brain, DTI allows the identification of fiber tracts even prior to the onset of myelination (reviewed by Mori & Zhang, 2006; Mori et al., 2001; Zhang et al., 2003; Zhang et al., 2006).

In the current study, DTI scans were conducted at the Center for *In Vivo* Microscopy at Duke University (Durham, NC) employing either a 7T Magnex /210 mm bore or a 9.4T Oxford/89 mm bore magnet controlled by GE EXCITE consoles (GE Healthcare, Milwaukee, WI). Specimens were placed in a custom-built holder inserted in a solenoid radiofrequency coil. During the period of this study, a holder was developed for simultaneous imaging of 2 fetal heads, effectively reducing the acquisition time by one half. A diffusion-weighted spin-echo pulse sequence was used to acquire 3D volume images (FOV=22×11×11 mm for two fetal heads or each postnatal brain or 20×10×10 mm for an entire fetus; matrix size=512×256×256 resulting in 43 μm or 39 μm isotropic resolution, TR=100 ms). For each subject, one non-diffusion weighted image and 6 [1] (NEX=2) or 12 [2] (NEX=1) unique gradient direction diffusion-weighted images with b-values of 800 to 1000 s/mm^2 were acquired over approximately 24 hours. The following gradients were used: 6 directions (Jiang and Johnson, 2010), or 12 directions (Papadakis et al., 1999).

Image processing and fiber tracking

As a first step, the two fetuses simultaneously imaged were separated into two individual image files before further processing. Diffusion tensor (DT)

images were then computed from the DWIs using weighted square estimation (Salvador et al., 2005). The Mean Diffusivity (MD) images were computed from the DT images and were used to find the transformations that rigidly reorient all images into the same coordinate space. These transformations were applied to the DT images (Alexander et al., 2001) using preservation of principal direction and MD, Fractional Anisotropy (FA), and color-coded FA images were computed from the aligned DTI images. These images were examined for gross anomalies in all three orthogonal planes utilizing 3D Slicer (www.slicer.org; Pieper et al., 2006). ITK-SNAP (www.itksnap.org; Yushkevich et al., 2006) was used to segment selected specimens' brain regions consistent with our previous report for 3D renderings (Parnell et al., 2009; Godin et al., 2010). For tractography of selected white matter tracts, DTIStudio (www.mristudio.org; Jiang et al., 2006) was applied. Using the Fiber Assignment by Continuous Tracking (FACT) algorithm, which employs a brute-force fiber searching approach (Mori et al., 1999a,b, Xue et al., 1999), 3D fiber tracts were generated from each data set. The following parameters were utilized: FA threshold for starting tracking = 0.25; FA threshold for ending tracking = 0.25, and fiber turning angle before ending tracking = 45°. For the CC, hippocampal commissure and anterior commissure, regions of interest (ROI) for fiber tracking were designated in the mid-sagittal plane, while the fasciculus retroflexus ROIs were delineated in the coronal plane. ROIs were placed along the possible paths of fibers utilizing knowledge from existing atlases based on normal fetal brain anatomy (Kaufman, 1992; Schambra

2008; Schambra et al., 1992). Image visualization of 3D fiber tract reconstructions was performed in DTIStudio.

RESULTS

General features of ethanol-exposed fetuses

Consistent with previous studies (eg. Godin et al., 2010; Lipinski et al., 2010; Sulik & Johnson, 1982; Sulik, 2005; Webster et al., 1983), ethanol exposure on day 7 of gestation induced a range of grossly observable defects, including both ocular and facial dysmorphology, in the fetal animals assessed. Ocular defects ranged from mild unilateral microphthalmia and abnormally shaped pupils, to iridial coloboma, and bilateral anophthalmia. Representing the severe end of the ethanol teratogenesis spectrum, a number of subjects selected for DTI analyses also presented with facies consistent with the HPE pattern of defect (see figure 3.3, b – g). HPE is a complex disorder characterized by a spectrum of anomalies affecting the median forebrain region and is accompanied by distinct facial abnormalities (reviewed by Cohen et al., 2006; Muenke & Cohen, 2000; Sulik & Johnson, 1982). HPE was confirmed in all but one of the animals with characteristic HPE faces, a finding that is consistent with the observation by DeMyer and colleagues (1964) that "the face predicts the brain (although not always)".

Gross and fiber tract anomalies in the brains of HPE fetuses

In the current study, DTI, coupled with active staining techniques that have been optimized for the fetal mouse (eg. Petiet et al., 2008; 2010), resulted in images having 39-43 micron isotropic resolution, allowing assessment of the brain in all 3 planes simultaneously. Among those ethanol-exposed fetuses with HPE, examination of the FA and color-coded directional anisotropy maps revealed significant gross and fiber tract anomalies. Characteristic findings are illustrated in figure 3.1, which includes coronal sections of a control and a HPE fetal brain that are shown at comparable levels throughout the forebrain. In this affected fetus, the brain anomalies are consistent with those in human lobar HPE and include rostral union of the cerebral cortices and lateral ventricles as well as complete absence of a septal region (figure 3.1, block arrow in control) and olfactory bulbs (see figure 3.4h). Additionally, the striatum of this HPE animal appears united across the midline as shown in the rostral-most section in figure 3.1. As shown by the color-coded FA maps, fiber tract anomalies involving commissural fibers are particularly pronounced. Notably, the CC (figure 3.1, white arrow in the control) is completely absent in the HPE subject. Furthermore, although both an anterior commissure (figure 3.1a, AC, pink arrow) and hippocampal commissure (figure 3.1, HC, yellow arrow) can be identified in the HPE animal; both of these major fiber tracts are clearly abnormal. The anterior commissure of the HPE animal is rostrally displaced, appears diffuse and completely lacks the olfactory projections as seen in a control fetus (figure 3.1a, AC, pink arrow). The hippocampal commissure (figure 3.1, HC, yellow arrow) is

also displaced, though in the caudal direction, and appears to be thickened and dysplastic as compared to the control subject.

In addition to major anomalies in commissural fibers, significant abnormalities in other fiber tracts were also identifiable. The columns of the fornix, which are readily identified in the control subject (figure 3.1c, F, blue arrowhead), are completely absent in the HPE subject. In addition, the external capsule (figure 3.1, EC, green arrow) of the HPE animal appears to be anomalously continuous at the most anterior sections shown. The fibers of both the internal capsule (figure 3.1, IC, pink arrowhead) and the fimbria (figure 3.1, Fim, orange arrow) appear to be thickened in the HPE subject as compared to the control. Additional regions of dysmorphology observed in the HPE subject include a band of fibers with a preferential right/left direction (red signal) just ventral to the large lateral ventricle as well as a large midline band of blue signal, indicating fibers projecting in the inferior/superior direction. Both of these anomalies can be observed at the level of the hippocampal commissure in the HPE subject (figure 3.1, white dashed arrows).

Despite the significant dysmorphology present in the HPE brain shown in figure 3.1, fiber tracts located caudal to the telencephalon in this animal appear to be relatively normal. These include the fiber tracts of the optic nerve (figure 3.1, ON, blue arrow), optic chiasm (figure 3.1, OC, red arrow), and optic tracts (figure 3.1, OT, purple arrow) as well as the fasciculus retroflexus (figure 3.1, FR, green arrowhead). Notably, while this HPE subject had bilateral iridial

colobomas accompanied by minor microphthalmia, the optic nerves and optic chiasm appeared relatively normal.

Cortical layers in the fetal mouse

DTI not only allows identification of brain fiber tracts, but affords excellent contrast in the cerebral cortex, where levels of anisotropy are high at this time in development. This allows the recognition of various cortical layers as shown in rodents (eg. Zhang et al., 2006; Zhang et al., 2003; Mori et al., 2001; reviewed by Mori & Zhang, 2006), as well as during the perinatal period in humans (eg. Huppi et al., 1998; Neil et al., 1998; Mukherjee et al., 2002 ; Huppi & Dubois, 2006).

As shown in figure 3.2, the cortical plate (figure 3.2, white arrows), intermediate zone (figure 3.2, white dashed arrows), and the subventricular zone (figure 3.2, yellow arrows) can be distinguished in color-coded maps (figure 3.2, a & b). Additionally, glyphs, representing the primary eigenvector and the preferential direction of the diffusion tensors, are shown overlaid on FA images, facilitating the visualization of the orientation of cellular components in these various cerebral cortical layers (figure 3.2, c & d). As expected, significant cortical layer alterations are a consequence of ethanol-induced HPE as shown in horizontal brain scans in figure 3.2, b & d. The cortical plate can be seen on the outermost surface of the brain in the control subject as a band of tissue with high FA which transitions from red on the lateral aspects of the cortex, to green at the most rostral end of the cortex, and back to red at the medial aspects of the brain (figure 3.2a, white arrow). The orientation of the cortical plate tissue is

perpendicular to the surface of the brain, which is clearly illustrated in figure 3.2c (white arrows). Despite significant dysmorphology in the HPE subject, the color-coded FA maps (figure 3.2, b, white arrow), as well as the glyphs (figure 3.2b, white arrow), illustrate that on the lateral aspects of the brain the cortical plate is quite similar to that of the control fetus. Rostro-medially, however, in the absence of a normal interhemispheric fissure, the cortical fiber orientation differs from that of the control (figure 3.2, b & d, white arrows). In addition to the cortical plate, the intermediate zone, a layer in which tangential cell migration occurs, is distinguishable in the control fetus with FA coding direction and glyph orientation being parallel to the surface of the cortex (figure 3.2, a & c, white dashed arrow). This layer is somewhat difficult to discern in the HPE subject (figure 3.2, b & d), as the cortical layers appear to be thickened and include a region of high intensity blue signal not seen in the control. This blue signal is indicative of projections in the superior/inferior direction (white dashed arrows, figure 3.2, b & c). Finally, regions of high signal intensity perpendicular to the surface of the ventricles surrounding the walls of the lateral ventricles are seen in both the control and HPE subject (figure 3.2, a-d, yellow dashed arrow) and are consistent with the subventricular zone which is a site of neurogenesis in the brain. Notable is that the subventricular zone of the HPE subject appears to be thickened and that the lateral aspects do not show the same red signal intensity as present in the control (figure 3.2a, yellow dashed arrow). Rather, regions of blue signal are seen (figure 3.2b, yellow dashed arrow), representing aberrant cellular organization in this region of the brain.

Spectrum of ethanol-induced HPE malformations

As is typical in humans who present with HPE, among those animals presenting with HPE in the current study, a large range of defects was evident. Light microscopic images of the faces of these subjects (figure 3.3b-g), illustrate varying degrees of abnormal approximation of the nostrils in all of the ethanol-exposed subjects shown. In all but the fetus shown in fig. 3.3b, the central notch in the upper lip is diminished. The latter condition is consistent with loss of philtral tissue. Note that the most severely affected animal shown is cebocephalic (figure 3.3g). Varying degrees of mandibular dysmorphology, ranging from moderate (as shown in figure 3.3, c, d, f, and g) to severe micrognathia (figure 3.3, e), are also an apparent feature. Notable is that in the severely micrognathic subject, cleft palate and aglossia were visualized in the MRIs, and low-set ears are evident. This collection of malformations is consistent with otocephaly.

For each of these HPE specimens and for a control animal, non-diffusion weighted coronal sections of the brain at the level of the anterior commissure are shown in figure 3.3 h-n. In the affected animals, varying degrees of interhemispheric fissure deficiency and median union of the lateral ventricles were noted, facilitating classification of the subjects as having lobar/semi-lobar (figure 3.3, b-f; i-m) or alobar (figure 3.3, g & n) HPE. The anterior horns of the lateral ventricles were not present in any of these subjects. Additionally in the HPE fetuses, the striatum, which can be appreciated bilaterally in the control animal (figure 3.3h, stars), is united across the midline to varying degrees (figure

3.3, i-m) or appears completely absent (figure 3.3, n). Other anomalies apparent in the non-diffusion weighted images among HPE animals and that are consistent with our earlier report (Godin et al., 2010) were varying degrees of forebrain deficiency including hypo- or agenesis of the olfactory bulbs, cortical heterotopias and pituitary defects.

In addition to visualizing defects in FA and color-coded images, utilization of the primary eigenvector (v_1) of the diffusion tensor to reconstruct pathways of fiber tracts in the brain (i.e. tractography), allows visualization of 3D fiber tract trajectories (reviewed by Mori & Zhang, 2006; Mukherjee et al., 2008; Huppi & Dubois, 2006, Melhem et al., 2002). Recent reviews describe the application of this methodology to the study of abnormal development (eg. Lee et al., 2005) and congenital brain malformations (eg. Wahl et al., 2009), including the utility of this imaging modality for discovery of HPE-related pathology. In the HPE fetuses described in the current study, selected 3D fiber tract reconstructions in forebrain regions illustrated significant dysmorphology (figure 3.3 p-u) as compared to the control fetus (figure 3.3 o). As illustrated in figure 1o, reconstructed tracts evident in the control fetus include the CC (red), anterior commissure (blue), fimbria/fornix (green) and fasciculus retroflexus (yellow). At the developmental stage examined (GD 17), the CC is rostrally placed and relatively small. Additionally identifiable are the anterior commissure with its bilateral olfactory projections (figure 3.3o, white arrow), and the fimbria/fornix (figure 3.3o, green fibers). The latter normally project from the hippocampus rostrally and medially to the septal region, then extend as the columns of the fornix ventrally and

caudally through the thalamus (figure 3.3o, pink arrow). Portions of these fibers normally cross the midline to form the hippocampal commissure. Bilateral tracts illustrated in yellow represent the fasciculus retroflexus, the fibers of which extend from the habenula ventrally to the interpeduncular nucleus of the midbrain (figure 3.3o).

All of the ethanol-exposed HPE fetuses examined presented with agenesis of the CC (figure 3.3, p-u). And in all of these fetuses, fiber tracts consistent with the right/left projections of the anterior commissure were present (figure 3.3, p-u, blue fiber reconstructions). However, the morphology of these tracts appeared diffuse and disorganized and the olfactory projections could not be readily identified (figure 3.3, p-u, blue fibers). Notable is that in the most severely affected animal (the fetus with alobar HPE), fibers presumed to be those of the anterior commissure were only identifiable on one side of the brain (figure 3.3u). Like the anterior commissure, the fimbria/fornix was clearly dysmorphic in all of the HPE fetuses (figure 3.3, p-u, green fibers). In these animals, the fibers from the fimbria projected rostrally, where they crossed the midline forming what appears to be the hippocampal commissure. However, these fiber tracts were significantly flattened, foreshortened and dysplastic. In most cases, the hippocampal commissure appeared to be thickened as compared to control (figure 3.3, p-u, green fibers and see also figure 3.5, l & p, yellow arrows) and the columns of the fornix (figure 3.3o, pink arrow) were absent in all of the HPE fetuses. Finally, in contrast to the significant dysmorphology of the telencephalic fiber tracts in the HPE fetuses, the fasciculus retroflexus, which projects from the

habenula to the midbrain region, appeared to be relatively normal. These fiber tracking results are consistent with the color-coded anisotropy maps shown in figure 3.1 and support the premise that ethanol exposure restricted to early gastrulation stages has a major selective impact on the telencephalic region.

In addition to the major fiber tract malformations shown in figures 3.1-3.3, the presence of Probst bundles in an ethanol exposed HPE subject was discovered by examination of the color-coded anisotropy maps (figure 3.4). Probst bundles are common in cases of CC agenesis and result from fibers not being able to cross the midline. Rather, these abnormal fibers project in an anterior/posterior direction, and interestingly, have been characterized using DTI in humans (eg. Lee et al., 2004; Tovar-Moll et al., 2005; Utsunomiya et al., 2006) as well as in a mouse knock out model (Ren et al., 2007). Here, the fibers of the CC should appear red, running horizontally as they cross the midline just dorsal to the septal region (white arrow in the control image shown in figure 3.4 b). In contrast, in the HPE subject, which has no septal region, bilateral regions of green color-coded high anisotropy, were located just dorsal to the united lateral ventricles (figure 3.4 d, e, white arrows). This represents fibers projecting in an anterior/posterior direction as characterizes Probst bundles. Subsequent histological assessments of this subject confirmed this finding (figure 3.4f, arrows).

Dysmorphology in non-HPE fetuses

Consistent with individuals with FASDs, some of the fetuses exposed to ethanol on GD7 did not present with frank facial or CNS dysmorphology. However, through the evaluation of color-coded anisotropy images, subtle deficits were identified. Figure 3.5 illustrates data from 2 of 7 representative ethanol-exposed fetuses included in this analysis that, due to their facial or brain phenotypes, are considered not to have HPE. For comparison, data from a control and a HPE subject are also included in this figure (figure 3.5 a,e,i,m; d,h,l,p, respectively). In one of these non-HPE ethanol-exposed fetuses, the face appears comparable to the control and the 3D brain reconstruction reveals only somewhat smaller olfactory bulbs than in the control (figure 3.5 b, f). Notably, however, as compared to both the horizontal and midsagittal color-coded anisotropy maps of the control fetus (figure 3.5, l & m), evidence of a CC (white arrows) cannot be discerned in this fetus (figure 3.5, j & n). Despite this, the hippocampal commissure (figure 3.5, j & n, yellow arrow), fornix columns (figure 3.5, j & n, blue arrowhead) and anterior commissure (figure 3.5, j & n, pink arrow) appear normal. In the fetus illustrated in the adjacent column in figure 3.5 (figure 3.5 c,g,k,o), while the facial features are consistent with HPE (compare to its littermate which has HPE, figure 3.3f), the CC is apparently normal (figure 3.5, k & o). However, the anterior commissure (pink arrow) appeared diffuse, consistent with that in HPE. The olfactory projections of this fiber tract were discernable, however.

Illustrated in the last column of figure 3.5 (d,h,i,p), is the fetus with HPE whose face is shown in figure 3.3d. 3D reconstruction of the brain of this animal illustrates rostral union of the cerebral cortices and absence of the olfactory bulbs. Further, as was shown in the fiber tract reconstructions in figure 3.3, color-coded maps show agenesis of the CC (figure 3.5, l & p, no white arrow as seen in figure 3.3 i & m), evidence of a dysplastic hippocampal commissure (figure 3.5, l & p, yellow arrow), and a diffuse anterior commissure (figure 3.5, p, pink arrow). Indicated by a blue arrowhead in figure 3.4p is a median band of blue signal (superior/inferior projecting fibers) that appears to be consistent with the appearance of the fornix columns (figure 3.5 m – o, blue arrowheads). These fibers are not picked up with fiber tracking, presumably due to their discontinuity with the fimbria/fornix (see figure 3.3r).

Persistence of fiber tract anomalies into the postnatal period

As for fetal stages, exposure to ethanol on day 7 of gestation results in fiber tract anomalies that can be identified in periadolescent animals (figure 3.6). As illustrated in figure 3.6, in the ethanol-exposed postnatal day 45 mice, the CC and other commissural fibers are abnormal. Shown are 2 animals, one of which is more mildly affected than the other. As compared to the control brain, shown in the coronal and midsagittal planes (figure 3.6, a & b, respectively), the CC of the more mildly affected animal shown in c & d is somewhat thinned, a reduction that is particularly evident in the region of the body (figure 3.6, d, white arrow). No other apparent dysmorphology was appreciated. In the more severely affected

brain shown in figure 3.6 e & f, reduction in the CC can be readily seen in both the coronal and mid-sagittal views (figure 3.6, e & f, white arrow). Again, the deficiency is most evident in the CC body, though, even in the control, this is the narrowest region. Additionally, this animal presented with thinning of the ventral hippocampal commissure (figure 3.6, e, yellow arrow) and readily apparent dilation of the lateral ventricles (figure 3.6, e, star). Importantly, the finding that animals with obvious CNS abnormalities resulting from acute GD7 high dose ethanol exposure remain viable to (and through) adolescence, strengthens the validity of this FASD model and allows for subsequent structure/function correlational analyses.

DISCUSSION

Reported are brain fiber tract anomalies in fetal and periadolescent mice that result from acute high dose ethanol exposure on GD7. Consistent with our previous report describing high-resolution MRM to characterize fetal brain anomalies resulting from ethanol exposure at this early developmental stage (Godin et al., 2010), defects representing a wide range of severity and including HPE were seen.

HPE is the term used to describe a spectrum of complex brain and facial anomalies, all of which are associated with median forebrain deficiency. Although HPE is apparent in only 1/10,000 live births (Croen et al., 1996; Rasmussen et al., 1996; reviewed by Leoncini et al., 2008), it is present in as many as 1/250 human conceptuses (Matsunaga & Shiota, 1977), making it the most common

birth defect. There are a number of HPE subtypes including, from most to least severe, alobar, semi-lobar, lobar and a middle interhemispheric variant (MIH) (reviewed by Hahn & Barnes, 2010). For the current study, the majority of the fetal HPE brains examined could be classified as lobar or semi-lobar (figure 3.3 b-f) as at least some degree of cerebral cortical separation was evident (see figure 3.3 i-m). Alobar HPE was identified in 1 fetus examined in this study, the cebocephalic animal shown in figure 3.3, f & m. As expected, marked fiber tract abnormalities including deficits in forebrain commissural fibers were found in all of the HPE fetuses examined.

CC abnormalities in human HPE include its complete absence in the alobar subtype and rostral to caudal loss of its fibers, with preservation of the splenium, as severity increases from lobar to semi-lobar forms (reviewed by Hahn & Barnes, 2010). In the fetal mice examined for the current report, the CC was not identified in any of those with HPE. Additionally, CC anomalies were detected in ethanol-exposed fetuses, as well as postnatal animals without overt HPE. It is important to note that only the rostral portion of the CC is normally visible in mice at the fetal stage examined. As shown by Ozaki & Wahlsten (1992), the first fibers of the CC that cross the midline form the genu and cross on approximately GD16.3 in the mouse, roughly 24 hours prior to the fetal assessments conducted here. This is consistent with a DTI-based study by Zhang and colleagues (2003) in which the CC was shown to be present in GD17 fetuses, but not in those examined 24 hours earlier. In the current study, among the fetal subjects in which a CC was not identified, the possibility that this was

due to a developmental delay in the crossings of these fibers is possible, but unlikely. This is because the overall size and morphology of the ethanol-exposed subjects was consistent with that of the GD17 controls and because defects in this fiber tract were also evident in animals examined at postnatal stages.

The finding that the CC is a major target of ethanol teratogenesis is not novel; some of the earliest reports documenting brain defects among individuals exposed to ethanol prenatally document anomalies in this fiber tract (eg. Jones & Smith, 1973; Clarren et al., 1978; Coulter et al., 1993). In more recent years, imaging applications have shown morphological alterations including agenesis and hypoplasia of this structure in individuals with full blown Fetal Alcohol Syndrome (FAS; eg. Autti-Ramo et al., 2002; Bhatara et al., 2002; Johnson et al., 1996; Mattson et al., 1992; Riley et al., 1995; reviewed by Norman et al., 2009), and more subtle shape changes or deficits in its volume in individuals with FASDs (eg. Astley et al., 2009; Bookstein et al., 2002a,b; Sowell et al., 2001). Extending these morphological analyses of the CC in individuals with FASDs are recent DTI-based white matter microstructure assessments in which alterations in CC FA and MD measures have been identified (Fryer et al., 2009; Lebel et al., 2008, 2010; Li et al., 2009; Ma et al., 2005; Sowell et al., 2008; Wozniak et al., 2006; 2009).

Overall, human DTI studies have illustrated microstructural anomalies in the genu, body, splenium and isthmus of the CC, with deficits in the posterior regions (splenium) being among the most consistent findings across studies (reviewed by Norman et al., 2009). In the fetal mice examined for the current

investigation, deficits involving the anterior part of the CC and including the genu could be confirmed, but assessment of the most posterior aspects of the CC was not possible given the CC's protracted development. Importantly, among the ethanol-exposed postnatal animals described, the entire CC appeared reduced in size, with the body of the CC appearing most affected. This could represent a relative change since the body is normally the narrowest region. MRI studies illustrating cases of CC hypoplasia after prenatal ethanol exposure also show patterns of effects consistent with our current findings in postnatal animals (eg. Mattson et al., 1992; Riley et al., 1994). Of additional interest, reduction to absence of the body, with retention of the genu and splenium is consistent with the pattern of CC anomalies present in the MIH variant of HPE (reviewed by Hahn & Barnes, 2010).

In addition to deficits in the CC, the other fiber tract anomalies found in the HPE subjects in this study were absence of the columns of the fornix and the olfactory projections of the anterior commissure, and dysplastic anterior commissures and fimbria/fornices. These defects are comparable to those reported in a DTI-based investigation of human HPE (eg. Rollins et al., 2005). Among the non-HPE ethanol-exposed fetuses the anterior commissure was also observed to be affected, though more subtly than in the HPE animals. Notably, while agenesis or hypoplasia of the anterior commissure has been reported in autopsy reports of individuals with FAS (Clarren et al., 1978; Peiffer et al., 1979; Coulter et al., 1993), neuroimaging studies have not identified deficits in this fiber tract. It is expected that in future human FASD studies in which measures of

diffusivity are employed, subtle alterations will be detected in many of the same fiber tracts shown in the current investigation to be targets of ethanol teratogenesis.

In addition to the major fiber tract anomalies reported herein, DTI allowed assessment of cellular orientation in the fetal cerebral cortex. As opposed to in the mature brain where anisotropy levels (FA) are low in cortical regions, in the fetal brain cortical FA values are normally high. This is presumably due to the presence of very ordered radial glia which provide the scaffolding for neuronal migration; a process that occurs during the developmental stage examined in this study (eg. Mori et al., 2001; Zhang et al., 2003). Aberrancies in cortical cellular orientation that were noted to accompany loss of median tissue in the frontal cortical regions in the fetal HPE mice are of particular interest due to an expected adverse effect on cell migration. In particular, this finding may help to explain the occurrence of cerebral cortical heterotopias as previously reported in mice following treatment with the same ethanol exposure paradigm as employed for this study (Godin et al., 2010) or in other models of prenatal ethanol exposure (Mooney et al., 2004; Komatsu et al., 2001, Sakata-Haga et al., 2004). More detailed histological analyses as well as examination of the potential functional consequences of the disordered cortex following GD7 ethanol exposure in mice are warranted. Recognizing the strong positive correlation of cortical migration errors with seizure activity (Verotti et al., 2009), in concert with the occurrence of increased seizure activity (eg. Sun et al., 2009) and cortical heterotopias (eg.

Jones et al., 1975; Coulter et al., 1993) in human FASD, makes these future studies particularly compelling.

Data provided in the current study clearly demonstrate that DTI is a valuable technique for dysmorphology investigations. As elegantly previously shown (eg. Zhang et al., 2003; 2006), and as also described herein, DTI affords excellent contrast in the developing brain, allowing not only the identification of major fiber tracts even prior to the onset of myelination, but delineation of various cerebral cortical layers. For the current investigation, utilization of high resolution isotropic scans allowed accurate assessments in every anatomical plane, greatly facilitating discovery of the teratogen-induced brain defects. This technique is not without limitations, however. The restricted availability of high field strength imaging systems is problematic, and hourly costs remain high with lengthy imaging times required for each specimen. Currently, therefore, it is not feasible to involve large numbers of subjects in DTI studies. As imaging technologies advance, new discoveries will undoubtedly be made, providing for shorter imaging times and larger cohorts sizes.

In conclusion, that DTI can be fruitfully applied to the study of stage-dependent effects of prenatal ethanol exposure in both fetal and postnatal animals was illustrated herein. Alterations were identified in a number of major fiber tracts following an acute ethanol exposure occurring at early gastrulation stages in mice. Importantly, the fiber deficits illustrated are consistent with white matter anomalies reported in individuals with severe cases of FASD and with HPE. Based on these results, planned and ongoing studies are directed toward

quantifying diffusion parameters in the brains of both fetal and postnatal mice, and to correlating changes in these diffusion parameters to behavioral and functional consequences of prenatal ethanol exposure.

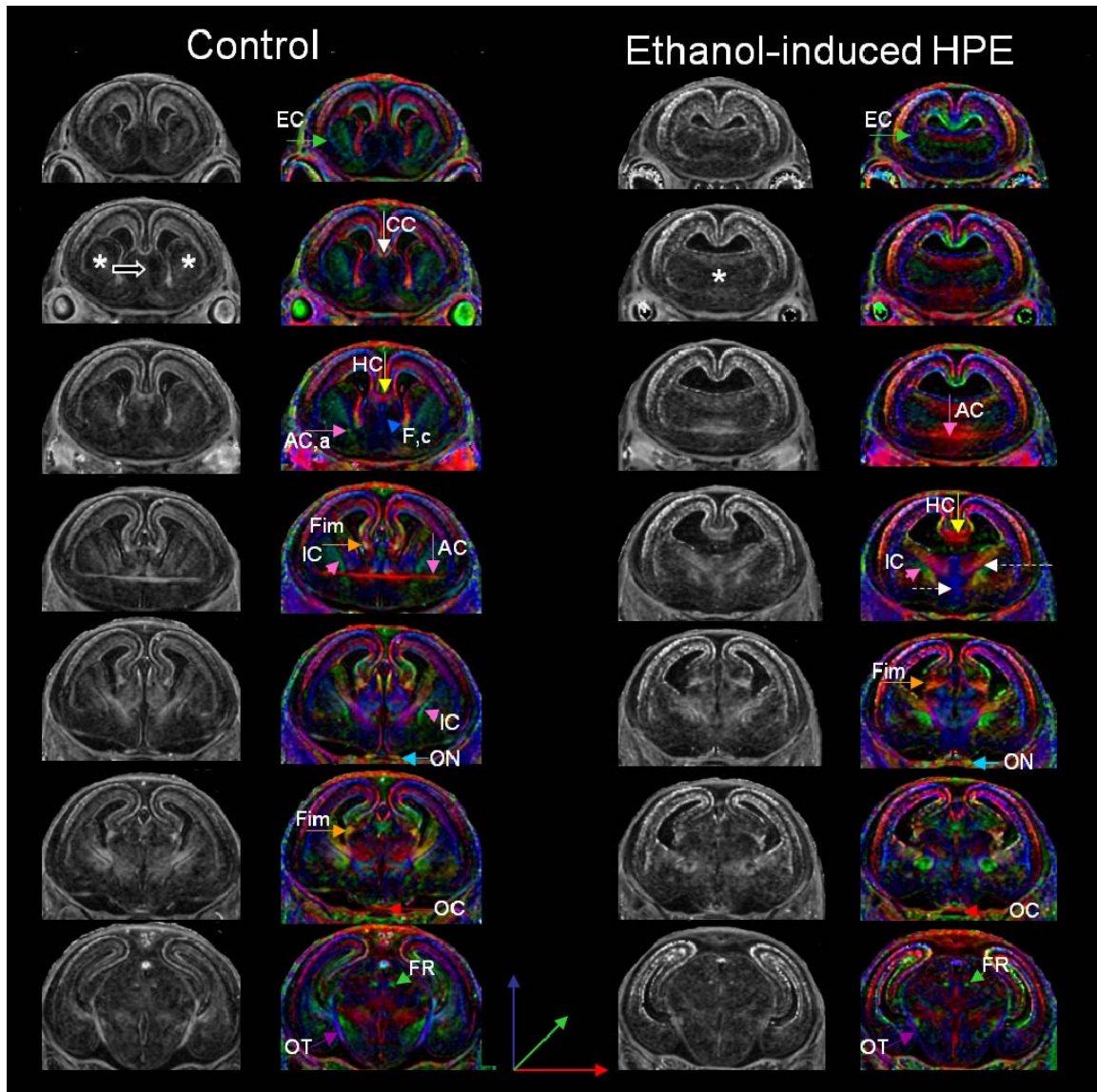


Figure 3.1: Illustrated are serial coronal sections of the brain showing fractional anisotropy (FA) (left) and color-coded directional FA maps (right) in a control and a prenatal ethanol-exposed HPE subject. The sections of the brain that are shown begin at the level of the eye and move caudally through the level of the thalamus. Major fiber tracts in the control animal and anomalies associated with HPE in the ethanol-exposed animal are indicated. Illustrated in the HPE subject are major fiber tract anomalies including agenesis of the CC, along with defects involving the anterior commissure, fimbria, fornix, hippocampal commissure, external capsule and internal capsule. Stars = striatum; block arrow = septal region; EC, green arrow = external capsule; CC, white arrow = CC; HC, yellow

arrow = hippocampal commissure; F. c, blue arrowhead = fornix columns; AC, pink arrow = anterior commissure; AC, a, pink arrow = olfactory projections of anterior commissure; IC, pink arrowhead = internal capsule; Fim, orange arrow = fimbria; ON, blue arrow = optic nerve; OC, red arrow = optic chiasm; OT, purple arrow = optic tract; FR, green arrowhead = fasciculus retroflexus. Color coded fiber tract directionality is indicated by blue (superior/inferior), green (anterior/posterior) and red (right/left) arrows.

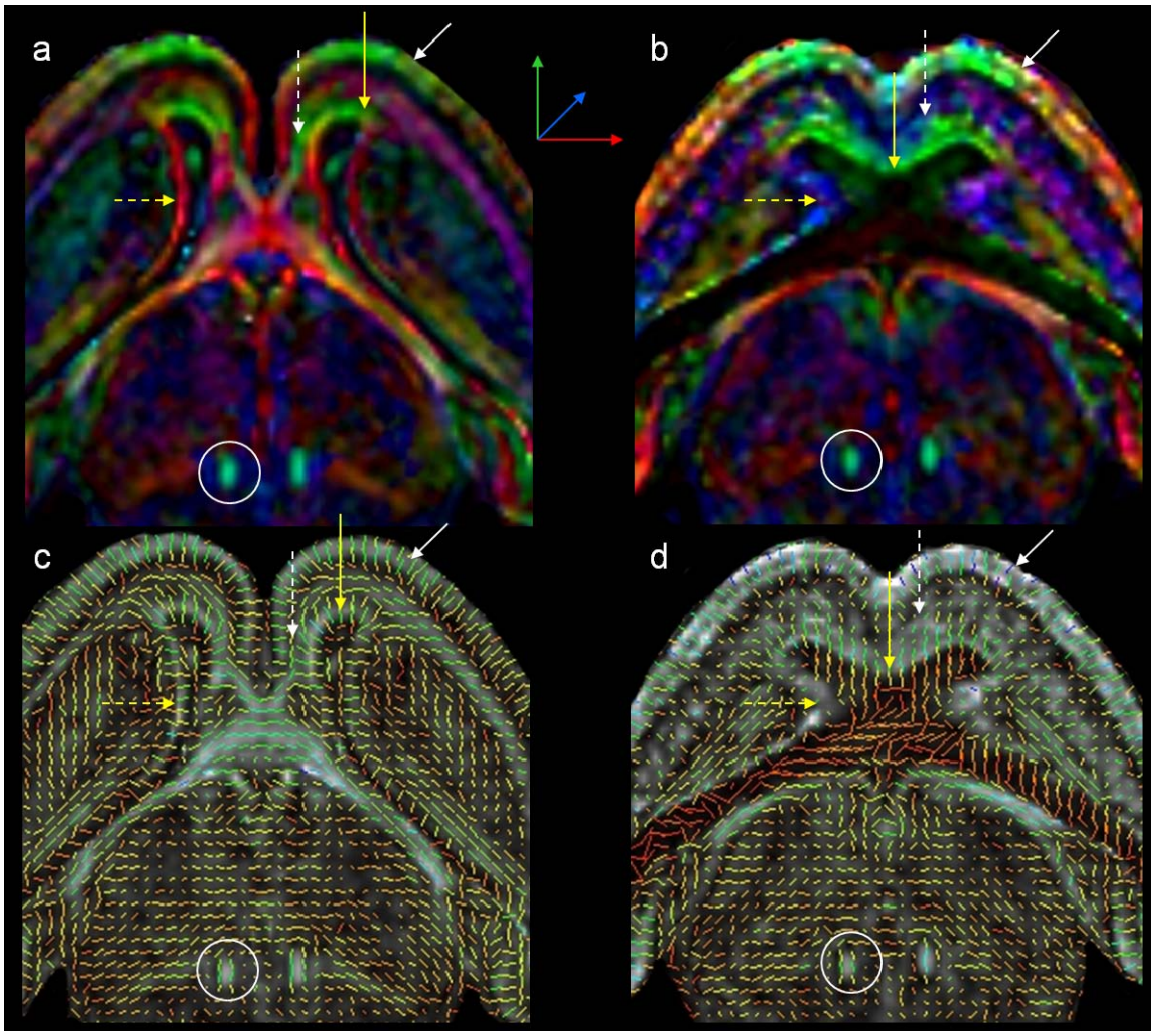


Figure 3.2: Shown are horizontal scans presented as color-coded anisotropy maps and glyphs overlaid on an FA image of a control (a & c) and an HPE subject (b & d). Illustrated are the various layers of the cerebral cortex. The cortical plate (white arrows), which contains cellular components that are oriented perpendicular to the surface of the cerebral cortices are evidenced by the transition of this region from green to red as one moves medially in the color coded FA maps (a) as well as the glyphs (c) in the control subject. The cortical plate, while seen in the HPE subject (b & d), lacks the medial regions. Additionally evident is the intermediate zone (dashed arrows) that contains cellular components that are oriented parallel to the surface of the brain as indicated by their green color in the midline of the control (a & c). The intermediate zone in the HPE animal is difficult to identify (b & d) and large

regions of blue signal (indicative of fibers projecting in the superior/inferior direction) in the middle cortical layers are seen. The subventricular zone, which is seen as a thin layer of high FA perpendicular to the ventricles in the control (a & c) is also apparent but appears to be thickened in the HPE subject (b & d). Color coded fiber tract directionality is indicated by blue (superior/inferior), green (anterior/posterior) and red (right/left) arrows.

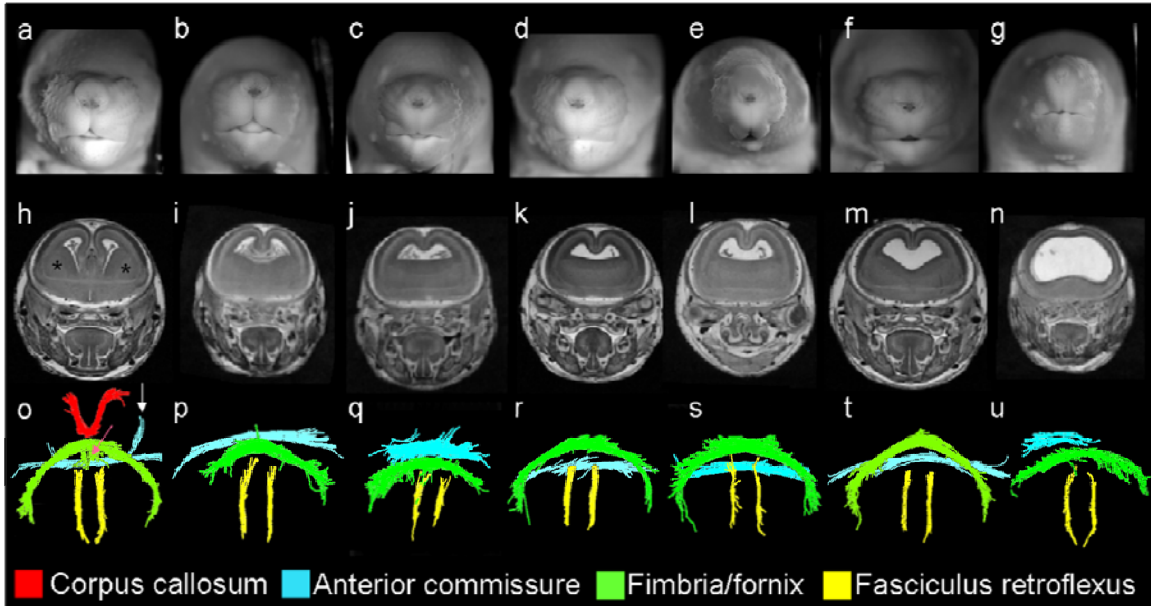


Figure 3.3: Illustrated are faces, coronal MRI scans at the level of the anterior commissure, and 3D reconstructed fiber tracts from a control (a, h, o) and 6 GD17 mouse fetuses with holoprosencephaly (HPE) (b-g; i-n; p-u). Varying degrees of dysmorphology involving the upper lip are present in the ethanol-treated subjects (b-g) as compared to the control (a). Brain dysmorphology is also evident and expression is variable in the ethanol-exposed fetuses (i-n) as compared to the control (h). In the animal having a single central nostril (the cebocephalic fetus in g), the brain was more severely affected than in any of the others in this group (n). Fibertracking results illustrate grossly observable abnormalities involving the CC (red), anterior commissure (blue), and fimbria/fornix (green). Notable are the lack of CC, olfactory projections of the anterior commissure (o, white arrow) and fornix columns (o, pink arrow) in ethanol-exposed HPE fetuses. In contrast to substantial forebrain dysmorphology, the fasciculus retroflexus (yellow) is present in all ethanol-exposed subjects bilaterally and appear in most cases to be relatively unaffected.

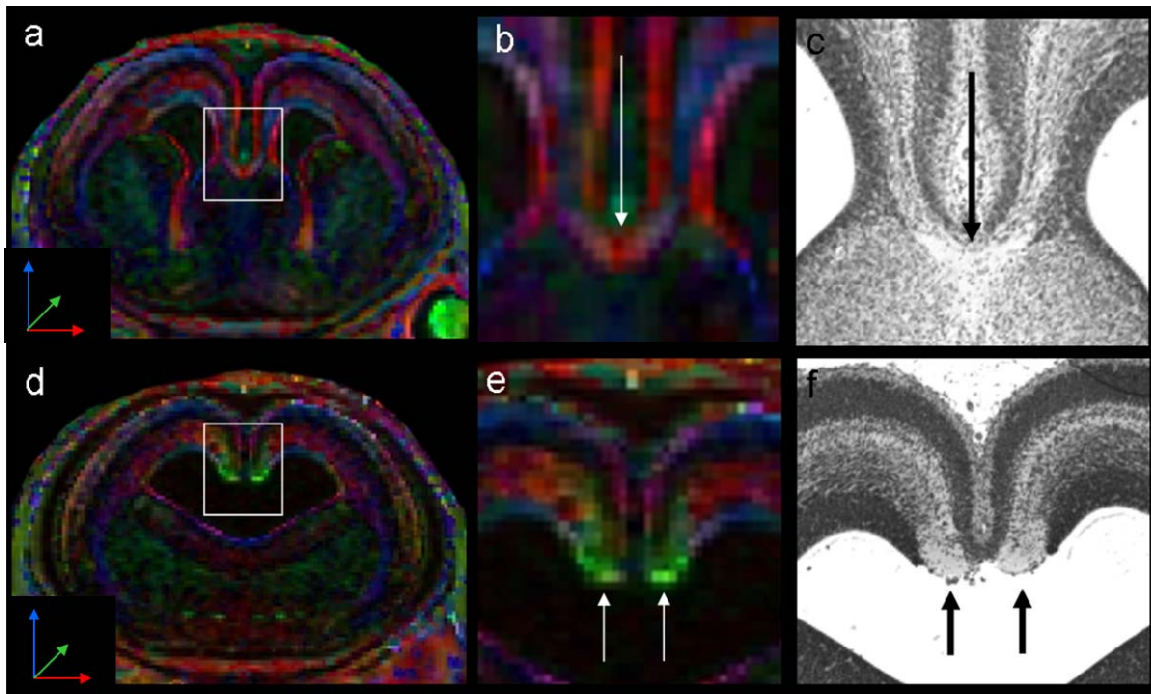


Figure 3.4: Shown are color-coded anisotropy maps (a,b; d,e) and histological sections (c, f) of a control (a-c) and prenatal ethanol-exposed HPE (d-f) mouse fetus. As evident in coronal scans, as compared to a control GD17 fetus (a & b), the HPE fetus (d & e) is lacking median-crossing CC fibers (b, arrow in control). Rather, regions of high anisotropy that are green, indicative of fibers that project in the anterior/posterior direction, are seen (e, white arrows). Routine histology confirmed this finding (compare c and f), illustrating a defect consistent with Probst bundles (f, black arrows). Color coded fiber tract directionality is indicated by blue (superior/inferior), green (anterior/posterior) and red (right/left) arrows.

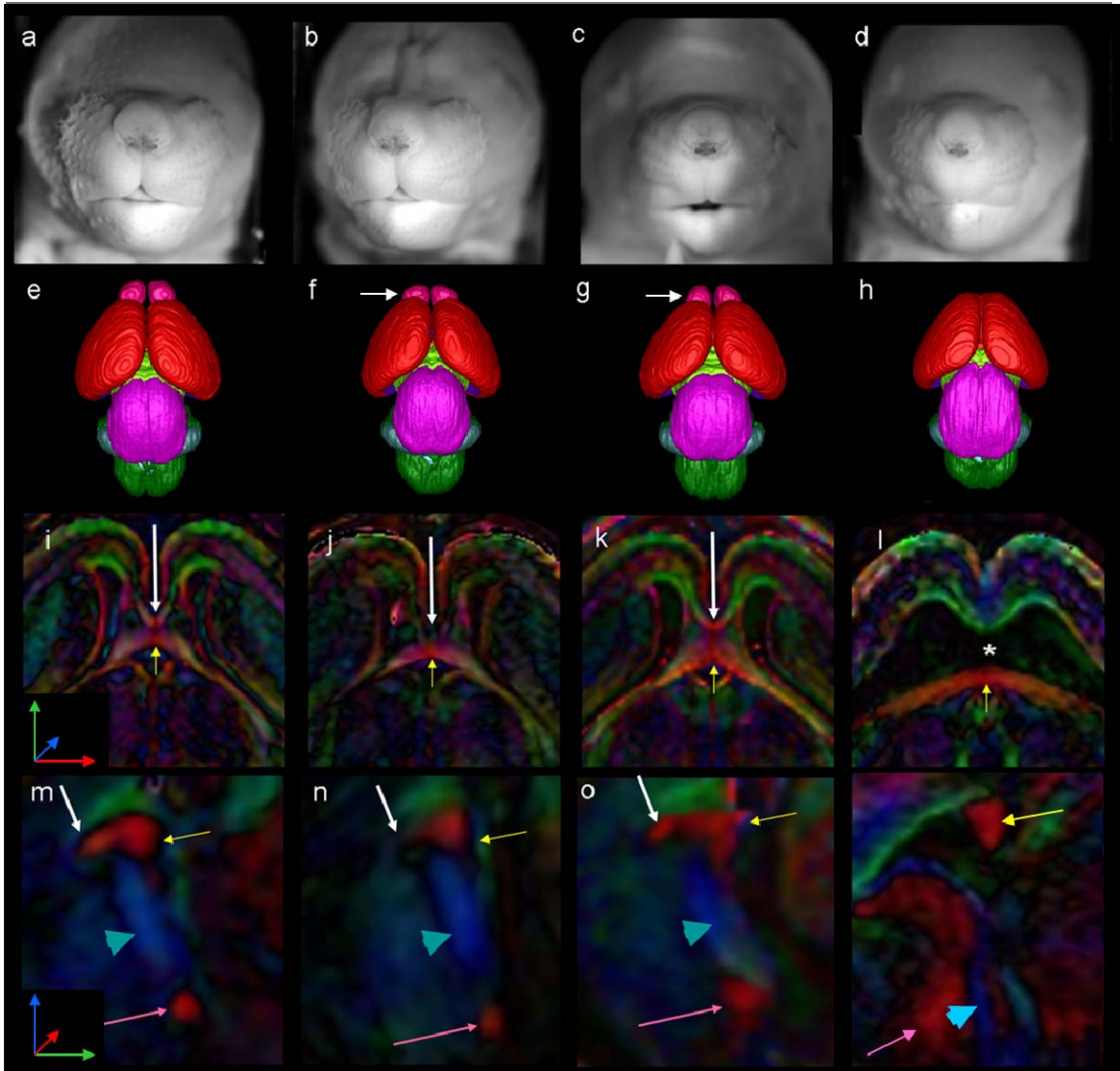


Figure 3.5: Illustrated are faces (a-d), 3D MRM brain reconstructions (e-h), and horizontal (i-l) and midsagittal (m-p) color-coded FA maps from a control mouse fetus (a, e, i, m) and three that were exposed to ethanol on GD 7(b-d; f-h; j-l; n-p). The facial images illustrate the normal morphology of the control (a), an ethanol exposed animal with no apparent facial dysmorphism (b), and two fetuses whose faces includes characteristic GD7 ethanol-induced facial dysmorphism (c & d). Note that the brain of the ethanol-exposed animal without facial dysmorphism (b) appears normal (as compared to the control brain show in e) with a slight reduction in the size of the olfactory bulbs (magenta, arrow), the brain of the fetus illustrated in c appears to have small and somewhat dysmorphic olfactory bulbs, with the left side being more affected (magenta,

arrow). The brain in h is characterized by considerable dysmorphology, corresponds to the most severely affected face (d) and is consistent with holoprosencephaly (HPE). Note the absence of olfactory bulbs and anterior interhemispheric fissure. In color-coded FA maps made in the axial (i-l) and mid-sagittal plane (m-p l), red, blue, and green indicate fibers running in the right/left, inferior/superior, and anterior/posterior directions, respectively. As compared to the control (i & m), in the ethanol-exposed fetuses shown in b and d, no CC (white arrow) could be identified. However, in the subject shown in c, a CC was apparent despite significant facial dysmorphology. The anterior commissure among ethanol-exposed animals appears diffuse, especially in the subjects with frank facial dysmorphology (pink arrow, o & p). In the holoprosencephalic animal, the hippocampal commissure (yellow arrow) appears thickened and dysplastic (p) and the columns of the fornix (blue arrowhead) are absent as compared to the other subjects though a region of high FA projecting in the superior/inferior direction is apparent. Color coded fiber tract directionality is indicated by blue (superior/inferior), green (anterior/posterior) and red (right/left) arrows.

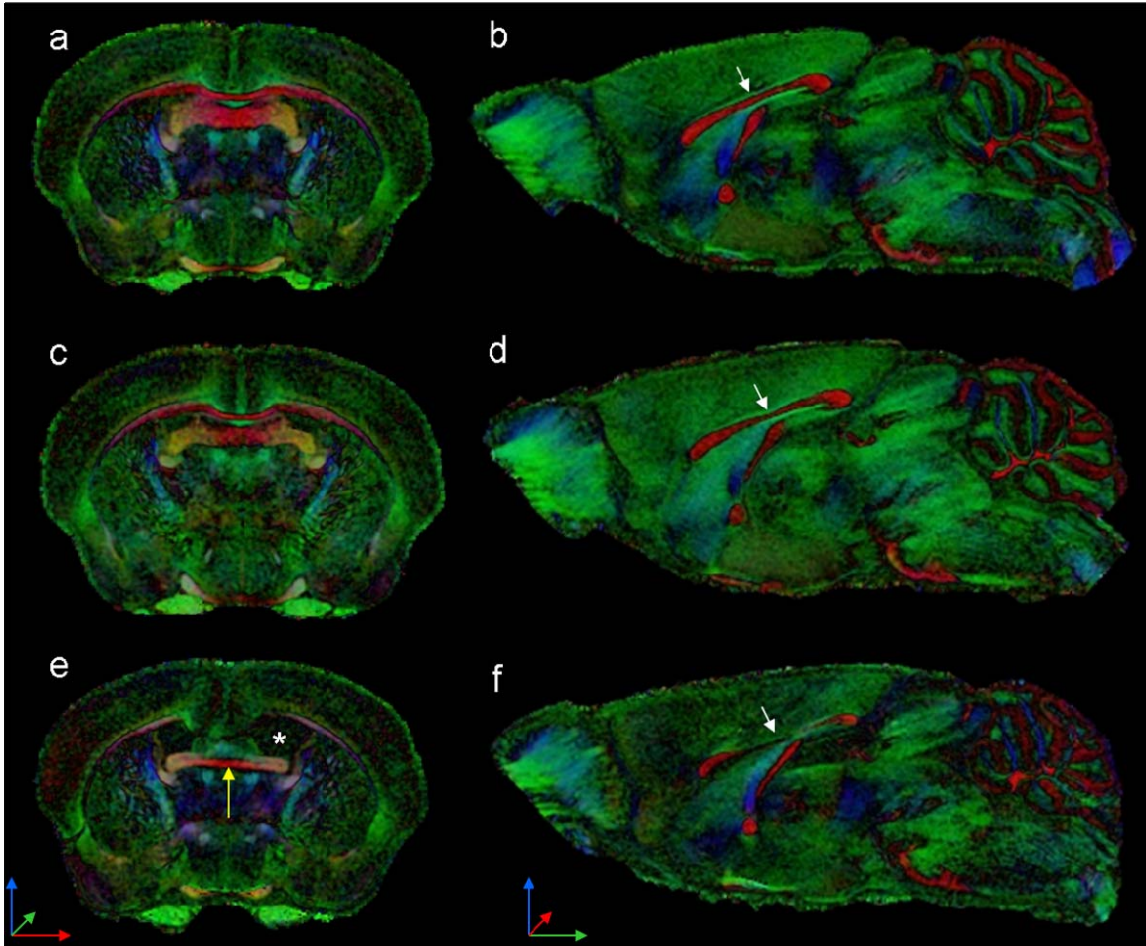


Figure 3.6: Illustrated are coronal and mid-sagittal color-coded anisotropy maps from a control (a & b) and two ethanol-exposed (c & d; e & f) male mice at postnatal day 45. As compared to the control (a & b), the subject depicted in c & d has a mild thinning of the CC which is especially apparent at the level of the body (d, white arrow). The subject depicted in e & f shows considerably dysmorphology of the CC (f, white arrow) consistent with partial agenesis of the CC. Also evident in this animal is dilation of the lateral ventricles (e, stars), as well as a deficient hippocampal commissure (e, yellow arrow). Color coded fiber tract directionality is indicated by blue (superior/inferior), green (anterior/posterior) and red (right/left) arrows.

REFERENCES

- Alexander DC, Pierpaoli C, Basser PJ, Gee JC (2001) Spatial transformations of diffusion tensor magnetic resonance images. *IEEE Trans Med Imaging* 20:1131-1139.
- Astley SJ, Aylward EH, Olson HC, Kerns K, Brooks A, Coggins TE, Davies J, Dorn S, Gendler B, Jirikowic T, Kraegel P, Maravilla K, Richards T (2009) Magnetic resonance imaging outcomes from a comprehensive magnetic resonance study of children with fetal alcohol spectrum disorders. *Alcohol Clin Exp Res* 33:1671-1689.
- Autti-Ramo I, Autti T, Korkman M, Kettunen S, Salonen O, Valanne L (2002) MRI findings in children with school problems who had been exposed prenatally to alcohol. *Dev Med Child Neurol* 44:98-106.
- Basser PJ, Mattiello J, LeBihan D (1994) MR diffusion tensor spectroscopy and imaging. *Biophys J* 66:259-267.
- Basser PJ, Pierpaoli C (1996) Microstructural and physiological features of tissues elucidated by quantitative-diffusion-tensor MRI. *J Magn Reson B* 111:209-219.
- Bhatara VS, Lovrein F, Kirkeby J, Swayze V, 2nd, Unruh E, Johnson V (2002) Brain function in fetal alcohol syndrome assessed by single photon emission computed tomography. *S D J Med* 55:59-62.
- Bonthius DJ, West JR (1990) Alcohol-induced neuronal loss in developing rats: increased brain damage with binge exposure. *Alcohol Clin Exp Res* 14:107-118.
- Bookstein FL, Sampson PD, Connor PD, Streissguth AP (2002) Midline corpus callosum is a neuroanatomical focus of fetal alcohol damage. *Anat Rec* 269:162-174.
- Bookstein FL, Streissguth AP, Sampson PD, Connor PD, Barr HM (2002) Corpus callosum shape and neuropsychological deficits in adult males with heavy fetal alcohol exposure. *Neuroimage* 15:233-251.
- Clarren SK, Alvord EC, Jr., Sumi SM, Streissguth AP, Smith DW (1978) Brain malformations related to prenatal exposure to ethanol. *J Pediatr* 92:64-67.

Cohen MM, Jr. (2006) Holoprosencephaly: clinical, anatomic, and molecular dimensions. *Birth Defects Res A Clin Mol Teratol* 76:658-673.

Coulter CL, Leech RW, Schaefer GB, Scheithauer BW, Brumback RA (1993) Midline cerebral dysgenesis, dysfunction of the hypothalamic-pituitary axis, and fetal alcohol effects. *Arch Neurol* 50:771-775.

Croen LA, Shaw GM, Lammer EJ (1996) Holoprosencephaly: epidemiologic and clinical characteristics of a California population. *Am J Med Genet* 64:465-472.

Demyer W, Zeman W, Palmer CG (1964) The Face Predicts the Brain: Diagnostic Significance of Median Facial Anomalies for Holoprosencephaly (Arhinencephaly). *Pediatrics* 34:256-263.

Fryer SL, Schweinsburg BC, Bjorkquist OA, Frank LR, Mattson SN, Spadoni AD, Riley EP (2009) Characterization of white matter microstructure in fetal alcohol spectrum disorders. *Alcohol Clin Exp Res* 33:514-521.

Gering D, Nabavi A, Kikinis R, Grimson W, Hata N, Everett P, Jolesz F, Wells W (1999) An Integrated Visualization System for Surgical Planning and Guidance using Image Fusion and Interventional Imaging. . In: *Int Conf Med Image Comput Comput Assist Interv.*

Godin EA, O'Leary-Moore SK, Khan AA, Parnell SE, Ament JJ, Dehart DB, Johnson BW, Allan Johnson G, Styner MA, Sulik KK Magnetic resonance microscopy defines ethanol-induced brain abnormalities in prenatal mice: effects of acute insult on gestational day 7. *Alcohol Clin Exp Res* 34:98-111.

Goodlett CR, Pearlman AD, Lundahl KR (1998) Binge neonatal alcohol intubations induce dose-dependent loss of Purkinje cells. *Neurotoxicol Teratol* 20:285-292.

Hahn JS, Barnes PD Neuroimaging advances in holoprosencephaly: Refining the spectrum of the midline malformation. *Am J Med Genet C Semin Med Genet* 154C:120-132.

Huppi PS, Maier SE, Peled S, Zientara GP, Barnes PD, Jolesz FA, Volpe JJ (1998) Microstructural development of human newborn cerebral white matter assessed in vivo by diffusion tensor magnetic resonance imaging. *Pediatr Res* 44:584-590.

Huppi PS, Dubois J (2006) Diffusion tensor imaging of brain development. *Semin Fetal Neonatal Med* 11:489-497.

Jiang Y, Johnson GA Microscopic diffusion tensor imaging of the mouse brain. *Neuroimage* 50:465-471.

Johnson VP, Swayze VW, II, Sato Y, Andreasen NC (1996) Fetal alcohol syndrome: craniofacial and central nervous system manifestations. *Am J Med Genet* 61:329-339.

Jones KL, Smith DW (1973) Recognition of the fetal alcohol syndrome in early infancy. *Lancet* 302:999-1001.

Jones KL, Smith DW (1975) The fetal alcohol syndrome. *Teratology* 12:1-10.

Kaufman MH (1992) *The Atlas of Mouse Development*. San Diego: Academic Press.

Komatsu S, Sakata-Haga H, Sawada K, Hisano S, Fukui Y (2001) Prenatal exposure to ethanol induces leptomeningeal heterotopia in the cerebral cortex of the rat fetus. *Acta Neuropathol* 101:22-26.

Lebel C, Rasmussen C, Wyper K, Andrew G, Beaulieu C Brain microstructure is related to math ability in children with fetal alcohol spectrum disorder. *Alcohol Clin Exp Res* 34:354-363.

Lebel C, Rasmussen C, Wyper K, Walker L, Andrew G, Yager J, Beaulieu C (2008) Brain diffusion abnormalities in children with fetal alcohol spectrum disorder. *Alcohol Clin Exp Res* 32:1732-1740.

Lee SK, Mori S, Kim DJ, Kim SY, Kim DI (2004) Diffusion tensor MR imaging visualizes the altered hemispheric fiber connection in callosal dysgenesis. *AJNR Am J Neuroradiol* 25:25-28.

Lee SK, Kim DI, Kim J, Kim DJ, Kim HD, Kim DS, Mori S (2005) Diffusion-tensor MR imaging and fiber tractography: a new method of describing aberrant fiber connections in developmental CNS anomalies. *Radiographics* 25:53-65; discussion 66-58.

Leoncini E et al. (2008) Frequency of holoprosencephaly in the International Clearinghouse Birth Defects Surveillance Systems: searching for population variations. *Birth Defects Res A Clin Mol Teratol* 82:585-591.

Li L, Coles CD, Lynch ME, Hu X (2009) Voxelwise and skeleton-based region of interest analysis of fetal alcohol syndrome and fetal alcohol spectrum disorders in young adults. *Hum Brain Mapp* 30:3265-3274.

Lipinski RJ, Godin EA, O'Leary-Moore SK, Parnell SE, Sulik KK Genesis of teratogen-induced holoprosencephaly in mice. *Am J Med Genet C Semin Med Genet* 154C:29-42.

Ma X, Coles CD, Lynch ME, Laconte SM, Zurkiya O, Wang D, Hu X (2005) Evaluation of corpus callosum anisotropy in young adults with fetal alcohol syndrome according to diffusion tensor imaging. *Alcohol Clin Exp Res* 29:1214-1222.

Maier SE, Miller JA, Blackwell JM, West JR (1999) Fetal alcohol exposure and temporal vulnerability: regional differences in cell loss as a function of the timing of binge-like alcohol exposure during brain development. *Alcohol Clin Exp Res* 23:726-734.

Matsunaga E, Shiota K (1977) Holoprosencephaly in human embryos: epidemiologic studies of 150 cases. *Teratology* 16:261-272.

Mattson SN, Riley EP, Jernigan TL, Ehlers CL, Delis DC, Jones KL, Stern C, Johnson KA, Hesselink JR, Bellugi U (1992) Fetal alcohol syndrome: a case report of neuropsychological, MRI and EEG assessment of two children. *Alcohol Clin Exp Res* 16:1001-1003.

Melhem ER, Mori S, Mukundan G, Kraut MA, Pomper MG, van Zijl PC (2002) Diffusion tensor MR imaging of the brain and white matter tractography. *AJR Am J Roentgenol* 178:3-16.

Mooney SM, Siegenthaler JA, Miller MW (2004) Ethanol induces heterotopias in organotypic cultures of rat cerebral cortex. *Cereb Cortex* 14:1071-1080.

Mori S, Crain BJ, Chacko VP, van Zijl PC (1999) Three-dimensional tracking of axonal projections in the brain by magnetic resonance imaging. *Ann Neurol* 45:265-269.

Mori S, Barker PB (1999) Diffusion magnetic resonance imaging: its principle and applications. *Anat Rec* 257:102-109.

Mori S, Itoh R, Zhang J, Kaufmann WE, van Zijl PC, Solaiyappan M, Yarowsky P (2001) Diffusion tensor imaging of the developing mouse brain. *Magn Reson Med* 46:18-23.

Muenke M, Cohen MM, Jr. (2000) Genetic approaches to understanding brain development: holoprosencephaly as a model. *Ment Retard Dev Disabil Res Rev* 6:15-21.

Mukherjee P, Miller JH, Shimony JS, Philip JV, Nehra D, Snyder AZ, Conturo TE, Neil JJ, McKinstry RC (2002) Diffusion-tensor MR imaging of gray and white matter development during normal human brain maturation. *AJNR Am J Neuroradiol* 23:1445-1456.

Mukherjee P, Berman JI, Chung SW, Hess CP, Henry RG (2008) Diffusion tensor MR imaging and fiber tractography: theoretic underpinnings. *AJNR Am J Neuroradiol* 29:632-641.

Neil JJ, Shiran SI, McKinstry RC, Schefft GL, Snyder AZ, Almlí CR, Akbudak E, Aronovitz JA, Miller JP, Lee BC, Conturo TE (1998) Normal brain in human newborns: apparent diffusion coefficient and diffusion anisotropy measured by using diffusion tensor MR imaging. *Radiology* 209:57-66.

Norman AL, Crocker N, Mattson SN, Riley EP (2009) Neuroimaging and fetal alcohol spectrum disorders. *Dev Disabil Res Rev* 15:209-217.

Ozaki HS, Wahlsten D (1992) Prenatal formation of the normal mouse corpus callosum: a quantitative study with carbocyanine dyes. *J Comp Neurol* 323:81-90.

Papadakis NG, Xing D, Huang CL, Hall LD, Carpenter TA. A comparative study of acquisition schemes for diffusion tensor imaging using MRI. *J Magn Reson* 1999;137:67-82

Parnell SE, O'Leary-Moore SK, Godin EA, Dehart DB, Johnson BW, Allan Johnson G, Styner MA, Sulik KK (2009) Magnetic resonance microscopy defines ethanol-induced brain abnormalities in prenatal mice: effects of acute insult on gestational day 8. *Alcohol Clin Exp Res* 33:1001-1011.

Peiffer J, Majewski F, Fischbach H, Bierich JR, Volk B (1979) Alcohol embryo- and fetopathy. Neuropathology of 3 children and 3 fetuses. *J Neurol Sci* 41:125-137.

Petiet A, Johnson GA Active staining of mouse embryos for magnetic resonance microscopy. *Methods Mol Biol* 611:141-149.

Petiet AE, Kaufman MH, Goddeeris MM, Brandenburg J, Elmore SA, Johnson GA (2008) High-resolution magnetic resonance histology of the embryonic and neonatal mouse: a 4D atlas and morphologic database. *Proc Natl Acad Sci U S A* 105:12331-12336.

Pieper S, Halle M, Kikinis R (2004) 3D SLICER. In: *Proceedings of the 1st IEEE International Symposium on Biomedical Imaging: From Nano to Macro*, pp 632-635.

Pieper S, Lorensen B, Soreder W, Kikinis R (2006) The NA-MIC Kit: ITK, VTK, Pipelines, Grids and 3D Slicer as an Open Platform for the Medical Image Computing Community. In: *Proceedings of the 3rd IEEE International Symposium on Biomedical Imaging: From Nano to Macro*, pp 689-701.

Pierpaoli C, Basser PJ (1996) Toward a quantitative assessment of diffusion anisotropy. *Magn Reson Med* 36:893-906.

Pierpaoli C, Jezzard P, Basser PJ, Barnett A, Di Chiro G (1996) Diffusion tensor MR imaging of the human brain. *Radiology* 201:637-648.

Rasmussen SA, Moore CA, Khoury MJ, Cordero JF (1996) Descriptive epidemiology of holoprosencephaly and arhinencephaly in metropolitan Atlanta, 1968-1992. *Am J Med Genet* 66:320-333.

Ren T, Zhang J, Plachez C, Mori S, Richards LJ (2007) Diffusion tensor magnetic resonance imaging and tract-tracing analysis of Probst bundle structure in Netrin1- and DCC-deficient mice. *J Neurosci* 27:10345-10349.

- Riley EP, Mattson SN, Sowell ER, Jernigan TL, Sobel DF, Jones KL (1995) Abnormalities of the corpus callosum in children prenatally exposed to alcohol. *Alcohol Clin Exp Res* 19:1198-1202.
- Riley EP, McGee CL, Sowell ER (2004) Teratogenic effects of alcohol: a decade of brain imaging. *Am J Med Genet C Semin Med Genet* 127C:35-41.
- Riley EP, McGee CL (2005) Fetal alcohol spectrum disorders: an overview with emphasis on changes in brain and behavior. *Exp Biol Med (Maywood)* 230:357-365.
- Rollins N (2005) Semilobar holoprosencephaly seen with diffusion tensor imaging and fiber tracking. *AJNR Am J Neuroradiol* 26:2148-2152.
- S P, B L, W S, R K (2006) The NA-MIC Kit: ITK, VTK, Pipelines, Grids and 3D Slicer as an Open Platform for the Medical Image Computing Community. In: *Proceedings of the 3rd IEEE International Symposium on Biomedical Imaging: From Nano to Macro*, pp 698-701.
- Sakata-Haga H, Sawada K, Ohnishi T, Fukui Y (2004) Hydrocephalus following prenatal exposure to ethanol. *Acta Neuropathol* 108:393-398.
- Schambra UB, Lauder JM, Silver K (1992) *Atlas of Prenatal Mouse Brain*. San Diego: Academic Press.
- Schambra UB (2008) *Prenatal Mouse Brain Atlas*. New York: Springer Science + Business Media.
- Sowell ER, Mattson SN, Thompson PM, Jernigan TL, Riley EP, Toga AW (2001) Mapping callosal morphology and cognitive correlates: effects of heavy prenatal alcohol exposure. *Neurology* 57:235-244.
- Sowell ER, Johnson A, Kan E, Lu LH, Van Horn JD, Toga AW, O'Connor MJ, Bookheimer SY (2008) Mapping white matter integrity and neurobehavioral correlates in children with fetal alcohol spectrum disorders. *J Neurosci* 28:1313-1319.
- Studholme C, Hill, D.L.G., Hawkes, D.J. (1999) An overlap invariant entropy measure of 3D medical image alignment. *Pattern Recognition* 32:71-86.

Sulik KK, Johnston MC, Webb MA (1981) Fetal alcohol syndrome: embryogenesis in a mouse model. *Science* 214:936-938.

Sulik KK, Johnston MC (1982) Embryonic origin of holoprosencephaly: interrelationship of the developing brain and face. *Scan Electron Microsc*:309-322.

Sulik KK (2005) Genesis of alcohol-induced craniofacial dysmorphism. *Exp Biol Med (Maywood)* 230:366-375.

Thomas JD, Wasserman EA, West JR, Goodlett CR (1996) Behavioral deficits induced by binge-like exposure to alcohol in neonatal rats: importance of developmental timing and number of episodes. *Dev Psychobiol* 29:433-452.

Tovar-Moll F, Moll J, de Oliveira-Souza R, Bramati I, Andreiuolo PA, Lent R (2007) Neuroplasticity in human callosal dysgenesis: a diffusion tensor imaging study. *Cereb Cortex* 17:531-541.

Utsunomiya H, Yamashita S, Takano K, Okazaki M (2006) Arrangement of fiber tracts forming Probst bundle in complete callosal agenesis: report of two cases with an evaluation by diffusion tensor tractography. *Acta Radiol* 47:1063-1066.

Verrotti A, Spalice A, Ursitti F, Papetti L, Mariani R, Castronovo A, Mastrangelo M, Iannetti P New trends in neuronal migration disorders. *Eur J Paediatr Neurol* 14:1-12.

Wahl M, Barkovich AJ, Mukherjee P Diffusion imaging and tractography of congenital brain malformations. *Pediatr Radiol* 40:59-67.

Webster WS, Walsh DA, McEwen SE, Lipson AH (1983) Some teratogenic properties of ethanol and acetaldehyde in C57BL/6J mice: implications for the study of the fetal alcohol syndrome. *Teratology* 27:231-243.

Wozniak JR, Mueller BA, Chang PN, Muetzel RL, Caros L, Lim KO (2006) Diffusion tensor imaging in children with fetal alcohol spectrum disorders. *Alcohol Clin Exp Res* 30:1799-1806.

Wozniak JR, Lim KO (2006) Advances in white matter imaging: a review of in vivo magnetic resonance methodologies and their applicability to the study of development and aging. *Neurosci Biobehav Rev* 30:762-774.

Wozniak JR, Muetzel RL, Mueller BA, McGee CL, Freerks MA, Ward EE, Nelson ML, Chang PN, Lim KO (2009) Microstructural corpus callosum anomalies in children with prenatal alcohol exposure: an extension of previous diffusion tensor imaging findings. *Alcohol Clin Exp Res* 33:1825-1835.

Xue R, van Zijl PC, Crain BJ, Solaiyappan M, Mori S (1999) In vivo three-dimensional reconstruction of rat brain axonal projections by diffusion tensor imaging. *Magn Reson Med* 42:1123-1127.

Yushkevich PA, Piven J, Hazlett HC, Smith RG, Ho S, Gee JC, Gerig G (2006) User-guided 3D active contour segmentation of anatomical structures: significantly improved efficiency and reliability. *Neuroimage* 31:1116-1128.

Zhang J, Richards LJ, Yarowsky P, Huang H, van Zijl PC, Mori S (2003) Three-dimensional anatomical characterization of the developing mouse brain by diffusion tensor microimaging. *Neuroimage* 20:1639-1648.

Zhang J, Richards LJ, Miller MI, Yarowsky P, van Zijl P, Mori S (2006) Characterization of mouse brain and its development using diffusion tensor imaging and computational techniques. *Conf Proc IEEE Eng Med Biol Soc* 1:2252-2255.

CHAPTER IV

VENTROMEDIAN FOREBRAIN DYSGENESIS FOLLOWS EARLY PRENATAL ETHANOL EXPOSURE IN MICE

Neurotoxicol Teratol. in prep

Abbreviated title: Prenatal ethanol-induced forebrain dysgenesis

Elizabeth A. Godin, Deborah B. Dehart, Scott E. Parnell, Shonagh K. O'Leary
Moore, Kathleen K. Sulik

Bowles Center for Alcohol Studies (EAG, DBD, SEP, SOM, KKS), University of
North Carolina, Chapel Hill, NC 27599

Corresponding Author: E.A.Godin, Fetal Toxicology Division, Bowles Center for
Alcohol Studies, University of North Carolina at Chapel Hill, CB #7178 Thurston
Bowles Building Chapel Hill, NC 27599-7178; (919) 966-3208. Email:
eamyers@med.unc.edu

Numbers of figures/tables: 5

Number of pages: 34

Key words: fetal alcohol spectrum disorders, ganglionic eminences,
holoprosencephaly, oligodendrocytes, interneurons

Sources of support: This work was supported by NIH/NIAAA grants AA007573, AA011605, AA017124; and was conducted in conjunction with the Collaborative Initiative on Fetal Alcohol Spectrum Disorders (CIFASD). Additional information about CIFASD can be found at www.cifasd.org.

ABSTRACT

Ethanol exposure on gestational day (GD) 7 in the mouse has previously been shown to result in ventromedian forebrain deficits along with facial anomalies characteristic of fetal alcohol syndrome (FAS). To further explore ethanol's teratogenic effect on the ventromedian forebrain in this mouse model, scanning electron microscopic and histological analyses were conducted. For this, time mated C57Bl/6J mice were injected with 2.9 g/kg ethanol or saline twice, at a four hour interval, on their 7th day of pregnancy. On GD 12.5, 13 and 17 control and ethanol-exposed specimens were collected and processed for light and scanning electron microscopic analyses. Gross morphological changes present in the forebrains of ethanol-exposed embryos included cerebral hemispheres that were too close in proximity or rostrally united, an enlarged foramen of Monro, enlarged or united lateral ventricles, and varying degrees of hippocampal and ventromedian forebrain deficiency. In GD12.5 control and ethanol-exposed embryos, in situ hybridization employing probes for Nkx2.1 or Fzd8 to distinguish the preoptic area (POA) and medial ganglionic eminences (MGEs) from the lateral (LGE) ganglionic eminences, respectively, confirmed the selective loss of ventromedian tissues. Immunohistochemical labeling of oligodendrocyte progenitors with Olig2, a transcription factor necessary for their specification, and of GABA, an inhibitory neurotransmitter showed ethanol-induced reductions in both. To investigate later consequences of ventromedian forebrain loss, MGE-derived somatostatin-expressing interneurons in the subpallial region of GD17 fetal mice were examined, with results showing that the somatostatin-expressing interneurons that were

present were dysmorphic in the ethanol-exposed fetuses. The potential functional consequences of this early prenatal ethanol exposure-induced reduction in interneurons and oligodendrocytes are discussed.

INTRODUCTION

Alcohol (ethanol) consumption during pregnancy is the leading known, yet preventable, cause of mental retardation in the western world (Abel and Sokol, 1986). The central nervous system (CNS) appears to be vulnerable to ethanol insult at virtually all prenatal stages, even as early as gastrulation, a process that begins during the third week of human development (Sulik, 2005). While the early vulnerability to ethanol teratogenesis has been demonstrated in a number of species, Fetal Alcohol Spectrum Disorder (FASD) studies employing mice have been particularly informative. In a well-described mouse FASD model, ethanol exposure limited to gestational day 7 (GD7), a time when gastrulation begins, has been shown to result in brain and facial abnormalities that occur in widely ranging degrees of severity (Sulik et al., 1984; Schambra et al., 1990; Godin et al., 2010). Within the spectrum of effects, are facial features and brain anomalies that are consistent with those in full-blown Fetal Alcohol Syndrome (FAS). Notable following acute GD 7 ethanol exposure in mice is deficiency involving the ventromedian forebrain, a region that in some cases is so severely diminished that the lateral ventricles are united, forming a holosphere (Sulik et al., 1984; Schambra et al., 1990; Godin et al., 2010).

For the current investigation, GD7 ethanol-induced forebrain defects in mice have been examined in greater detail than previously reported. Particular attention has been paid to the preoptic area (POA) along with the ganglionic eminences (GEs) and their derivative cell populations. The POA is that median forebrain region that is just rostral to the optic recess, at the ventral boundary of the telencephalon and diencephalon (Puelles et al., 2000). Rostral to the POA is the anterior entopeduncular area (AEP). Immediately lateral are the ganglionic eminences, which are comprised of 3 distinct regions; medial (MGE), caudal (CGE) and lateral (LGE), each of which give rise to specific cell types that migrate tangentially into the cortical plate (Anderson, 2001; Wichterle, 2001; Anderson, 2002; Valcanis and Tan, 2003; Xu, 2004; reviewed in Marin and Rubinstein, 2001). Among these cellular derivatives are interneurons, all of which express the inhibitory neurotransmitter γ -Aminobutyric acid (GABA). These GABAergic cells are divisible into subpopulations based on their molecular expression patterns. Each of the GABAergic subpopulations is derived from specific regions within the ventral telencephalon. Interneurons that migrate to the olfactory bulbs are derived from the LGEs (Menezes, 1995, Wichterle, 1999), while the CGEs give rise to calretinin (Cr)-expressing cortical interneurons (Nery, 2002). Neuropeptide Y (NPY)-expressing interneurons come from both the CGEs and POA (Gelman et al., 2009). And, derived from the MGEs are both somatostatin (Sst) and parvalbumin (Pv)-expressing cortical interneurons (Wichterle, 2001; Xu, 2003; Butt, 2007). Regarding the MGEs, it has recently been shown that it is the dorsal MGE from which the Sst-expressing interneurons arise and that the ventral MGE gives rise to the Pv-

expressing cells (Flames, 2007; Fogarty, 2007; Wonders, 2008; Xu, 2010). Sst expression is detectable prenatally while Pv-expressing interneurons are not detectable until postnatal stages.

For specification of MGE-derived interneuron subtypes, the transcription factor Nkx2.1 is required (Butt, 2008). In mice Nkx2.1 is first expressed at the 1-somite stage in the median aspect of the anterior neural plate. By the time that 11 somites have formed (approximately GD 8.5), this gene is expressed in the ventromedian telencephalon, the region from which the ganglionic eminences arise (Shimamura et al., 1995). Maintenance of Nkx2.1 expression requires both Sonic hedgehog (Shh) (Gulacsi and Anderson, 2006) and Fgf8 signaling (Storm, 2006).

In addition to interneurons, the ganglionic eminences give rise to oligodendrocytes, cells that form the myelin that insulates axons of the CNS. Oligodendrocytes arise from Nkx2.1-expressing progenitor cells that are found in the MGEs, POA, and AEP (Kessaris, 2006; Nery, 2001; Parras, 2007; Rowitch, 2004; Tekki-Kessaris, 2001). For the specification and maturation of oligodendrocyte progenitor cells, the expression of Olig2, a Shh-induced basic helix loop helix (bHLH) transcription factor, is required (Nery, 2001).

Previous studies have demonstrated prenatal ethanol exposure-mediated insult to both oligodendrocyte (Ozer, 2000) and interneuron populations (Moore, 1997; Moore, 1998; Bailey, 2004; Granato, 2006; Cuzon, 2008; Isayama, 2009). In contrast to the current investigation, however, the former studies employed chronic ethanol exposure paradigms. Here we present evidence that ethanol exposure limited to a very narrow window of time prior to neural plate formation reduces the

tissue that gives rise to cortical interneurons and oligodendrocytes, with the degree of affect being variable among ethanol-exposed embryos and fetuses. The potential consequences of this ethanol-induced reduction in ventromedian telencephalic tissues are discussed.

METHODS

Animal husbandry and treatment paradigm

C57Bl/6J mice (The Jackson Laboratory, Bar Harbor, ME) were maintained on an *ad libitum* diet of standard laboratory chow and water. Early in the light cycle 2 females were placed with a single male for a 2 hour period, and then examined for the presence of a copulation plug. The beginning of this breeding period was defined as gestational day (GD) 0. On their 7th day of pregnancy, mice in the experimental group were administered two doses of 25% (v/v) ethanol in lactated Ringer's solution at a dosage of 2.9 g/kg maternal body weight by intraperitoneal (i.p.) injection. The injections were given 4 h apart, with the first administered at GD 7, 0 h, and resulting in maternal peak blood ethanol concentrations averaging 440 mg/dl (range: 400-466 mg/dl) 30 minutes after the second dose (Godin et al., 2010). Control animals were injected with an equivalent volume of lactated Ringer's solution according to the above treatment paradigm.

For the studies described herein, on day 12.5, 13, or 17 of pregnancy, dams were anesthetized via CO₂ inhalation followed by cervical dislocation. The majority of severely affected ethanol-exposed animals [i.e. those with holoprosencephaly (HPE)] do not survive beyond the first few postnatal days, therefore only prenatal

animals were utilized for this study. Following laparotomy, the uteri were removed and the embryos or fetuses were immediately dissected free of decidua in ice-cold phosphate buffered-saline (PBS) and examined for the presence of gross abnormalities. Ethanol-exposed fetuses were selected, based on the degree of ocular and facial dysmorphology, to provide a spectrum of affected animals. For this study, all of the selected ethanol-exposed specimens had ocular defects. Some of these had apparently normal facies, while others had facial features characteristic of FAS (as described in Sulik, et al., 1981). Control animals were stage-matched to corresponding ethanol-exposed animals based on the degree of limb (GD12.5 and 13), skin and hair follicle (GD17) development (Thieler, 1989). All animal treatment protocols were approved by the University of North Carolina at Chapel Hill, Institutional Animal Care and Use Committee (IACUC).

Scanning electron microscopy

GD13 Embryos chosen for scanning electron microscopy were decapitated, dissected and immersion fixed for 48 hours in a 2.5% glutaraldehyde fixative. Specimens were rinsed in Sorenson's phosphate buffer at which time the lateral wall of both left and right cerebral hemispheres were removed. Embryos were post-fixed in 2% osmium tetroxide for 1 hour and dehydrated in a graded ethanol series, then critical point dried in CO₂. Embryos were then mounted on aluminum stubs and sputter coated with gold palladium. Scanning was performed at 15 kV on a JEOL scanning electron microscope.

Routine histology

GD13 embryos were immersed in Bouins fixative (Sigma Aldrich) for a week, and then rinsed with 70% ethanol until the residual fixative was no longer evident. Specimens were routinely processed overnight for paraffin embedding using a tissue processor. Coronal sections were cut at 8 μm , mounted on glass slides, stained with aqueous hemotoxylin and eosin (H & E), cover-slipped and viewed with a light microscope. Photographs of sections were taken using a Nikon photomicroscope.

In situ hybridization

For in situ hybridization, GD12.5 embryos were immersion fixed overnight at 4° in RNase free 4% paraformaldehyde. They were then transferred to a 15% sucrose solution, in which they remained for 24 hours prior to freezing in OCT medium and storage at -80°. Serial cryosections were cut at 20 μm and collected on glass slides, followed by storage at -20°. Following treatment with proteinase K and triethanolamine, sections were hybridized overnight at 60° with digoxigenin-labeled riboprobes for either Nkz2.1 or Fzd8 (generated by Yongquin Wu of the *In Situ* Hybridization Core Facility at UNC). After washing and blocking, the sections were incubated with an anti-digoxigenin alkaline phosphatase (AP) antibody and developed using BM Purple AP Substrate (Roche). After development, the sections were fixed in 4% paraformaldehyde to quench the AP activity and then were mounted with CC/Mount (Sigma), followed by photography employing a Nikon photomicroscope.

Immunohistochemistry

For immunohistochemistry, GD12.5 and 17 specimens were immersion fixed with 4% paraformaldehyde, then processed using a tissue processor and embedded in paraffin. Specimens were sectioned in the coronal plane at 10 μm , followed by deparaffination, rehydration, and quenching with H_2O_2 . Steam antigen retrieval was performed in combination with an antigen retrieval citra solution (Biogenex). The following primary antibodies were used: rabbit anti-GABA (1:1000, Sigma-Aldrich), rabbit anti-Olig2 (DF308 at 1:20,000 generously provided by C. Stiles and J. Alberta, Dana Farber Cancer Institute), and rabbit anti-somatostatin (1:500, Millipore). Following incubation with anti-rabbit secondary antibody and avidin/biotin-immunoperoxidase reactions (Vector Laboratories), antigen was detected using diaminobenzidine as a substrate (Innovex Biosciences). Sections from both control and ethanol-exposed animals were stained at the same time to control for any variability in technique. Photographs of sections were taken using a Nikon photomicroscope.

RESULTS

Embryos that had been acutely exposed to ethanol on GD 7 were collected on GD13 and selected, based on ocular and facial morphology, for subsequent scanning electron microscopic or histological analyses. All of the treated animals selected had some degree of ocular abnormality, with defects ranging from slight microphthalmia to apparent anophthalmia. Abnormal facial features, which consisted

of a long upper lip, narrow snout with closely apposed nostrils, and small mandible (Fig 1 d, g) were present in only the most severely affected animals examined.

In ethanol-exposed embryos from which the lateral aspects of the cerebral cortices were removed, scanning electron microscopy revealed abnormalities involving the hippocampus, which was diminished in size, with reduction being most evident in the rostral aspect (Fig 1 e,f; h,i). Additionally, the Foramen of Monro was enlarged and the cortical wall thickness appeared reduced in these affected animals.

These CNS abnormalities can also be appreciated in routine histological sections of GD 13 embryos. Shown in Figure 2 are coronal sections of a control (Fig 2 a/e) and 3 differentially-affected ethanol-exposed animals (Fig 2 b-d, f-h). Two sections made at comparable anterior-posterior levels are shown for each of the four embryos included. The images from the affected embryos are arranged, from the viewers' left to right, in increasing degrees of severity based on ventromedian forebrain deficiency. In the most mildly affected animal (Fig 2 b,f), a rostral section thorough the cerebral hemispheres illustrates the close proximity of the ventral aspect of the cortex and ganglionic eminences. Further posteriorly, instead of the normally distinct bilateral LGE, MGE, and the centrally-located POA, there are only 3 prominent basal forebrain elevations. Additionally, the lateral ventricles and foramen of Monro (arrow in Fig 2e) appear larger than normal, while the hippocampus is slightly reduced in its dorso-ventral dimension. In an animal that was somewhat more severely affected and that is shown in Figure 2 c, g, the cerebral hemispheres remain separate dorsally, but are approximated ventrally. Rostrally, the GEs are positioned on the ventromedial aspect of the basal forebrain, as compared to their

normal ventrolateral location (Fig 2c). Further posterior the basal forebrain has 3 major tissue elevations, as in the more mildly affected animal, but the median tissue mass is smaller (Fig 2g). In this specimen, the reduction in the hippocampus is also more pronounced and the foramen of Monro is notably enlarged. In the most severely affected ethanol-exposed animal shown the cerebral hemispheres are united, as are the lateral ventricles (Fig 2d). The basal forebrain of this specimen is comprised of a single tissue mass both rostrally and caudally (Fig 2 d,h). In this animal, the hippocampus is very reduced and the cortex is notably thin relative to the control (Fig 2h). Examination of sections from each of the ethanol-exposed animals at more caudal levels than shown illustrated a relatively spared mid- and hindbrain, confirming previous reports that the ventromedian forebrain shows the most severe gross brain dysmorphology following GD7 ethanol insult.

In situ hybridization employing region-specific probes was used to more precisely identify tissues affected in embryos following GD 7 ethanol exposure. As illustrated in Figure 3 (a,e), on GD12.5 in mice *Nkx2.1* expression is normally localized to the POA and MGEs, while *Fzd8* expression is limited to the ventricular zone of the LGEs and the cerebral cortex (as described in Tucker et al., 2008). As in the control, in a mildly affected ethanol-exposed embryo, *Nkx2.1* heavily labels the POA even though the width of this region is diminished (Fig 3b,f). This median tissue loss is accompanied by abnormally close proximity of the *Fzd8*-labeled tissue (Fig 3f). The ethanol-exposed animal shown in Figure 3c and g is affected to a somewhat greater degree than the animal shown in Figure 2 c and g. In this animal, median union of the *Nkx2.1*-labeled tissue is apparent. Notably, the ventral midline region

remains heavily labeled (arrowhead in Fig 3c). Although the ethanol-induced reduction in the ventromedian forebrain tissues is evident, and although too closely approximated, the Fzd8-labeled LGEs and cortex appear quite normal (Fig 3g). In this animal the hippocampus is much reduced and the foramen of Monro is very enlarged. In another, somewhat more severely affected embryo, Nkx2.1 labeling is limited to a median strip, with the normally intense ventromedian staining being notably reduced (Fig 3d). This is accompanied by Fzd8 expression which extends to the midline of the basal forebrain.

To further examine ethanol's effect on the basal forebrain, antibodies for Olig2, a transcription factor necessary for the specification of oligodendrocyte progenitor cells, and for GABA, an inhibitory neurotransmitter, were employed. As shown in sections from a control GD 12.5 embryo, expression of Olig2 is normally restricted to the POA as well as both the MGEs and LGEs, with staining being least intense in the LGEs (Fig 4a). It is primarily localized to the ventricular zone, although some darkly stained cells are also located in the subjacent subventricular zone. At this stage in development, immunohistochemical labeling identifies GABA expression throughout the subventricular and mantle zones of the basal forebrain (Fig 4e). In embryos affected to degrees comparable to those shown in Figure 3, an expected reduction in Olig2 and GABA labeling was found. As shown in Figure 4 (b), a mild degree of affect is evidenced by a reduced POA, along with a deficiency in the POA-associated Olig2 and GABA staining. In severely affected animals (Fig 4c,d; g,h), with loss of much of the MGE area, there is concomitant loss of Olig2 and GABA staining.

In order to examine some of the later consequence of ethanol-induced ventromedian forebrain deficiency, immunohistochemical staining for somatostatin (Sst)-expressing interneurons was conducted on brain sections from GD17 fetuses. At this time in development, these cells normally are migrating tangentially from the MGEs to the cerebral cortex. As shown in sections from a control fetus (Fig 5a,c) Sst-expressing cells are evident in the subpallium. Shown in Figure 5c is a high magnification view that illustrates the normal morphology of these cells. Figures 5 b and d show low and high magnification views of a Sst-labeled section from a GD17 fetus that had been exposed acutely to ethanol on GD7. In this animal, the size and shape of the striatum appear abnormal, the septal nuclei are not present, and the anterior commissure appears thickened, a finding that is consistent with previous analyses of this animal model (Godin et al., 2010; O'Leary-Moore, submitted). The Sst-labeled cells are clearly dysmorphic.

DISCUSSION

While it has long been recognized that acute high dose ethanol exposure at early gastrulation stages in mice selectively impacts the forebrain (Sulik and Johnston, 1982; Sulik et al., 1984; Schambra et al., 1990), there is only one previous study employing this FASD model in which a detailed examination of ethanol-induced insult to specific forebrain populations is reported (Schambra et al., 1990). In this previous report, a reduction in choline acetyltransferase (ChAT)-expressing neurons in the forebrain of fetal mice following GD 7 ethanol exposure was shown. Within the past fifteen years, the fact that the ventromedian forebrain serves as a

source for tangentially-migrating interneurons and oligodendrocytes has been firmly established (Anderson, 1997; reviewed by Marin and Rubenstein, 2001; Wonders and Anderson, 2006). More recently, transcription factors that regulate the differentiation of interneurons have been identified, and mechanisms controlling tangential migration have been defined (e.g Polleux, 2002, reviewed in Ayala et al., 2007). This new information is critical for examining and more fully understanding the impact of ethanol-induced ventromedian forebrain deficiency. In the current study the region or cell type-specific markers, Nkx2.1, Fzd8, Olig2, and GABA, were employed, to further examine ethanol's teratogenic effect. Reductions in MGE and POA tissues and effects on oligodendrocyte and GABAergic interneuron progenitor populations have been shown.

The Nkx2.1 and Fzd8 expression pattern alteration identified in this study are remarkably similar to that in the Nkx2.1 mutant mouse described by Sussel and colleagues (1999). This study was the first to show that Nkx2.1 is required for normal development of the pallidal-related ventral telencephalon. The mutant mice lacked a morphological and molecular MGE, although the dorsal telencephalon was relatively normal. The globus pallidus, a derivative of the MGE, was absent at later stages of development, and instead, was replaced by striatal-like tissue. Also, there was an overall reduction in an isoform of the glutamic acid decarboxylase (Gad67), a GABA synthesizing enzyme. Similar to the results of the ethanol-teratogenesis studies of Schambra et al.(1990), cholinergic neurons, another subset of progenitor cells derived from the MGE/POA region, were absent in the Nkx2.1 mutant (Sussel, 1999).

Nkx2.1 expression is dependent on Shh signaling. Shh is a ventralizing morphogen that is necessary for cell proliferation, differentiation, and embryonic patterning. At early gastrulation stages, Shh is expressed in the notochord, prechordal plate, and floor plate of the neural tube. In mouse embryos having approximately 8 somites (approximately GD 8.5), its expression can be localized to the median aspect of the anterior neural plate. By about GD 9.5, Shh is expressed in the mantle zone of the MGEs (Shimamura et al., 1995). Importantly, mutations in Shh result in HPE, one of the severe manifestations of early prenatal alcohol exposure (Sulik and Johnston, 1982; Ronen and Andrews, 1991; Siebert, 1991; Coulter et al., 1993).

Recognizing that early gastrulation stages represent a critical exposure time for FAS and that Shh is a key signaling pathway at this point in time, a number of investigations have explored insult to this pathway as a primary mechanism of ethanol's teratogenesis (Blader and Strahle, 1998; Ahlgren et al., 2002; Yamada et al., 2005; Higashiyama et al., 2007; Li et al., 2007; Loucks et al., 2007; Aoto et al., 2008; Loucks and Ahlgren, 2009). The results of studies employing a variety of animal models, including zebrafish, chicks, and mice, have provided evidence indicating that ethanol exposure occurring during gastrulation does decrease Shh expression, with resulting craniofacial and CNS abnormalities being consistent with HPE. Strongly supporting a role for diminished Shh signaling is that the ethanol-induced defects can be rescued by Shh (Ahlgren et al., 2002; Loucks and Ahlgren, 2009) or by other molecules involved in Shh signaling [i.e. cholesterol (Li et al.,

2006)]. Despite a considerable amount of work, however, it remains unclear whether the ethanol-mediated effects on Shh signaling are direct or indirect.

The results of the current work highlight the potential of acute, early ethanol insult to have a protracted effect on the structure and function of the developing brain. Reduction in the tissues from which GABAergic populations are derived is expected to have functional consequences that might include disruption in the balance of excitation and inhibition in the CNS. In this regard it is notable that ADHD is the highest co-morbidity in FASD (Fryer, 2007; Herman, 2008); an outcome that may, at least in part, result from reduced GABAergic neurotransmission (Viggiano et al., 2002; Sagvolden et al., 2005). Another result of inhibitory interneuron loss is seizure activity (Cobos et al., 2005). Importantly, seizures are estimated to occur in 3-21% of children with FASD (Jones and Smith, 1975; Olegard et al., 1979; Iosub et al., 1981; Majewski, 1981; Murray-Lyon, 1985; Marcus, 1987; Ioffe and Chernick, 1990; O'Malley and Barr, 1998; Sun et al., 2008; Bell et al., 2010). The developmental basis for this remains unknown, though Bonthuis and colleagues (Bonthuis et al., 2001 a, b) have suggested that ethanol-induced hippocampal dysfunction may be one cause and Godin et al. (2010) have related this consequence to cell migration errors leading to the development of cerebral cortical heterotopias. Additionally notable are that seizures are common in patients with HPE (DeMyer and White, 1964; Takahashi et al., 2001); a decrease in interneurons in individuals with HPE has been reported (Fertzunihos et al., 2009); and individuals with Shh mutations that have microcephaly, but lack overt HPE features present with hyperactivity and seizures. Also, in the Nkx2.1 mutant mouse, there are reduced

populations of interneurons (Sussel, 1999). In fact, Nkx2.1 has been suggested to regulate the balance of excitation and inhibition in the postnatal cerebral cortex (Gulacsi, 2006). Although the mutant mice do not survive postnatally because of lung and thyroid problems, a conditional knockout of the gene on either GD9.5 or 10.5 is consistent with viability. These conditional knockouts develop spontaneous seizures as juveniles, a finding thought to be related to decreased GABA activity (Butt, 2008). Clearly, studies directed toward examining seizure thresholds in the FASD mouse model employed for the current study are needed.

In addition to hyperactivity and seizures, another potential consequence of abnormal GABA levels is altered sensitivity to GABA-modulating drugs, including ethanol. Ethanol is a GABA-agonist, an action that yields relaxing, anti-anxiety effects. That most individuals with FASD have an increased risk for developing both alcohol and drug abuse problems may, in part, be related to their need to drink more in order to achieve a desired effect (reviewed in O'Connor and Paley, 2009; Baer et al., 1998, 2003; Alati et al., 2006, 2008; Barr et al., 2006; Famy et al., 1998; Streissguth et al., 2004; Kodituwakku, 2007).

In addition to consideration of the consequences of damage to GABAergic populations, additional consideration of early ethanol-mediated insult involving oligodendrocyte populations is warranted. A marked reduction in the tissue from which oligodendrocyte progenitor cell populations originate was shown in this study. Importantly, in human FASD, fiber tracts, including the corpus callosum, are affected. Defects in the corpus callosum have been shown to range from complete agenesis to decreased white matter organization/integrity (Riley et al., 1995;

Johnson et al., 1996; Swayze et al., 1997; Autti-Ramo et al., 2002; Bhatara et al., 2002; Bookstein et al., 2002a,b, 2007; Ma et al., 2005; Wozniak et al., 2006; 2009; Sowell et al., 2008; Astley et al., 2009; Lebel et al., 2008; 2010; Fryer et al., 2009; Li et al., 2009). While the existence of functionally redundant oligodendrocyte progenitor cells that may compensate if another population is affected has been suggested (Ivanova et al., 2003; Kessaris, 2006; Menn, 2006), it remains possible that loss of ventromedian derived-oligodendrocyte progenitor cells may contribute to the white matter integrity changes that follow prenatal ethanol exposure. Additional investigations directed toward examining early ethanol exposure mediated effects on myelination in later prenatal and postnatal stages are indicated.

In conclusion, the results of this study show that in mice, acute ethanol exposure occurring at a time in development equivalent to that in the third week of pregnancy in humans adversely affects the ventromedian forebrain, reducing the tissues that are required for the generation of interneurons and oligodendrocytes. The functional consequences of this insult are expected to include an increased potential for hyperactivity, seizures and susceptibility to drug and alcohol abuse. This work highlights the need for additional pre- and postnatal studies directed toward a more comprehensive examination of ethanol-induced ventromedian forebrain-derived cell loss and resulting structural and functional changes.

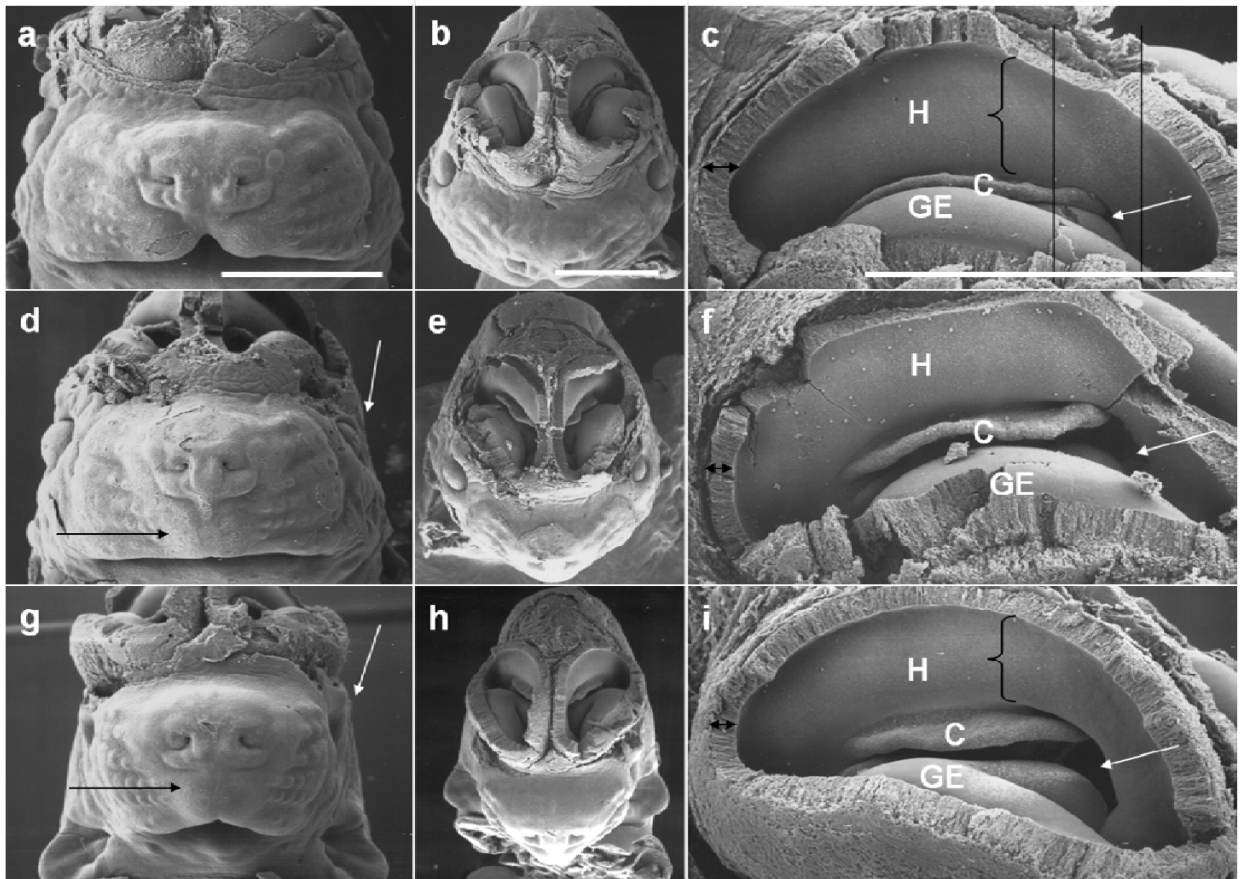


Figure 4.1: Scanning electron microscopic analyses of control (a,b,c) and two ethanol- exposed GD 13 embryos (d-i) illustrate that abnormal facial features accompany forebrain anomalies. The facial defects correspond to those in fetal alcohol syndrome and include an indistinct philtrum and long upper lip (black arrows in d and g), small eyes, (white arrows in d and g) small nose and decreased head circumference. Removal of both left and right lateral walls of the cerebral hemispheres allowed 3-D -like views of the medial walls and ganglionic eminences (GE) of the forebrain (b,c,e,f,h,i). Obvious ethanol-induced abnormalities seen by comparing views of the right side of the control (c) and affected (f and i) forebrains include an enlarged foramen of Monro (arrows in f and i) and reduction in the dorso-ventral dimension of the hippocampus (H; compare { in c and i). Additionally, the thickness of the cerebral cortex appeared reduced (doubleheaded arrows in c, f, i). C = choroid plexus. Lines in c indicate level of sections for Figure 2. Bars in a - c = 1mm

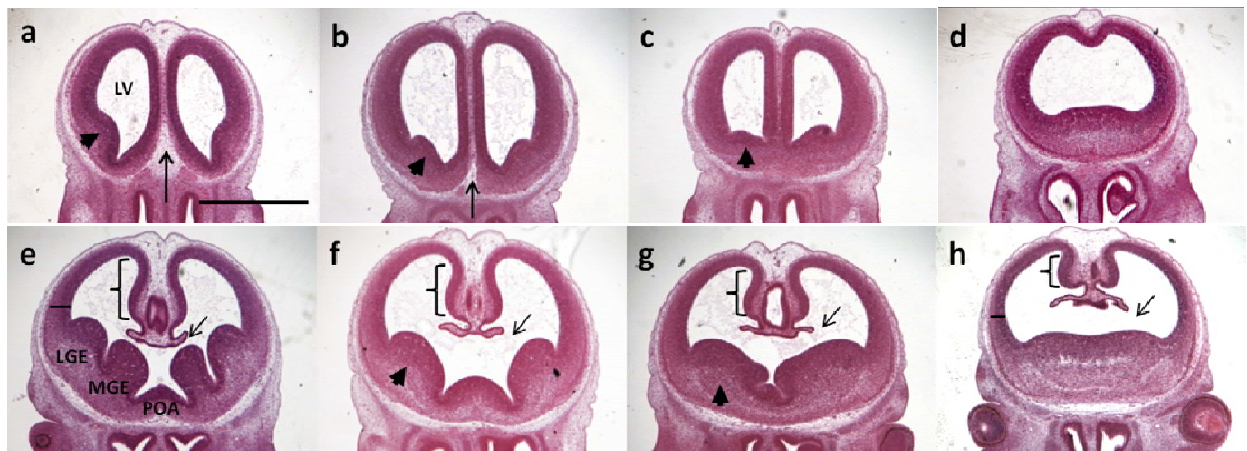


Figure 4.2: Routine H&E-stained histological sections of a control (a, e) and 3 ethanol-exposed (b-d, f-h) GD13 embryos illustrate a spectrum of forebrain abnormality. Two coronal sections from each animal are shown, made at the level of the two lines in Figure 4.1 c, with the most anterior (a-d) being near the level at which the ganglionic eminences are first evident and the more posterior section being at the level of the foramen of Monro (arrow in e-h). In the ethanol-exposed embryos, notable are close apposition of the ganglionic eminences in both the anterior (arrowhead in b, c) and posterior sections (asterisks in f, g). Accompanying this are cerebral cortices that are too close in proximity (indicated by the arrow in a and b), enlarged lateral ventricles and an expanded foramen of Monro (arrow in e-h). Additionally, the rostral aspect of the hippocampus is reduced in its dorso-ventral dimension ({} in e-h) in the affected specimens and the cerebral cortex is thin (compare line in h to line in e). In the ethanol-exposed animal shown in d and h, rostrally the lateral ventricles are merged and the brain is holoprosencephalic (d). LV = lateral ventricles, LGE = lateral ganglionic eminence, MGE = medial ganglionic eminence, POA = preoptic area. Bar in a = 1mm

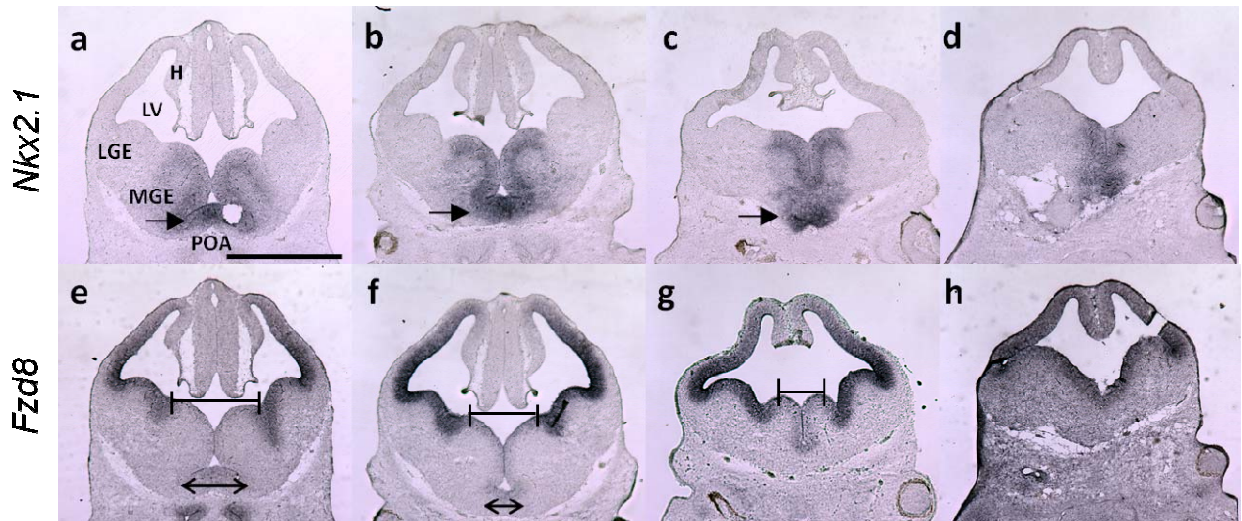


Figure 4.3: *In situ* hybridization, to label Nkx2.1 and Fzd8 expression in control (a, e) and ethanol-exposed (b-d; f-h) GD12.5 embryos illustrates median forebrain deficiency involving the POA and MGEs. As shown in the control animal (a), these regions express Nkx2.1. In ethanol-exposed mice, ordered in increasing severity, from left to right, the Nkx2.1-labeled tissue can be seen to diminish accordingly (b-d). In the most mildly affected embryo, the densely stained POA (arrow in a-c) is reduced in width (double-headed arrow in e & f) and in the most severely affected embryo (d, h) it is absent. Cells of the ventricular zone of the LGE and cortex are labeled with Fzd8, as shown in the control (e). In the ethanol-exposed animals (f-h) Fzd8 expression appears to be relatively unchanged in the LGE and cortical areas. With increasing severity of insult, the distance between the LGEs is reduced (bracket in e-g) to the point where Fzd8 expression surrounds the entire ventricle (h). H = hippocampus, LV = lateral ventricles, LGE = lateral ganglionic eminence, MGE = medial ganglionic eminence, POA = preoptic area. Bar in a = 1mm

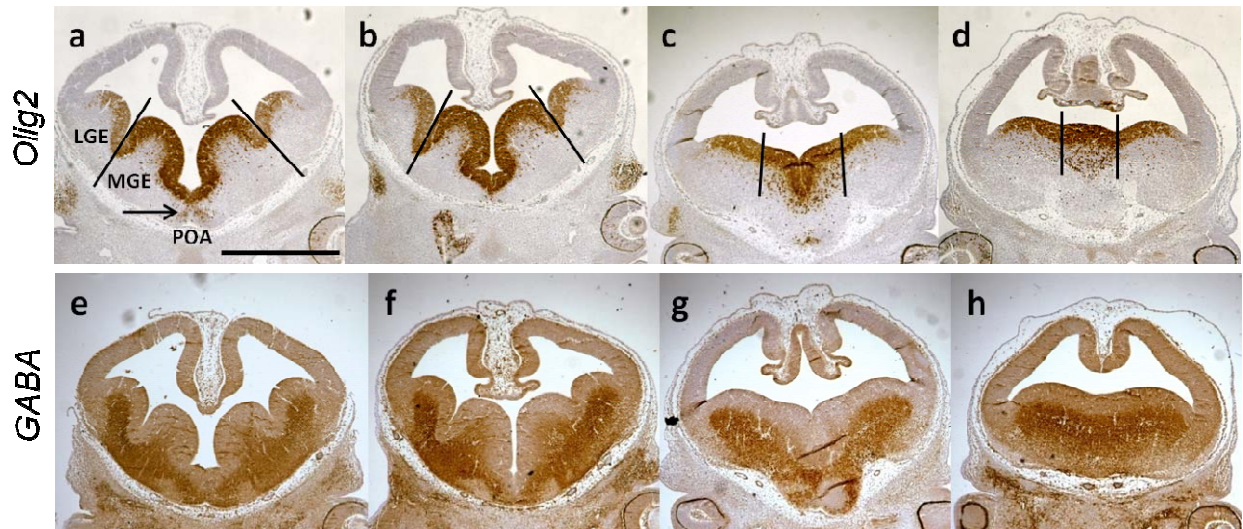


Figure 4.4: Immunohistochemical labeling of Olig2 and GABA illustrates deficiency of these basal forebrain markers in ethanol-exposed GD12.5 mice (b-d, f-h) in comparison to a control (a, e). Olig2 (a-d), which is necessary for the specification of oligodendrocyte progenitor cells, is strongly expressed in the ventricular zone of the POA and MGEs (the region between the lines in a) and is more weakly expressed in the LGEs. Patches of cells within the MGE and POA subventricular zone are also Olig2 positive. Accompanying the loss of median tissue, Olig2 expression is reduced in the ethanol-exposed animals (note the region between the lines in b-d). Normally, as shown in the control section in (e), expression of the inhibitory neurotransmitter GABA is restricted to the subventricular and mantle zones of the basal telencephalon on GD 12.5 in mice. In sections from the same three ethanol-exposed embryos as labeled for Olig2, GABA expression is reduced in accord with the ethanol-induced reduction in the median forebrain tissue mass (f, g, h). LGE = lateral ganglionic eminence, MGE = medial ganglionic eminence, POA = preoptic area. Bar in a = 1mm

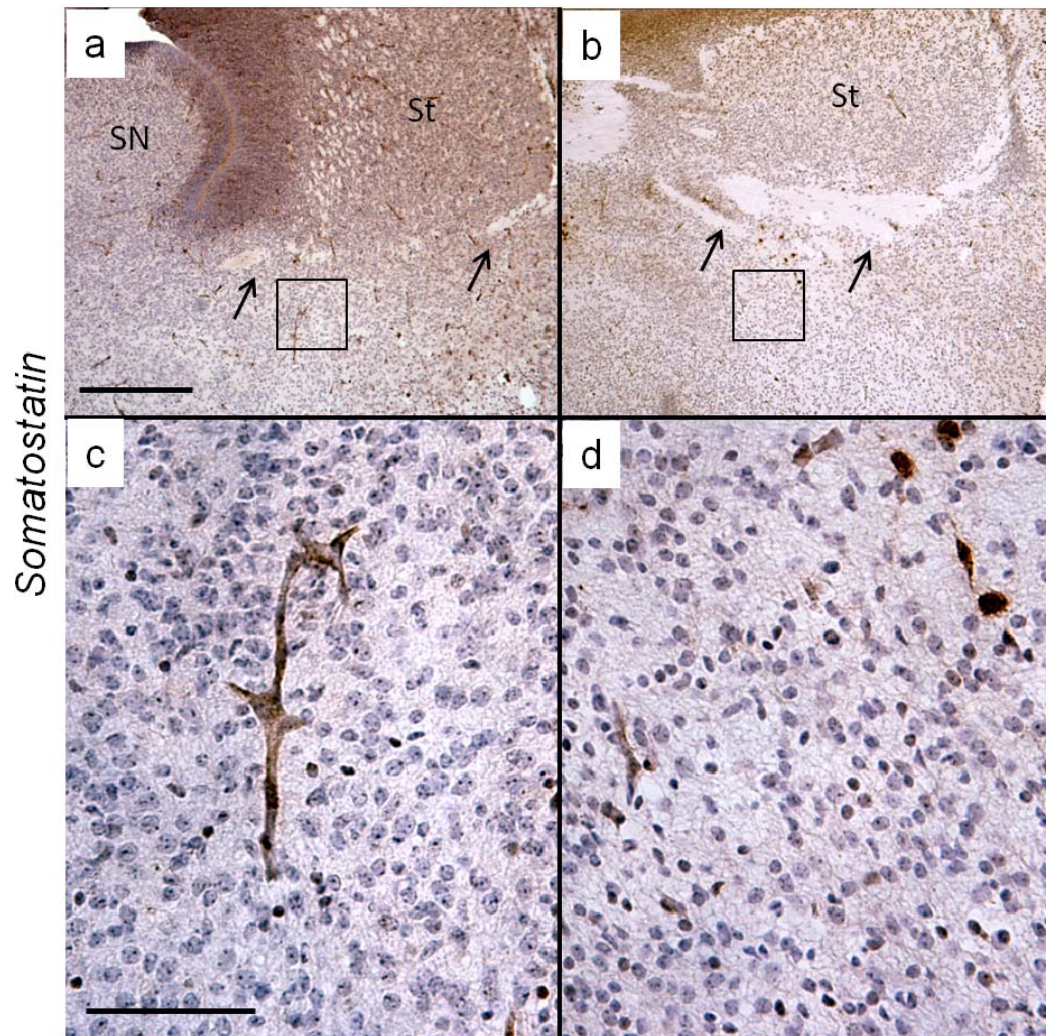


Figure 4.5: Shown are representative images of somatostatin (Sst)-immunohistochemical staining in the subpallium of GD17 mice (a,b;10X) (c,d; 40X). In comparison to a control (a), the striatum (St) appears small and mis-shapen and the anterior commissure (arrows) is noticeably thickened in the ethanol-exposed holoprosencephalic fetus (b). High magnification views (boxed area shown in a&b) illustrate robust Sst-expressing interneurons in the subpallium of the control (c). In comparison, the Sst-labeled cells in the ethanol-exposed fetuses appear small and dysmorphic (d). SN = septal nucleus, St = Striatum. Bar in a = 50 μ m; c = 10 μ m

REFERENCES

- Abel EL, Sokol RJ (1986) Fetal alcohol syndrome is now leading cause of mental retardation. *Lancet* 2(8517):1222.
- Ahlgren SC, Thakur V, Bronner-Fraser M (2002) Sonic hedgehog rescues cranial neural crest from cell death induced by ethanol exposure. *Proc Natl Acad Sci U S A* 99(16):10476-81.
- Alati R, Al Mamun A, Williams GM, O'Callaghan M, Najman JM, Bor W (2006) In utero alcohol exposure and prediction of alcohol disorders in early adulthood: a birth cohort study. *Arch Gen Psychiatry* 63(9):1009-16.
- Alati R, Clavarino A, Najman JM, O'Callaghan M, Bor W, Mamun AA, Williams GM (2008) The developmental origin of adolescent alcohol use: findings from the Mater University Study of Pregnancy and its outcomes. *Drug Alcohol Depend* 98(1-2):136-43.
- Anderson SA, Eisenstat DD, Shi L, Rubenstein JL (1997) Interneuron migration from basal forebrain to neocortex: dependence on Dlx genes. *Science* 278(5337):474-6.
- Anderson SA, Kaznowski CE, Horn C, Rubenstein JL, McConnell SK (2002) Distinct origins of neocortical projection neurons and interneurons in vivo. *Cereb Cortex* 12(7):702-9.
- Anderson SA, Marin O, Horn C, Jennings K, Rubenstein JL (2001) Distinct cortical migrations from the medial and lateral ganglionic eminences. *Development* 128(3):353-63.
- Aoto K, Shikata Y, Higashiyama D, Shiota K, Motoyama J (2008) Fetal ethanol exposure activates protein kinase A and impairs Shh expression in prechordal mesendoderm cells in the pathogenesis of holoprosencephaly. *Birth Defects Res A Clin Mol Teratol* 82(4):224-31.
- Astley SJ, Aylward EH, Olson HC, Kerns K, Brooks A, Coggins TE, Davies J, Dorn S, Gendler B, Jirikowic T, Kraegel P, Maravilla K, Richards T (2009) Magnetic resonance imaging outcomes from a comprehensive magnetic resonance study of children with fetal alcohol spectrum disorders. *Alcohol Clin Exp Res* 33(10):1671-89.

Autti-Ramo I, Autti T, Korkman M, Kettunen S, Salonen O, Valanne L (2002) MRI findings in children with school problems who had been exposed prenatally to alcohol. *Dev Med Child Neurol* 44(2):98-106.

Ayala R, Shu T, Tsai LH (2007) Trekking across the brain: the journey of neuronal migration. *Cell* 128(1):29-43.

Baer JS, Sampson PD, Barr HM, Connor PD, Streissguth AP (2003) A 21-year longitudinal analysis of the effects of prenatal alcohol exposure on young adult drinking. *Arch Gen Psychiatry* 60(4):377-85.

Bailey CD, Brien JF, Reynolds JN (2004) Chronic prenatal ethanol exposure alters the proportion of GABAergic neurons in layers II/III of the adult guinea pig somatosensory cortex. *Neurotoxicol Teratol* 26(1):59-63.

Barr HM, Bookstein FL, O'Malley KD, Connor PD, Huggins JE, Streissguth AP (2006) Binge drinking during pregnancy as a predictor of psychiatric disorders on the Structured Clinical Interview for DSM-IV in young adult offspring. *Am J Psychiatry* 163(6):1061-5.

Bell SH, Stade B, Reynolds JN, Rasmussen C, Andrew G, Hwang PA, Carlen PL (2010) The Remarkably High Prevalence of Epilepsy and Seizure History in Fetal Alcohol Spectrum Disorders. *Alcohol Clin Exp Res*.

Bhatara VS, Lovrein F, Kirkeby J, Swayze V, 2nd, Unruh E, Johnson V (2002) Brain function in fetal alcohol syndrome assessed by single photon emission computed tomography. *S D J Med* 55(2):59-62.

Blader P, Strahle U (1998) Ethanol impairs migration of the prechordal plate in the zebrafish embryo. *Dev Biol* 201(2):185-201.

Bonthius DJ, Pantazis NJ, Karacay B, Bonthius NE, Taggard, Da, Lothman EW (2001) Alcohol exposure during the brain growth spurt promotes hippocampal seizures, rapid kindling, and spreading depression. *Alcohol Clin Exp Res* 25(5):734-45.

Bonthius DJ, Woodhouse J, Bonthius NE, Taggard DA, Lothman EW (2001) Reduced seizure threshold and hippocampal cell loss in rats exposed to alcohol during the brain growth spurt. *Alcohol Clin Exp Res* 25(1):70-82.

Bookstein FL, Connor PD, Huggins JE, Barr HM, Pimentel KD, Streissguth AP (2007) Many infants prenatally exposed to high levels of alcohol show one particular anomaly of the corpus callosum. *Alcohol Clin Exp Res* 31(5):868-79.

Bookstein FL, Sampson PD, Connor PD, Streissguth AP (2002) Midline corpus callosum is a neuroanatomical focus of fetal alcohol damage. *Anat Rec* 269(3):162-74.

Bookstein FL, Streissguth AP, Sampson PD, Connor PD, Barr HM (2002) Corpus callosum shape and neuropsychological deficits in adult males with heavy fetal alcohol exposure. *Neuroimage* 15(1):233-51.

Butt SJ, Cobos I, Golden J, Kessar N, Pachnis V, Anderson S (2007) Transcriptional regulation of cortical interneuron development. *J Neurosci* 27(44):11847-50.

Butt SJ, Sousa VH, Fuccillo MV, Hjerling-Leffler J, Miyoshi G, Kimura S, Fishell G (2008) The requirement of Nkx2-1 in the temporal specification of cortical interneuron subtypes. *Neuron* 59(5):722-32.

Coulter CL, Leech RW, Schaefer GB, Scheithauer BW, Brumback RA (1993) Midline cerebral dysgenesis, dysfunction of the hypothalamic-pituitary axis, and fetal alcohol effects. *Arch Neurol* 50(7):771-5.

Cuzon VC, Yeh PW, Yanagawa Y, Obata K, Yeh HH (2008) Ethanol consumption during early pregnancy alters the disposition of tangentially migrating GABAergic interneurons in the fetal cortex. *J Neurosci* 28(8):1854-64.

Demyer W, White PT (1964) Eeg in Holoprosencephaly (Arhinencephaly). *Arch Neurol* 11:507-20.

Famy C, Streissguth AP, Unis AS (1998) Mental illness in adults with fetal alcohol syndrome or fetal alcohol effects. *Am J Psychiatry* 155(4):552-4.

Fertuzinhos S, Krsnik Z, Kawasawa YI, Rasin MR, Kwan KY, Chen JG, Judas M, Hayashi M, Sestan N (2009) Selective depletion of molecularly defined cortical interneurons in human holoprosencephaly with severe striatal hypoplasia. *Cereb Cortex* 19(9):2196-207.

Flames N, Pla R, Gelman DM, Rubenstein JL, Puelles L, Marin O (2007) Delineation of multiple subpallial progenitor domains by the combinatorial expression of transcriptional codes. *J Neurosci* 27(36):9682-95.

Fogarty M, Grist M, Gelman D, Marin O, Pachnis V, Kessaris N (2007) Spatial genetic patterning of the embryonic neuroepithelium generates GABAergic interneuron diversity in the adult cortex. *J Neurosci* 27(41):10935-46.

Fryer SL, McGee CL, Matt GE, Riley EP, Mattson SN (2007) Evaluation of psychopathological conditions in children with heavy prenatal alcohol exposure. *Pediatrics* 119(3):e733-41.

Fryer SL, Schweinsburg BC, Bjorkquist OA, Frank LR, Mattson SN, Spadoni AD, Riley EP (2009) Characterization of white matter microstructure in fetal alcohol spectrum disorders. *Alcohol Clin Exp Res* 33(3):514-21.

Gelman DM, Martini FJ, Nobrega-Pereira S, Pierani A, Kessaris N, Marin O (2009) The embryonic preoptic area is a novel source of cortical GABAergic interneurons. *J Neurosci* 29(29):9380-9.

Godin EA, O'Leary-Moore SK, Khan AA, Parnell SE, Ament JJ, Dehart DB, Johnson BW, Allan Johnson G, Styner MA, Sulik KK (2010) Magnetic resonance microscopy defines ethanol-induced brain abnormalities in prenatal mice: effects of acute insult on gestational day 7. *Alcohol Clin Exp Res* 34(1):98-111.

Granato A (2006) Altered organization of cortical interneurons in rats exposed to ethanol during neonatal life. *Brain Res* 1069(1):23-30.

Gulacsi A, Anderson SA (2006) Shh maintains Nkx2.1 in the MGE by a Gli3-independent mechanism. *Cereb Cortex* 16 Suppl 1:i89-95.

Herman LE, Acosta MC, Chang PN (2008) Gender and attention deficits in children diagnosed with a Fetal Alcohol Spectrum Disorder. *Can J Clin Pharmacol* 15(3):e411-9.

Higashiyama D, Saitsu H, Komada M, Takigawa T, Ishibashi M, Shiota K (2007) Sequential developmental changes in holoprosencephalic mouse embryos exposed to ethanol during the gastrulation period. *Birth Defects Res A Clin Mol Teratol* 79(7):513-23.

Ioffe S, Chernick V (1990) Prediction of subsequent motor and mental retardation in newborn infants exposed to alcohol in utero by computerized EEG analysis. *Neuropediatrics* 21(1):11-7.

Iosub S, Fuchs M, Bingol N, Gromisch DS (1981) Fetal alcohol syndrome revisited. *Pediatrics* 68(4):475-9.

Isayama RN, Leite PE, Lima JP, Uziel D, Yamasaki EN (2009) Impact of ethanol on the developing GABAergic system. *Anat Rec (Hoboken)* 292(12):1922-39.

Johnson VP, Swayze VW, II, Sato Y, Andreasen NC (1996) Fetal alcohol syndrome: craniofacial and central nervous system manifestations. *Am J Med Genet* 61(4):329-39.

Jones KL, Smith DW (1975) The fetal alcohol syndrome. *Teratology* 12(1):1-10.

Kessaris N, Fogarty M, Iannarelli P, Grist M, Wegner M, Richardson WD (2006) Competing waves of oligodendrocytes in the forebrain and postnatal elimination of an embryonic lineage. *Nat Neurosci* 9(2):173-9.

Kodituwakku PW (2007) Defining the behavioral phenotype in children with fetal alcohol spectrum disorders: a review. *Neurosci Biobehav Rev* 31(2):192-201.

Lebel C, Rasmussen C, Wyper K, Andrew G, Beaulieu C Brain microstructure is related to math ability in children with fetal alcohol spectrum disorder. *Alcohol Clin Exp Res* 34(2):354-63.

Lebel C, Rasmussen C, Wyper K, Walker L, Andrew G, Yager J, Beaulieu C (2008) Brain diffusion abnormalities in children with fetal alcohol spectrum disorder. *Alcohol Clin Exp Res* 32(10):1732-40.

Li L, Coles CD, Lynch ME, Hu X (2009) Voxelwise and skeleton-based region of interest analysis of fetal alcohol syndrome and fetal alcohol spectrum disorders in young adults. *Hum Brain Mapp* 30(10):3265-74.

Li YX, Yang HT, Zdanowicz M, Sicklick JK, Qi Y, Camp TJ, Diehl AM (2007) Fetal alcohol exposure impairs Hedgehog cholesterol modification and signaling. *Lab Invest* 87(3):231-40.

- Loucks EJ, Ahlgren SC (2009) Deciphering the role of Shh signaling in axial defects produced by ethanol exposure. *Birth Defects Res A Clin Mol Teratol* 85(6):556-67.
- Loucks EJ, Schwend T, Ahlgren SC (2007) Molecular changes associated with teratogen-induced cyclopia. *Birth Defects Res A Clin Mol Teratol* 79(9):642-51.
- Ma X, Coles CD, Lynch ME, Laconte SM, Zurkiya O, Wang D, Hu X (2005) Evaluation of corpus callosum anisotropy in young adults with fetal alcohol syndrome according to diffusion tensor imaging. *Alcohol Clin Exp Res* 29(7):1214-22.
- Majewski F (1981) Alcohol embryopathy: some facts and speculations about pathogenesis. *Neurobehav Toxicol Teratol* 3(2):129-44.
- Marcus JC (1987) Neurological findings in the fetal alcohol syndrome. *Neuropediatrics* 18(3):158-60.
- Marin O, Rubenstein JL (2001) A long, remarkable journey: tangential migration in the telencephalon. *Nat Rev Neurosci* 2(11):780-90.
- Menezes JR, Smith CM, Nelson KC, Luskin MB (1995) The division of neuronal progenitor cells during migration in the neonatal mammalian forebrain. *Mol Cell Neurosci* 6(6):496-508.
- Menn B, Garcia-Verdugo JM, Yaschine C, Gonzalez-Perez O, Rowitch D, Alvarez-Buylla A (2006) Origin of oligodendrocytes in the subventricular zone of the adult brain. *J Neurosci* 26(30):7907-18.
- Moore DB, Quintero MA, Ruygrok AC, Walker DW, Heaton MB (1998) Prenatal ethanol exposure reduces parvalbumin-immunoreactive GABAergic neuronal number in the adult rat cingulate cortex. *Neurosci Lett* 249(1):25-8.
- Moore DB, Ruygrok AC, Walker DW, Heaton MB (1997) Effects of prenatal ethanol exposure on parvalbumin-expressing GABAergic neurons in the adult rat medial septum. *Alcohol Clin Exp Res* 21(5):849-56.
- Murray-Lyon IM (1985) Alcohol and foetal damage. *Alcohol Alcohol* 20(2):185-8.
- Nery S, Fishell G, Corbin JG (2002) The caudal ganglionic eminence is a source of distinct cortical and subcortical cell populations. *Nat Neurosci* 5(12):1279-87.

Nery S, Wichterle H, Fishell G (2001) Sonic hedgehog contributes to oligodendrocyte specification in the mammalian forebrain. *Development* 128(4):527-40.

O'Connor MJ, Paley B (2009) Psychiatric conditions associated with prenatal alcohol exposure. *Dev Disabil Res Rev* 15(3):225-34.

O'Leary-Moore SK, Godin EA, Jiang Y, Styner MA, Budin F, Parnell SE, Dehart DB, Johnson GA, Oguz I, Sulik KK Diffusion tensor imaging and tractography define a spectrum of fiber tract dysmorphology in the brains of prenatal ethanol-exposed mice. *J Neurosci* submitted.

Olegard R, Sabel KG, Aronsson M, Sandin B, Johansson PR, Carlsson C, Kyllerman M, Iversen K, Hrbek A (1979) Effects on the child of alcohol abuse during pregnancy. Retrospective and prospective studies. *Acta Paediatr Scand Suppl* 275:112-21.

O'Malley KD, Barr H (1998) Fetal alcohol syndrome and seizure disorder. *Can J Psychiatry* 43(10):1051.

Ozer E, Sarioglu S, Gure A (2000) Effects of prenatal ethanol exposure on neuronal migration, neuronogenesis and brain myelination in the mice brain. *Clin Neuropathol* 19(1):21-5.

Parras CM, Hunt C, Sugimori M, Nakafuku M, Rowitch D, Guillemot F (2007) The proneural gene *Mash1* specifies an early population of telencephalic oligodendrocytes. *J Neurosci* 27(16):4233-42.

Polleux F, Whitford KL, Dijkhuizen PA, Vitalis T, Ghosh A (2002) Control of cortical interneuron migration by neurotrophins and PI3-kinase signaling. *Development* 129(13):3147-60.

Puelles L, Kuwana E, Puelles E, Bulfone A, Shimamura K, Keleher J, Smiga S, Rubenstein JL (2000) Pallial and subpallial derivatives in the embryonic chick and mouse telencephalon, traced by the expression of the genes *Dlx-2*, *Emx-1*, *Nkx-2.1*, *Pax-6*, and *Tbr-1*. *J Comp Neurol* 424(3):409-38.

Riley EP, Mattson SN, Sowell ER, Jernigan TL, Sobel DF, Jones KL (1995) Abnormalities of the corpus callosum in children prenatally exposed to alcohol. *Alcohol Clin Exp Res* 19(5):1198-202.

Ronen GM, Andrews WL (1991) Holoprosencephaly as a possible embryonic alcohol effect. *Am J Med Genet* 40(2):151-4.

Rowitch DH (2004) Glial specification in the vertebrate neural tube. *Nat Rev Neurosci* 5(5):409-19.

Sagvolden T, Johansen EB, Aase H, Russell VA (2005) A dynamic developmental theory of attention-deficit/hyperactivity disorder (ADHD) predominantly hyperactive/impulsive and combined subtypes. *Behav Brain Sci* 28(3):397-419; discussion 419-68.

Schambra UB, Lauder JM, Petrusz P, Sulik KK (1990) Development of neurotransmitter systems in the mouse embryo following acute ethanol exposure: a histological and immunocytochemical study. *Int J Dev Neurosci* 8(5):507-22.

Shimamura K, Hartigan DJ, Martinez S, Puelles L, Rubenstein JL (1995) Longitudinal organization of the anterior neural plate and neural tube. *Development* 121(12):3923-33.

Siebert JR, Astley SJ, Clarren SK (1991) Holoprosencephaly in a fetal macaque (*Macaca nemestrina*) following weekly exposure to ethanol. *Teratology* 44(1):29-36.

Sowell ER, Mattson SN, Kan E, Thompson PM, Riley EP, Toga AW (2008) Abnormal cortical thickness and brain-behavior correlation patterns in individuals with heavy prenatal alcohol exposure. *Cereb Cortex* 18(1):136-44.

Storm EE, Garel S, Borello U, Hebert JM, Martinez S, McConnell SK, Martin GR, Rubenstein JL (2006) Dose-dependent functions of *Fgf8* in regulating telencephalic patterning centers. *Development* 133(9):1831-44.

Streissguth AP, Bookstein FL, Barr HM, Sampson PD, O'Malley K, Young JK (2004) Risk factors for adverse life outcomes in fetal alcohol syndrome and fetal alcohol effects. *J Dev Behav Pediatr* 25(4):228-38.

Sulik KK (2005) Genesis of alcohol-induced craniofacial dysmorphism. *Exp Biol Med (Maywood)* 230(6):366-75.

Sulik KK, Johnston MC (1982) Embryonic origin of holoprosencephaly: interrelationship of the developing brain and face. *Scan Electron Microsc (Pt 1)*:309-22.

Sulik KK, Johnston MC, Webb MA (1981) Fetal alcohol syndrome: embryogenesis in a mouse model. *Science* 214(4523):936-8.

Sulik KK, Lauder JM, Dehart DB (1984) Brain Malformations in Prenatal Mice Following Acute Maternal Ethanol Administration. *Int J Dev Neurosci* 2(3):203-214.

Sun Y, Strandberg-Larsen K, Vestergaard M, Christensen J, Nybo Andersen AM, Gronbaek M, Olsen J (2009) Binge drinking during pregnancy and risk of seizures in childhood: a study based on the Danish National Birth Cohort. *Am J Epidemiol* 169(3):313-22.

Sussel L, Marin O, Kimura S, Rubenstein JL (1999) Loss of Nkx2.1 homeobox gene function results in a ventral to dorsal molecular respecification within the basal telencephalon: evidence for a transformation of the pallidum into the striatum. *Development* 126(15):3359-70.

Swayze VW, 2nd, Johnson VP, Hanson JW, Piven J, Sato Y, Giedd JN, Mosnik D, Andreasen NC (1997) Magnetic resonance imaging of brain anomalies in fetal alcohol syndrome. *Pediatrics* 99(2):232-40.

Takahashi S, Takahashi Y, Kondo N, Orii T (2001) Epileptic seizures and structural abnormalities in a patient with holoprosencephaly. *Brain Dev* 23(4):264-8.

Tekki-Kessarlis N, Woodruff R, Hall AC, Gaffield W, Kimura S, Stiles CD, Rowitch DH, Richardson WD (2001) Hedgehog-dependent oligodendrocyte lineage specification in the telencephalon. *Development* 128(13):2545-54.

Theiler K (1989) *The House Mouse: Atlas of Embryonic Development*. Springer-Verlag, New York.

Tucker ES, Segall S, Gopalakrishna D, Wu Y, Vernon M, Polleux F, Lamantia AS (2008) Molecular specification and patterning of progenitor cells in the lateral and medial ganglionic eminences. *J Neurosci* 28(38):9504-18.

Valcanis H, Tan SS (2003) Layer specification of transplanted interneurons in developing mouse neocortex. *J Neurosci* 23(12):5113-22.

Viggiano D, Grammatikopoulos G, Sadile AG (2002) A morphometric evidence for a hyperfunctioning mesolimbic system in an animal model of ADHD. *Behav Brain Res* 130(1-2):181-9.

Wichterle H, Garcia-Verdugo JM, Herrera DG, Alvarez-Buylla A (1999) Young neurons from medial ganglionic eminence disperse in adult and embryonic brain. *Nat Neurosci* 2(5):461-6.

Wichterle H, Turnbull DH, Nery S, Fishell G, Alvarez-Buylla A (2001) In utero fate mapping reveals distinct migratory pathways and fates of neurons born in the mammalian basal forebrain. *Development* 128(19):3759-71.

Wonders CP, Anderson SA (2006) The origin and specification of cortical interneurons. *Nat Rev Neurosci* 7(9):687-96.

Wonders CP, Taylor L, Welagen J, Mbata IC, Xiang JZ, Anderson SA (2008) A spatial bias for the origins of interneuron subgroups within the medial ganglionic eminence. *Dev Biol* 314(1):127-36.

Wozniak JR, Mueller BA, Chang PN, Muetzel RL, Caros L, Lim KO (2006) Diffusion tensor imaging in children with fetal alcohol spectrum disorders. *Alcohol Clin Exp Res* 30(10):1799-806.

Wozniak JR, Muetzel RL, Mueller BA, McGee CL, Freerks MA, Ward EE, Nelson ML, Chang PN, Lim KO (2009) Microstructural corpus callosum anomalies in children with prenatal alcohol exposure: an extension of previous diffusion tensor imaging findings. *Alcohol Clin Exp Res* 33(10):1825-35.

Xu Q, Cobos I, De La Cruz E, Rubenstein JL, Anderson SA (2004) Origins of cortical interneuron subtypes. *J Neurosci* 24(11):2612-22.

Xu Q, de la Cruz E, Anderson SA (2003) Cortical interneuron fate determination: diverse sources for distinct subtypes? *Cereb Cortex* 13(6):670-6.

Xu Q, Guo L, Moore H, Waclaw RR, Campbell K, Anderson SA Sonic hedgehog signaling confers ventral telencephalic progenitors with distinct cortical interneuron fates. *Neuron* 65(3):328-40.

Yamada Y, Nagase T, Nagase M, Koshima I (2005) Gene expression changes of sonic hedgehog signaling cascade in a mouse embryonic model of fetal alcohol syndrome. *J Craniofac Surg* 16(6):1055-61; discussion 1062-3.

CHAPTER V

GENERAL CONCLUSIONS

“Alcohol is a teratogen. Because of its common availability and usage, alcohol is more than just a teratogen; it is the most prominent behavioral teratogen in the world.”

Warren and Hewitt, 2009

Elegantly stated by Warren and Hewitt, alcohol [ethanol] is a very frequently used teratogen. In an effort to increase the awareness about the dangers of ethanol exposure during pregnancy, we first must understand the full scope of its teratogenic effects. Because the effects of prenatal ethanol exposure are dependent on the timing, dose, and pattern of exposure (Coles et al., 1994), it is critical to fully characterize stage dependent effects. While others have focused on third trimester-equivalent exposures, the Sulik laboratory has been among the few that have concentrated on research regarding the teratogenic effects of ethanol exposures occurring during the first trimester of pregnancy. Employing the mouse FASD model that has been commonly utilized for the work of Dr. Sulik and her colleagues, the effort described in this dissertation was to further characterize the biological consequences of an ethanol exposure occurring during early gastrulation. This

developmental event occurs in the middle of the third week (approximately gestational day 17) of pregnancy in humans. For this work, state of the art imaging methodologies, i.e. magnetic resonance microscopy (MRM) and diffusion tensor imaging (DTI), as well as more routine techniques for morphological analyses (routine histology, immunohistochemical labeling, *in situ* hybridization, and scanning electron microscopy) were employed for examination of embryonic and fetal mice. The results of the studies described herein have confirmed and extended those in previous reports regarding ethanol's teratogenesis.

For the studies described in Chapters II and III of this dissertation, the hypothesis tested was that the pioneering application of magnetic resonance-based imaging (MRM and DTI) to examination of brain morphology, regional volumes and fiber tracts in fetal mice would facilitate discovery of ethanol-induced CNS damage. This has proven true as evidenced, in part, by the novel MRM-based finding of cerebral cortical heterotopias in ethanol-affected brains and by DTI-based identification of ethanol-induced changes in major forebrain fiber tracts, as well as in cerebral cortical organization. The significance of this work is reflected, in part, by the fact that the entire second chapter has been selected for inclusion as part of the National Organization for Fetal Alcohol Syndrome (NOFAS)-UK Fetal Alcohol Forum (<http://www.nofas-uk.org/>), an organization dedicated to helping families of individuals with FASD and promoting public awareness about the risks of drinking alcohol during pregnancy.

The MRM-based findings in this work regarding the consequences of acute GD7 ethanol insult in mice differ from those recently reported (Parnell et al., 2009)

and described (O'Leary-Moore et al., in press and personal communication) for other exposure times. Exposure occurring just 24 hours after that reported herein results in a different pattern of affect, targeting the hindbrain regions as well as forebrain. Reported by Parnell et al. are reduced crown rump lengths and whole brain and body volumes. For regional brain assessment, asymmetric reductions in the right olfactory bulb, hippocampus, and cerebellum resulting from a GD8 ethanol exposure were found. Similarly, an exposure occurring on GD10 resulted in a global developmental delay. For this, GD17 ethanol-exposed fetuses were more comparable to GD16.5 control animals. Despite the developmental delay, ethanol-exposed fetuses had extended third ventricles and reduced cortical volumes, a pattern that appears to be specific to exposure on GD10.

While this work clearly shows the utility of these imaging techniques for studies of normal and abnormal development, their availability and costs limit the potential for their broad application. This is, however, changing. Indeed, for the initial DTI studies conducted for this work, approximately 24 hours were required in order to scan one fetal brain. With the development of specimen holders that enable scanning two fetuses at once, the valuable scan time has been reduced by one half. Undoubtedly, future innovations will increase the use and availability of these advanced imaging techniques for both basic and clinical research.

Additionally, advances in image processing and analysis have greatly improved. Open source software including ITK-Snap (utilized in Chap II) and Slicer3 (employed in Chap III) are continually updated, adding new tools to aid in image analysis. These programs and others, including ImageJ and DTIStudio, have been

critical for image analysis for the studies described in Chapters II and III of this dissertation. For Chapter II, the process of manually segmenting regions of the CNS was exceptionally time intensive. Atlas building and automatic segmentation will undoubtedly reduce this burden.

In contrast to the MRM and DTI-based work, the studies described in Chapter IV employ methodologies that are now considered routine. However, while broadly applied in animal models for examination of normal development and for studies of genetic alterations, immunohistochemical and *in situ* hybridization techniques have not been widely used to investigate early ethanol-induced dysmorphogenesis. The Nkx2.1, Olig2 and GABA labeling studies conducted for this work have extended the current understanding of the scope of GD7 ethanol-induced alterations in the ventromedian forebrain. While it has long been recognized that this brain region is a target of GD7 ethanol exposure in mice, the potential of this insult to have cascading effects as a result of reduction in the progenitors for interneurons and oligodendrocytes has been highlighted.

As previously stated in this work, a limitation of the mouse model employed is that severely affected animals typically do not survive postnatally. For the studies described in Chapter IV, this has been particularly limiting. One specific interneuron population of interest is parvalbumin (Pv)-expressing interneurons because they are derived from the ventral area of the medial ganglionic eminence (MGE), an area shown in Chapter IV to be affected by a GD7 ethanol exposure. Examination of Pv-expressing interneurons was not possible in severely affected animals because Pv is not expressed until postnatal stages. Studies were conducted to examine postnatal

expression of Pv in more subtly affected animals, though due to poor tissue quality, results were inconsistent. To circumvent this issue, future studies should include examination of the transcription factors Dlx5 & 6, which are only expressed in the ventral area of the MGE. Additionally, characterization of transgenic mice expressing GFP in MGE-derived cells would be of interest (i.e. Lhx6, Nkx2.1, Dlx5 or Dlx6). This would allow for real-time viewing of tangential migration of the interneurons, as well.

In addition to the above, obvious extensions of the current work include MRM-based correlative analyses of CNS and facial dysmorphia and examination of postnatal stages for both morphological and functional consequences. Regarding the former, isotropic MR scans make possible accurate 3D reconstruction of not only the brain, but also the face. Ongoing work employing dense surface modeling (Hammond et al., 2005) holds significant promise for identification of a wide range of ethanol-exposure-mediated facial dysmorphologies. That ethanol-induced teratogenesis affects both the craniofacies and forebrain has been well documented. In fact, as previously described, facial dysmorphia is diagnostic for Fetal Alcohol Syndrome (Hoyme et al., 2005). A more comprehensive understanding of the more subtle facial features resulting from prenatal ethanol exposure could aid in diagnosing less severe individuals, and is currently being examined in clinical populations as well (reviewed in Douglas et al., 2010).

Regarding postnatal studies, clearly it is important to determine whether those GD7 ethanol-induced changes seen at fetal stages persist and how they might impact function, including behavior. As described in Chapter III, and in an extension

of this work recently conducted by O'Leary-Moore and her colleagues (personal communication), structural deficits consistent with those in fetal animals have been identified in periadolescent mice. In future structural analyses of postnatal animals the application of quantitative measures for examination of fiber tract integrity [i.e. determination of fractional anisotropy (FA) and mean diffusivity (MD)] promises to provide important information regarding both severe and subtle insult.

Studies directed toward examination of behavioral abnormalities following GD7 ethanol insult have recently been initiated (SOM, personal communication). Preliminary findings in PND45 mice include a decreased sensitivity to ethanol-induced hypothermia and reduced impairment on the rotorod following an acute ethanol exposure. Future studies directed towards examining the correlation between fiber tract anomalies and behavior is of importance. Areas of interest include learning and memory tasks, cross-hemisphere tasks, and olfaction.

Of particular note are this work's findings indicating the need for future studies directed toward examining seizure thresholds following early prenatal ethanol exposure. The presence of cerebral cortical heterotopias as noted in the MRI studies described in Chapter II, the cortical disorganization seen in the DTI studies described in Chapter III, and the loss of interneuron-producing tissues shown in the work described in Chapter IV all are highly suggestive that the GD7-exposed animals will have low seizure thresholds. Identification of early gastrulation stages as a time when ethanol insult may result in seizures/epilepsy has important clinical and public health implications. It is likely that individuals prenatally exposed to ethanol who present to epilepsy clinics are not properly diagnosed. The FASD diagnosis is

important because it allows for intervention services and strategies. Therefore, the implications of the work described within this dissertation suggest there is a need for inquiry regarding in utero ethanol exposure at seizure clinics.

In addition to informing clinical investigations and practice, the results of the work presented herein are readily applicable to FASD prevention, in particular to education efforts. Recognizing the world-wide breadth of the FASD problem, it is important that everyone be aware that the developing embryo is sensitive to ethanol's devastating effects and that damage can result from ethanol exposure occurring even as early as the third week of gestation, prior to the time that most pregnancies are recognized. The graphic quality of MR-based images, as presented in Chapters II and III, allows ready appreciation of the severe effects that prenatal ethanol exposure can have on the developing brain. Consequently, some of these images have already been incorporated into educational materials, including the UNC Morehead Planetarium's Science360 program, The Developing Brain (<http://www.moreheadplanetarium.org>). This program was developed to expose students in grades 3 through 12 to current and innovative science, and to make them aware of factors that can alter the developing brain. Additionally, the most recent (9th) edition of the widely used Developmental Biology text by S.F. Gilbert, includes illustrations from this study of a normal and ethanol-exposed fetal brain, as do two articles regarding FASD that are currently in press in NIAAA's Alcohol and Health Journal.

In conclusion, this work has not only contributed to the goals of the basic science community of FASD, but also promises to aid in prevention methods as well.

Clearly, to fully appreciate the entire spectrum of ethanol's teratogenesis, acute and chronic exposure paradigms occurring at all stages of development should be examined to this extent.

REFERENCES

Coles CD (1994) Critical periods for prenatal alcohol exposure: evidence from animal and human studies. *Alcohol Health and Research World* 18(1):22.

Douglas TS, Mutsvangwa TE A review of facial image analysis for delineation of the facial phenotype associated with fetal alcohol syndrome. *Am J Med Genet A* 152A(2):528-36.

Hammond P, Hutton TJ, Allanson JE, Buxton B, Campbell LE, Clayton-Smith J, Donnai D, Karmiloff-Smith A, Metcalfe K, Murphy KC, Patton M, Pober B, Prescott K, Scambler P, Shaw A, Smith AC, Stevens AF, Temple IK, Hennekam R, Tassabehji M (2005) Discriminating power of localized three-dimensional facial morphology. *Am J Hum Genet* 77(6):999-1010.

Hoyme HE, May PA, Kalberg WO, Kodituwakku P, Gossage JP, Trujillo PM, Buckley DG, Miller JH, Aragon AS, Khaole N, Viljoen DL, Jones KL, Robinson LK (2005) A practical clinical approach to diagnosis of fetal alcohol spectrum disorders: clarification of the 1996 institute of medicine criteria. *Pediatrics* 115(1):39-47.

Parnell SE, O'Leary-Moore SK, Godin EA, Dehart DB, Johnson BW, Allan Johnson G, Styner MA, Sulik KK (2009) Magnetic Resonance Microscopy Defines Ethanol-Induced Brain Abnormalities in Prenatal Mice: Effects of Acute Insult on Gestational Day 8. *Alcohol Clin Exp Res* 33(6):1001-1011.

Warren KR, Hewitt BG (2009) Fetal alcohol spectrum disorders: when science, medicine, public policy, and laws collide. *Dev Disabil Res Rev* 15(3):170-5.